

Strongly-ordered infrared counterterms from factorisation

Lorenzo Magnea,^a Calum Milloy,^a Chiara Signorile-Signorile,^b Paolo Torrielli^a

^a*Dipartimento di Fisica, Università di Torino, and INFN, Sezione di Torino,
Via P. Giuria 1, I-10125 Torino, Italy*

^b*Max-Planck-Institut für Physik, Boltzmannstrasse 8, 85748 Garching, Germany*

E-mail: lorenzo.magnea@unito.it, calumwilliam.milloy@unito.it,
signoril@mpp.mpg.de, paolo.torrielli@unito.it

ABSTRACT: In the context of infrared subtraction algorithms beyond next-to-leading order, it becomes necessary to consider multiple infrared limits of scattering amplitudes, in which several particles become soft or collinear in a strongly-ordered sequence. We study these limits from the point of view of infrared factorisation, and we provide general definitions of strongly-ordered soft and collinear kernels in terms of gauge-invariant operator matrix elements. With these definitions in hand, it is possible to construct local subtraction counterterms for strongly-ordered configurations. Because of their factorised structure, these counterterms cancel infrared poles of real-virtual contributions by construction. We test these ideas at tree level for multiple emissions, and at one loop for single and double emissions, contributing to NNLO and N³LO distributions, respectively.

KEYWORDS: QCD corrections, factorisation, infrared subtraction

Contents

1	Introduction	1
2	The architecture of infrared subtraction	3
2.1	Subtraction at NLO	3
2.2	Subtraction at NNLO	5
2.3	Subtraction at higher orders	7
3	The factorisation approach to subtraction	9
3.1	A top-down approach to subtraction at NLO	12
3.2	Factorisation structure at NNLO	13
4	Factorisation of radiative functions in strongly-ordered limits at tree level	17
4.1	Tree-level radiative soft functions	18
4.2	Tree-level radiative jet functions	20
5	Factorisation of single-radiative functions at one loop	23
5.1	Single-radiative soft function at one loop	23
5.2	Single-radiative jet functions at one loop	27
5.3	Computing radiative jet functions at one loop	28
6	A top-down approach to strongly-ordered counterterms	31
6.1	Soft sector	31
6.2	Collinear sector	32
6.3	Extracting strongly-ordered counterterms	33
7	Summary and future prospects	35
A	Soft and collinear cancellations at NLO	36
A.1	Soft cancellation	37
A.2	Collinear cancellation	38
B	Tree-level radiative jet functions for different partonic processes	39
C	On the computation of radiative jet functions at one loop	41
D	Consistency relations	43

1 Introduction

In the era of precision high-energy physics, significant efforts and excitement in the particle physics community focus on developing methods to explore high orders in perturbation theory, and improving on the precision of theoretical predictions, to meet the standards set by current and future experiments (refer to Refs. [1–3] for recent reviews). An important requirement to access the calculation of hard processes at lepton and hadron colliders is to have a detailed control on infrared singularities (arising from configurations where one or more particles become soft or collinear), that

plague both real and virtual corrections. While this problem is completely solved at next-to-leading order (NLO) [4–10], the issue of treating infrared singularities in a fully general manner remains a challenge at NNLO. Numerous *subtraction* and *slicing* schemes are currently available [11–34], as reviewed in [35], and a few of them have already been applied to a variety of NNLO calculations (see [36–60] for some representative results). However, none of the existing methods have so far provided an explicit demonstration of the cancellation of infrared singularities for arbitrary hadron collider processes at NNLO. Although recent work made substantial progress in this direction, in the context of *antenna subtraction* [34, 61] and *nested soft-collinear subtraction* [33], such a proof for generic final states is still beyond the current state of the art for hadronic scattering. For e^+e^- collisions, this cancellation for arbitrary final states has only been displayed within the framework of the *local analytic sector subtraction* scheme [30, 31, 62].

Given this scenario, perfecting our understanding of the physical mechanisms governing infrared divergences is crucial. It is intriguing to observe an “asymmetry” in the control we have on soft and collinear singularities in *virtual* corrections to scattering amplitudes, compared to our understanding of the behaviour of *real-radiation* corrections in the same regimes. The infrared content of virtual corrections has been deeply scrutinised in the past [63–74], and, in the case of massless gauge amplitudes, it has been shown that it is governed to all orders by a limited set of universal functions defined by gauge-invariant operator matrix elements. These functions, in turn, obey evolution equations that can be solved in terms of soft and collinear anomalous dimensions, which have been computed in the massless case up to three loops [75–78], and in some cases also beyond [79–81]. Our knowledge of the behaviour of real-radiation matrix elements under unresolved limits is somewhat more limited, as most existing results have been derived at fixed order. Nevertheless, it has been demonstrated that, under a variety of conditions, these matrix elements factorise in soft and collinear limits into universal kernels and lower-multiplicity amplitudes [82–84]. The necessary kernels for NNLO calculations are fully known [82–87], while partial results are available at N³LO [88–101].

A theoretical framework to systematically construct unresolved radiative contributions, serving as local subtraction counterterms, and leveraging the well-understood structure of infrared divergences in virtual corrections, would greatly benefit the ultimate organisation of subtraction methods. This paper aims at filling this gap, complementing the study performed in Ref. [102]. In that paper, a general method was proposed to identify local infrared subtraction counterterms, to any order in perturbation theory. The core idea of the method consists in exploiting completeness relations and general theorems on the cancellation of infrared singularities, to infer the expression of real-radiation counterterms from the factorised form of virtual corrections. In the latter, soft and collinear divergences are organised in gauge-invariant matrix elements of fields and Wilson lines. Ref. [102] also tested the agreement between the expressions of the candidate counterterms and the known results at NLO, and presented the organisation of the relevant counterterms at NNLO. An interesting aspect of NNLO calculations that was not addressed in Ref. [102], and which is the focus of the present paper (see also Ref. [103]), is the issue of identifying and dealing with strongly-ordered soft and collinear limits, where groups of particles become unresolved in a hierarchical manner. For example, at NNLO, up to two partons can become soft and up to three partons can become collinear at the same time. When these double-unresolved limits are analysed, one needs to disentangle *uniform limits*, where soft and collinear emissions become unresolved at the same rate, and *strongly-ordered* limits, where one or more particles become unresolved at a faster rate than the others. These hierarchical configurations, upon integration, play the delicate role of cancelling singularities arising in mixed real-virtual contributions. In the present paper, we will tackle the problem of systematically building strongly-ordered subtraction counterterms, exploiting the principles of infrared factorisation. Through specific examples, we will illustrate how matrix elements involving fields and Wilson lines, that describe the factorised emission of soft and collinear particles, can be *re-factorised* in strongly-ordered configurations. We will then exploit this nested

factorisation structure to display the required cancellation of singularities between strongly-ordered limits and real-virtual contributions.

The paper is organised as follows: in Section 2 we present the architecture of infrared subtraction in full generality, starting at NLO and then illustrating the organisation of relevant counterterms up to N³LO. The resulting structure smoothly generalises to any order, and we discuss the counting of necessary counterterms at N^kLO, for generic k . In Section 3, we discuss the factorisation approach to explicitly construct the counterterms introduced in Section 2. Given such a construction, we will focus on strongly-ordered limits at tree level in Section 4. We will show that ordered configurations can be easily modelled by products of soft and jet functions, with appropriate colour and spin contractions. This result paves the way for a formal, all-order definitions of hierarchical limits. We then recall that strongly-ordered configurations must interplay with the real-virtual corrections. For this reason, in Section 5, we analyse the single radiative contributions at one-loop order, and we obtain the relevant counterterms. Combining the results of Section 4 and Section 5 will allow us to derive the form of strongly-ordered counterterms in terms of factorised soft and jet functions, presented in Section 6. We conclude in Section 7 with a summary of our results and a brief discussion of future prospects. Four Appendices present some technical aspects: in particular, Appendix A discusses in detail how the cancellation of singularities in terms of universal matrix elements is achieved at NLO, emphasising the role played by phase-space mappings in the collinear case.

2 The architecture of infrared subtraction

Consider renormalised scattering amplitudes $\mathcal{A}_n(p_i)$ involving n massless coloured particles carrying momenta p_i ($i = 1, \dots, n$). For simplicity, we focus on the case of final-state particles with a total momentum $Q = \sum_{i=1}^n p_i$, generated by the decay of a colour-singlet current, and we do not display the dependence on the strong coupling $\alpha_s(\mu^2)$ and the dimensional infrared regulator $\epsilon = (4 - d)/2 < 0$, where d is the number of space-time dimensions. We expand the amplitude in perturbation theory as

$$\mathcal{A}_n(p_i) = \mathcal{A}_n^{(0)}(p_i) + \mathcal{A}_n^{(1)}(p_i) + \mathcal{A}_n^{(2)}(p_i) + \dots, \quad (2.1)$$

where $\mathcal{A}_n^{(k)}(p_i)$ is the k -loop correction, including the appropriate power of the strong coupling constant. Given the amplitude, one can compute finite differential distributions for a generic infrared-safe observable X , whose perturbative expansion we write as

$$\frac{d\sigma}{dX} = \frac{d\sigma_{\text{LO}}}{dX} + \frac{d\sigma_{\text{NLO}}}{dX} + \frac{d\sigma_{\text{NNLO}}}{dX} + \dots \quad (2.2)$$

For example, the leading-order distribution is given by

$$\frac{d\sigma_{\text{LO}}}{dX} = \int d\Phi_n B_n \delta_n(X), \quad (2.3)$$

where $B_n \equiv |\mathcal{A}_n^{(0)}|^2$ is the Born-level squared amplitude, Φ_n is the n -particle phase space, and $\delta_n(X) \equiv \delta(X - X_n)$ fixes X_n , the expression for the observable appropriate for an n -particle configuration, to the prescribed value X . At higher orders, infrared divergences arise from both loop and phase-space integrations, and must be properly handled. We begin our discussion with a brief overview of the structure of the problem, order by order in perturbation theory.

2.1 Subtraction at NLO

At NLO, there are infrared divergent contributions from the one-loop virtual correction in eq. (2.1), and further divergences arising from the phase-space integration of unresolved real radiation. These

divergences cancel in the sum, so that one can compute¹

$$\frac{d\sigma_{\text{NLO}}}{dX} = \lim_{d \rightarrow 4} \left[\int d\Phi_n V_n \delta_n(X) + \int d\Phi_{n+1} R_{n+1} \delta_{n+1}(X) \right], \quad (2.4)$$

where $V_n \equiv 2\text{Re}[\mathcal{A}_n^{(0)\dagger} \mathcal{A}_n^{(1)}]$, and $R_{n+1} \equiv |\mathcal{A}_{n+1}^{(0)}|^2$. The main idea of infrared subtraction is to introduce *local counterterms* mimicking the phase-space behaviour of real radiation in all singular regions, but simple enough to be analytically integrated over the unresolved degrees of freedom. At NLO, this amounts to defining a single function in Φ_{n+1} (in practice, a sum of contributions from non-overlapping singular regions), which we denote with $K_{n+1}^{(1)}$, where the superscript emphasises the fact that only one particle can become unresolved at NLO. A proper definition of a local counterterm requires several steps, and a detailed construction was described for example in Refs. [30, 104]. For the purposes of this paper, we will not need a complete implementation, so we will provide here only a brief outline, which does not depend on the detailed definitions of the counterterms.

The first step in our construction is to define *projection operators* that extract leading-power contributions to R_{n+1} , for all singular regions, in the relevant variables. Since divergences arise only in soft and collinear limits, at NLO the required operators are \mathbf{S}_i , extracting the soft limit for particle i (where $\mathbf{S}_i R_{n+1}$ is singular only if i is a gluon), and \mathbf{C}_{ij} , extracting the collinear limit for particles i and j . In our approach, we then split the real-radiation phase space by introducing *sector functions* \mathcal{W}_{ij} , inspired by the method of Ref. [6], forming a partition of unity, so that each radiation sector has at most one soft and one collinear singularity. This makes it possible to define a single operator collecting all NLO singular limits, without double counting, as

$$\mathbf{L}^{(1)} R_{n+1} = \sum_{i=1}^{n+1} \sum_{\substack{j=1 \\ j \neq i}}^{n+1} \left(\mathbf{S}_i + \mathbf{C}_{ij} - \mathbf{S}_i \mathbf{C}_{ij} \right) R_{n+1} \mathcal{W}_{ij}. \quad (2.5)$$

The next step is to introduce *phase-space mappings*, following Ref. [7], in order to factor the radiative phase space as the product of a Born-level phase space times a measure for the degrees of freedom of the unresolved radiation, according to²

$$d\Phi_{n+1} \equiv \frac{\varsigma_{n+1}}{\varsigma_n} d\Phi_n d\Phi_{\text{rad},1}^{n+1}, \quad (2.6)$$

where we explicitly display the appropriate symmetry factors ς_p . The soft and collinear operators can then be *improved* by expressing the limits in terms of mapped variables, allowing for a complete factorisation of soft and collinear kernels (which depend only on radiative degrees of freedom) from Born-level squared matrix elements (depending only on the momenta of the resolved particles). Note that different mappings can be implemented for different sectors, and even for different terms in the soft and collinear kernels, in order to simplify subsequent integrations. Note also that one can, if needed, adjust the actions of improved limits on sector functions, or include subsets of non-singular terms, in order to ensure the consistency of nested improved limits, or to ameliorate numerical stability. A detailed discussion about different mappings and strategies to adapt them to the various singular kernels can be found in Ref. [31].

We denote the improved operators by $\bar{\mathbf{S}}_i$, $\bar{\mathbf{C}}_{ij}$, and $\bar{\mathbf{S}}_i \bar{\mathbf{C}}_{ij}$, respectively, and we use them to build an improved version of the subtraction operator defined in eq. (2.5), which we denote by

¹The same formula can be found in eq. (2.3) in Ref. [31]. However, we point out that in this paper we will adopt a slightly different notation. For instance, we will always specify the number of partons contributing to the matrix elements, for example V_n and R_{n+1} . We will use the same convention for the various counterterms. We believe this choice to be beneficial for clarity, in the context of the general discussion pursued here.

²Such factorisation is identical to the one presented in eq. (2.5) in Ref. [31], with the convention $d\Phi_{\text{rad},1}^{n+1} \equiv d\Phi_{\text{rad}}$. Analogously, we will use $d\Phi_{\text{rad},2}^{n+2}$ as a synonym for $d\Phi_{\text{rad},2}$ used in Ref. [31].

$\bar{\mathbf{L}}^{(1)}$. We can then finally define our NLO counterterm as

$$K_{n+1}^{(1)} = \bar{\mathbf{L}}^{(1)} R_{n+1}. \quad (2.7)$$

With these definitions, we are now in a position to integrate the local counterterm $K_{n+1}^{(1)}$ over the unresolved degrees of freedom, for any fixed Born configuration, defining the *integrated counterterm*

$$I_n^{(1)} = \int d\Phi_{\text{rad},1}^{n+1} K_{n+1}^{(1)}. \quad (2.8)$$

The infrared poles of $I_n^{(1)}$ are, by construction, the same as those arising from the exact integration of R_{n+1} in eq. (2.4), and thus must cancel the explicit poles of the virtual correction V_n . Similarly, subtracting the counterterm $K_{n+1}^{(1)}$ from R_{n+1} yields a function that is integrable in Φ_{n+1} directly in $d = 4$. It is then possible to rewrite eq. (2.4) *identically* as

$$\frac{d\sigma_{\text{NLO}}}{dX} = \int d\Phi_n [V_n + I_n^{(1)}] \delta_n(X) + \int d\Phi_{n+1} [R_{n+1} \delta_{n+1}(X) - K_{n+1}^{(1)} \delta_n(X)]. \quad (2.9)$$

Both combinations in square brackets are suitable for a direct numerical evaluation in $d = 4$. Importantly, the infrared (IR) safety of the observable is necessary for the cancellation, which ensures $\delta_{n+1}(X)$ to turn smoothly into $\delta_n(X)$ in all unresolved limits.

2.2 Subtraction at NNLO

The intricacy of the subtraction problem starts to show up at NNLO, where the cancellation of divergences requires mixing double-virtual corrections, to be integrated in the n -particle phase space, with real-virtual contributions, to be integrated in the $(n+1)$ -particle phase space, and with integrated double-real radiation in Φ_{n+2} . The observable distribution is then

$$\frac{d\sigma_{\text{NNLO}}}{dX} = \lim_{d \rightarrow 4} \left[\int d\Phi_n VV_n \delta_n(X) + \int d\Phi_{n+1} RV_{n+1} \delta_{n+1}(X) + \int d\Phi_{n+2} RR_{n+2} \delta_{n+2}(X) \right], \quad (2.10)$$

where

$$VV_n = \left| \mathcal{A}_n^{(1)} \right|^2 + 2\text{Re} \left[\mathcal{A}_n^{(0)\dagger} \mathcal{A}_n^{(2)} \right], \quad RV_{n+1} = 2\text{Re} \left[\mathcal{A}_{n+1}^{(0)\dagger} \mathcal{A}_{n+1}^{(1)} \right], \quad RR_{n+2} = \left| \mathcal{A}_{n+2}^{(0)} \right|^2. \quad (2.11)$$

The double-virtual matrix element VV_n features up to quadruple poles in ϵ , while the real-virtual correction RV_{n+1} displays up to double poles in ϵ , and up to two phase-space singularities. Finally, the double-real matrix element is finite in $d = 4$, but is affected by up to four phase-space singularities. Following the procedure outlined at NLO, at this order we need to consider all possible double-unresolved limits of RR_{n+2} , to be added to the single-unresolved ones that we have already introduced. The relevant configurations involve: *i*) double-soft emission of two partons i and j , described by the projection operator \mathbf{S}_{ij} , *ii*) triple-collinear splitting of a single Born-level parton, described by the operator \mathbf{C}_{ijk} , *iii*) double-collinear splitting of two different Born-level partons, given by the operator $\mathbf{C}_{ij,kl}$, and, finally, *iv*) joint emission of a soft parton i and a collinear pair jk , given by the operator $\mathbf{S}\mathbf{C}_{i,jk}$. Since up to four particles are involved in these limits, the partition of the double-radiative phase space will involve sector functions \mathcal{W}_{ijkl} , with up to four different partonic labels. Each sector is designed to contain up to two soft singularities and up to two collinear singularities. Importantly, the relevant limits of RR_{n+2} can be organised into three sets, which, in analogy with eq. (2.5), we denote by

$$\mathbf{L}^{(1)} RR_{n+2}, \quad \mathbf{L}^{(2)} RR_{n+2}, \quad \mathbf{L}^{(12)} RR_{n+2} \equiv \mathbf{L}^{(1)} \mathbf{L}^{(2)} RR_{n+2}. \quad (2.12)$$

As was the case at NLO, $\mathbf{L}^{(1)}RR_{n+2}$ collects (without double-counting) all singular contributions associated with *single-unresolved* radiation: it is given by eq. (2.5) with the replacement $R_{n+1} \rightarrow RR_{n+2}$, and with NNLO sector functions. Similarly, $\mathbf{L}^{(2)}RR_{n+2}$ collects all singularities due to *double-unresolved* radiation. Finally, $\mathbf{L}^{(12)}RR_{n+2}$ collects all *strongly-ordered* limits, in which two particles become unresolved at different rates. These singular limits lie in the overlap of single-unresolved and double-unresolved radiation, and must be subtracted from their sum in order to avoid double counting. The operators $\mathbf{L}^{(1)}$, $\mathbf{L}^{(2)}$ and $\mathbf{L}^{(12)}$ are given by iterations of the fundamental soft and collinear limits, and each term in these sums must be *improved*, in order to construct a fully subtracted form of the distribution in eq. (2.10). To this end, we need to factorise the $(n+2)$ -particle phase space as in eq. (2.6). In this case we have

$$d\Phi_{n+2} = \frac{\varsigma_{n+2}}{\varsigma_{n+1}} d\Phi_{n+1} d\Phi_{\text{rad},1}^{n+2}, \quad d\Phi_{n+2} = \frac{\varsigma_{n+2}}{\varsigma_n} d\Phi_n d\Phi_{\text{rad},2}^{n+2}. \quad (2.13)$$

The procedure to improve the NNLO singular limits, beginning with the choice of suitable mappings of the double-radiative phase space, is intricate, and highly constrained by consistency requirements: in the case of massless final-state radiation it is described in Ref. [31]. Ultimately, improved limits can be used to define the required local counterterms for double-real radiation, as

$$K_{n+2}^{(1)} = \bar{\mathbf{L}}^{(1)}RR_{n+2}, \quad K_{n+2}^{(2)} = \bar{\mathbf{L}}^{(2)}RR_{n+2}, \quad K_{n+2}^{(12)} = \bar{\mathbf{L}}^{(12)}RR_{n+2}. \quad (2.14)$$

When a phase-space parametrisation yielding eq. (2.13) is in place, one can define *integrated counterterms* for double-real radiation as

$$I_{n+1}^{(1)} = \int d\Phi_{\text{rad},1}^{n+2} K_{n+2}^{(1)}, \quad I_n^{(2)} = \int d\Phi_{\text{rad},2}^{n+2} K_{n+2}^{(2)}, \quad I_{n+1}^{(12)} = \int d\Phi_{\text{rad},1}^{n+2} K_{n+2}^{(12)}. \quad (2.15)$$

The last ingredient to construct a fully subtracted version of eq. (2.10) is a local counterterm for the phase-space singularities of the real-virtual contribution RV_{n+1} . Since only one particle is radiated, and can become unresolved, it is natural to mimic the NLO procedure, and make use of the limit $\mathbf{L}^{(1)}RV_{n+1}$, defined as in eq. (2.5). The corresponding improved real-virtual counterterm reads

$$K_{n+1}^{(\text{RV})} = \bar{\mathbf{L}}^{(1)}RV_{n+1}. \quad (2.16)$$

As discussed below, however, the improvement of the real-virtual local counterterm is non-trivial, due to the presence of explicit infrared poles in RV_{n+1} , which are not associated with phase-space singularities. Once the appropriate improvement has been identified, we can define the real-virtual integrated counterterm as

$$I_n^{(\text{RV})} = \int d\Phi_{\text{rad},1}^{n+1} K_{n+1}^{(\text{RV})}. \quad (2.17)$$

Putting together the ingredients assembled so far, we can now write a fully subtracted form of the generic NNLO distribution, eq. (2.10), which is the NNLO equivalent of eq. (2.9). It is given by

$$\begin{aligned} \frac{d\sigma_{\text{NNLO}}}{dX} &= \int d\Phi_n \left[VV_n + I_n^{(2)} + I_n^{(\text{RV})} \right] \delta_n(X) \\ &+ \int d\Phi_{n+1} \left[\left(RV_{n+1} + I_{n+1}^{(1)} \right) \delta_{n+1}(X) - \left(K_{n+1}^{(\text{RV})} + I_{n+1}^{(12)} \right) \delta_n(X) \right] \\ &+ \int d\Phi_{n+2} \left[RR_{n+2} \delta_{n+2}(X) - K_{n+2}^{(1)} \delta_{n+1}(X) - \left(K_{n+2}^{(2)} - K_{n+2}^{(12)} \right) \delta_n(X) \right]. \end{aligned} \quad (2.18)$$

With the definitions we have presented above, eq. (2.18) is an *identical* rewriting of eq. (2.10). To analyse eq. (2.18), we begin by noting that the third line is integrable in Φ_{n+2} by construction,

since all singular regions have been subtracted with no double counting. The analysis of the second line, which involves both explicit poles in ϵ and phase-space singularities, is more delicate. With a minimal definition of the local counterterms (including only leading-power contributions to the singular limits), standard theorems for the cancellation of IR divergences imply that the integral $I_{n+1}^{(1)}$ must cancel the poles of RV_{n+1} . The resulting sum, however, will still be affected by phase-space singularities, when the radiated particle becomes unresolved. To take care of this problem, the counterterm $K_{n+1}^{(\mathbf{RV})}$ is designed to cancel the phase-space singularities of RV_{n+1} . Furthermore, the integral $I_{n+1}^{(12)}$ must share the phase-space singularities of $I_{n+1}^{(1)}$, since the limit taken in defining $K_{n+2}^{(12)}$ from $K_{n+2}^{(1)}$ does not affect the leading-power contributions in the variables relative to the first unresolved particle. We conclude that the second line in eq. (2.18) is free of phase space singularities, and the first parenthesis is finite in $d = 4$. However, with a minimal definition of $K_{n+1}^{(\mathbf{RV})}$, we are not guaranteed that the second parenthesis will be finite: for example, the poles in $K_{n+1}^{(\mathbf{RV})}$ will depend on the phase-space mappings used in eq. (2.16), while the poles in $I_{n+1}^{(12)}$ will depend on the mappings and parametrisations used in the double-radiation phase space, and incorporated in eq. (2.14). Nevertheless, the complete cancellation of poles in the second parenthesis of the second line can be enforced by adjusting the definition of $K_{n+1}^{(\mathbf{RV})}$ to match the poles of $I_{n+1}^{(12)}$, without affecting phase-space singularities. Since this adjustment involves only terms that are not singular when the radiated particle becomes unresolved, we understand it here as part of the necessary improvement of the $\mathbf{L}^{(1)}$ operator, leading to the definition of $\bar{\mathbf{L}}^{(1)}$, when acting on RV_{n+1} . Having established the finiteness and integrability of both the second and the third line in eq. (2.18), the cancellation of poles in the first line follows directly from the KLN theorem.

2.3 Subtraction at higher orders

It is interesting to attempt to extrapolate the patterns appearing at NLO and at NNLO to higher orders. At N³LO the required matrix elements are

$$\begin{aligned} VVV_n &= 2\text{Re} \left[\mathcal{A}_n^{(0)\dagger} \mathcal{A}_n^{(3)} + \mathcal{A}_n^{(1)\dagger} \mathcal{A}_n^{(2)} \right], & RVV_{n+1} &= \left| \mathcal{A}_{n+1}^{(1)} \right|^2 + 2\text{Re} \left[\mathcal{A}_{n+1}^{(0)\dagger} \mathcal{A}_{n+1}^{(2)} \right], \\ RRV_{n+2} &= 2\text{Re} \left[\mathcal{A}_{n+2}^{(0)\dagger} \mathcal{A}_{n+2}^{(1)} \right], & RR_{n+3} &= \left| \mathcal{A}_{n+3}^{(0)} \right|^2. \end{aligned} \quad (2.19)$$

The uniform limits in which three particles become unresolved are

$$\mathbf{S}_{ijk}, \quad \mathbf{C}_{ijkl}, \quad \mathbf{C}_{ij,klm}, \quad \mathbf{C}_{ij,kl,mn}, \quad \mathbf{SC}_{i,jkl}, \quad \mathbf{SC}_{i,jk,lm}, \quad \mathbf{SC}_{ij,kl}, \quad (2.20)$$

where, following the conventions introduced at NNLO, we use commas to separate clusters of particles originating from the same hard parton, and we treat all soft particles as a single cluster. Thus, for example, in the limit $\mathbf{C}_{ij,klm}$ particles i, j and particles k, l, m form two distinct collinear clusters, while in the limit $\mathbf{SC}_{ij,kl}$ particles i and j are soft, while particles k and l form a collinear pair. These limits must of course be added on top of the single- and double-unresolved ones. Importantly, at N³LO there are several new possibilities for strong ordering of infrared limits. In fact, in analogy with eq. (2.12), one must introduce triple-unresolved limits

$$\begin{aligned} \mathbf{L}^{(3)} RRR_{n+3}, & \quad \mathbf{L}^{(13)} RRR_{n+3} \equiv \mathbf{L}^{(1)} \mathbf{L}^{(3)} RRR_{n+3}, & (2.21) \\ \mathbf{L}^{(23)} RRR_{n+3} \equiv \mathbf{L}^{(2)} \mathbf{L}^{(3)} RRR_{n+3}, & \quad \mathbf{L}^{(123)} RRR_{n+3} \equiv \mathbf{L}^{(1)} \mathbf{L}^{(2)} \mathbf{L}^{(3)} RRR_{n+3}. \end{aligned}$$

Here $\mathbf{L}^{(3)}$ gives the uniform limit, where three particles become unresolved at the same rate, $\mathbf{L}^{(13)}$ gives the strongly-ordered limits in which one particle becomes unresolved much faster than the other two, $\mathbf{L}^{(23)}$ covers the case in which two particles become unresolved at the same rate, but much faster than the third particle. Finally $\mathbf{L}^{(123)}$ gives the completely ordered limits in which

each particle becomes unresolved at a different rate. All of the limits in eq. (2.21) will be expressed as iterations of the fundamental limits in eq. (2.20), and each term in these sums will have to be improved, using the phase-space factorisations

$$d\Phi_{n+3} = \frac{\zeta_{n+3}}{\zeta_{n+2}} d\Phi_{n+2} d\Phi_{\text{rad},1}^{n+3}, \quad d\Phi_{n+3} = \frac{\zeta_{n+3}}{\zeta_{n+1}} d\Phi_{n+1} d\Phi_{\text{rad},2}^{n+3}, \quad d\Phi_{n+3} = \frac{\zeta_{n+3}}{\zeta_n} d\Phi_n d\Phi_{\text{rad},3}^{n+3}. \quad (2.22)$$

The required counterterms for limits involving three unresolved particles will then be of the form

$$K_{n+3}^{(\mathbf{h})} = \bar{\mathbf{L}}^{(\mathbf{h})} RRR_{n+3}, \quad (2.23)$$

with $\mathbf{h} \in \{\mathbf{3}, \mathbf{13}, \mathbf{23}, \mathbf{123}\}$, and the corresponding integrated counterterms will be given by

$$I_{n+3-q}^{(\mathbf{h})} = \int d\Phi_{\text{rad},q}^{n+3} K_{n+3}^{(\mathbf{h})}, \quad (2.24)$$

where q is the number of particles going unresolved at the highest rate, as in eq. (2.15). In order to complete the $N^3\text{LO}$ subtraction formula, one will further need a single local counterterm for single real radiation in RVV_{n+1} , which we denote by $K_{n+1}^{(\text{RVV})}$, and three local counterterms for double real radiation in RRV_{n+2} , which we denote by $K_{n+2}^{(\text{RRV}, \mathbf{h})}$, with $\mathbf{h} \in \{\mathbf{1}, \mathbf{2}, \mathbf{12}\}$, following the pattern set in eq. (2.14). These RVV and RRV counterterms must be integrated in the appropriate phase spaces, according to the rules introduced at NLO and at NNLO. Thus we define

$$I_n^{\text{RVV}} = \int d\Phi_{\text{rad},1}^{n+1} K_{n+1}^{(\text{RVV})}, \quad I_{n+2-q}^{(\text{RRV}, \mathbf{h})} = \int d\Phi_{\text{rad},q}^{n+2} K_{n+2}^{(\text{RRV}, \mathbf{h})}. \quad (2.25)$$

We are finally in a position to write a *master formula* for (final-state) $N^3\text{LO}$ subtraction. It takes the form

$$\begin{aligned} \frac{d\sigma_{N^3\text{LO}}}{dX} = & \int d\Phi_n \left[VVV_n + I_n^{(\mathbf{3})} + I_n^{(\text{RRV}, \mathbf{2})} + I_n^{(\text{RVV})} \right] \delta_n(X) \\ & + \int d\Phi_{n+1} \left[\left(RVV_{n+1} + I_{n+1}^{(\mathbf{2})} + I_{n+1}^{(\text{RRV}, \mathbf{1})} \right) \delta_{n+1}(X) - \left(K_{n+1}^{(\text{RVV})} + I_{n+1}^{(\mathbf{23})} + I_{n+1}^{(\text{RRV}, \mathbf{12})} \right) \delta_n(X) \right] \\ & + \int d\Phi_{n+2} \left\{ \left(RRV_{n+2} + I_{n+2}^{(\mathbf{1})} \right) \delta_{n+2}(X) - \left(K_{n+2}^{(\text{RRV}, \mathbf{1})} + I_{n+2}^{(\mathbf{12})} \right) \delta_{n+1}(X) \right. \\ & \quad \left. - \left[\left(K_{n+2}^{(\text{RRV}, \mathbf{2})} + I_{n+2}^{(\mathbf{13})} \right) - \left(K_{n+2}^{(\text{RRV}, \mathbf{12})} + I_{n+2}^{(\mathbf{123})} \right) \right] \delta_n(X) \right\} \\ & + \int d\Phi_{n+3} \left[RRR_{n+3} \delta_{n+3}(X) - K_{n+3}^{(\mathbf{1})} \delta_{n+2}(X) - \left(K_{n+3}^{(\mathbf{2})} - K_{n+3}^{(\mathbf{12})} \right) \delta_{n+1}(X) \right. \\ & \quad \left. - \left(K_{n+3}^{(\mathbf{3})} - K_{n+3}^{(\mathbf{13})} - K_{n+3}^{(\mathbf{23})} + K_{n+3}^{(\mathbf{123})} \right) \delta_n(X) \right]. \quad (2.26) \end{aligned}$$

In a concrete implementation, each one of the four phase space integrands in eq. (2.26) will be free of non-integrable singularities, and finite in $d = 4$. For example, in the $(n+3)$ -particle phase space, single-unresolved and double-unresolved singular contributions have been subtracted, and their overlap added back, in the first line. Triple-unresolved singular contributions are subtracted in the second line, with their overlap with single- and double-unresolved ones removed, and the overlap of the overlaps added back in. In the $(n+2)$ -particle phase space, infrared poles will cancel in the first parenthesis according to general theorems, and the phase-space singularities of RRV_{n+2} are fully subtracted by construction. Furthermore, the phase-space singularities of the three local counterterms are matched by the three corresponding integrated counterterms, also by construction. This would leave out possible uncanceled explicit poles, not associated with phase-space singularities, in each one of the last three parentheses: these can be handled in the process

of improving the relevant limit operators, as was done at NNLO. A similar pattern applies to the integrand in the $(n + 1)$ -particle phase space.

We see that a general-purpose subtraction algorithm at N³LO requires the construction of 11 local counterterm functions³, out of which 5 involve various forms of strong ordering, while 6 correspond to uniform limits. At the price of introducing some more formal notations, it is not too difficult to generalise this counting to N^kLO, for generic k . We find that the total number of local counterterms is then

$$c(k) = 2^{k+1} - 2 - k, \quad (2.27)$$

and, of these, only $k(k + 1)/2$ correspond to uniform limits, while the remaining ones involve strong ordering: for example, already for $k = 4$ the number of strongly-ordered counterterms (16) exceeds the number of uniform ones (10). Moreover, as we have seen, the pattern of cancellations involving mixed real-virtual local counterterms and the integrated versions of counterterms with extra real radiation is especially delicate, due to the interplay of phase-space singularities and explicit poles. Clearly, a general understanding of infrared subtraction will require mastering strongly-ordered infrared limits, and the cancellation of their singularities. We believe that a factorisation-based approach will be instrumental to this understanding, and we now turn to illustrate this viewpoint.

3 The factorisation approach to subtraction

Conceptually, the approach to subtraction that was discussed in the previous section can be described as *bottom-up*, according to the ordering used to analyse the lines in eq. (2.18) and eq. (2.26): one starts by considering the singular limits for multiple real-radiation matrix elements, and subsequently integrates the resulting counterterms, finally achieving the cancellation of virtual poles. However, we believe that it is interesting to consider a complementary *top-down* viewpoint, beginning with an analysis of infrared poles in the virtual correction, with the tools of factorisation, and then constructing infrared-finite soft and collinear cross sections, from which one can extract local counterterms. This approach was pursued in Ref. [102], where a general prescription was given to construct local counterterms for uniform soft and collinear limits, in terms of matrix elements of fields and Wilson lines. We now discuss how this approach can be extended to strongly-ordered local counterterms: this extension will ultimately guarantee the cancellation of infrared poles and phase-space singularities in the intermediate lines of eq. (2.18) and eq. (2.26).

To begin our discussion, we recall the well-known infrared factorisation formula for massless gauge-theory scattering amplitudes [69, 70, 73, 74]

$$\mathcal{A}_n(\{p_i\}) = \prod_{i=1}^n \left[\frac{\mathcal{J}_i(p_i, n_i)}{\mathcal{J}_{E_i}(\beta_i, n_i)} \right] \mathcal{S}_n(\{\beta_i\}) \mathcal{H}_n(\{p_i\}, \{n_i\}), \quad (3.1)$$

where we introduced four-velocities $\beta_i \equiv \sqrt{2} p_i / \mu$, and reference vectors n_i , for each one of the external legs. The soft function \mathcal{S}_n captures long-wavelength gluon exchanges between external particles: it does not depend on the spin of the latter, but it is a non-trivial operator in colour space, acting on the finite hard coefficient \mathcal{H}_n . A jet function \mathcal{J}_i is associated to each external particle, capturing collinear singularities: these depend only on the momentum and spin of the hard particle i , and are proportional to the identity in colour space. The eikonal jets \mathcal{J}_{E_i} encapsulates the overlap of soft and collinear singularities, that is present both in \mathcal{S}_n and in \mathcal{J}_i , and would otherwise be double-counted.

³We have described the structure of subtraction for final-state emissions only, however the inclusion of initial-state radiation does not essentially affect this counting. Rather, in a sector approach, some terms in the collinear parts of the counterterms, associated with initial-state radiation sectors, must be treated and integrated separately.

The factorisation functions \mathcal{S}_n , \mathcal{J}_i and \mathcal{J}_{E_i} appearing in eq. (3.1) have explicit operator definitions involving semi-infinite Wilson lines aligned with the external-particle trajectories,

$$\Phi_{\beta_i}(\infty, 0) \equiv P \exp \left\{ i g_s \mathbf{T}^a \int_0^\infty dz \beta_i \cdot A_a(z) \right\}, \quad (3.2)$$

where the symbol P identifies the path ordering, A_a is the gluon field, and g_s is the strong coupling. These Wilson lines capture soft-gluon radiation off external particles; further Wilson lines along the unphysical directions n_i are employed in the definition of the jet and eikonal jet functions. In the context of subtraction, it is useful to consider the virtual soft and jet functions in eq. (3.1) as special cases of more general objects, which we describe as *radiative* soft and jet functions, and can be used to organise soft and collinear *real* radiation. In the soft case, we begin by defining *eikonal form factors*

$$\mathcal{S}_{n, f_1 \dots f_m}(\{\beta_i\}; \{k_j, \lambda_j\}) \equiv \langle \{k_j, \lambda_j\} | T \left[\prod_{i=1}^n \Phi_{\beta_i}(\infty, 0) \right] | 0 \rangle, \quad (3.3)$$

where T is the time-ordering operator. The equation above describes the radiation of m particles of flavours f_j , momenta k_j and spin polarisations λ_j ($j = 0, \dots, m$), from the Wilson lines representing hard particles, including virtual corrections in the soft approximation. Similarly, we define *collinear form factors*, in order to describe collinear radiation from external particle i . These are spin-dependent quantities, involving the quantum field responsible for the creation or absorption of the hard particle. For final-state quarks we write

$$\mathcal{J}_{q, f_1 \dots f_m}^\alpha(x; n; \{k_j, \lambda_j\}) \equiv \langle \{k_j, \lambda_j\} | T [\bar{\psi}^\alpha(x) \Phi_n(x, \infty)] | 0 \rangle, \quad (3.4)$$

where one of the final-state particles is the quark created by the field $\bar{\psi}$ at point x . For final-state gluons, on the other hand, we choose [105]

$$g_s \mathcal{J}_{g, f_1 \dots f_m}^\nu(x; n; \{k_j, \lambda_j\}) \equiv \langle \{k_j, \lambda_j\} | T [\Phi_n(\infty, x) (iD^\nu \Phi_\beta(x, \infty))] | 0 \rangle, \quad (3.5)$$

where the Φ_β Wilson line is in the adjoint representation, oriented along the direction of a final-state gluon within the set $\{k_j\}$, and $D_\nu = \partial_\nu - ig_s A_\nu$. In eq. (3.4) and eq. (3.5), the index j ranges in $\{1, \dots, m\}$, where the $m = 1$ case reads $\mathcal{J}_{f_i, f_i} = \mathcal{J}_i$.

Finally, the eikonal versions of collinear form factors are spin-independent, and only characterised by the colour representation of the hard emitter. We can thus use the definition in eq. (3.4), and replace the field by a Wilson line along the classical quark or gluon trajectory, which gives

$$\mathcal{J}_{E_i, f_1 \dots f_m}(\beta_i; n_i; \{k_j, \lambda_j\}) \equiv \langle \{k_j, \lambda_j\} | T [\Phi_{\beta_i}(\infty, 0) \Phi_{n_i}(0, \infty)] | 0 \rangle. \quad (3.6)$$

The purely virtual soft and jet functions appearing in eq. (3.1) are instances of these form factors in the cases $m = 0$ (for the eikonal form factors and eikonal jets, corresponding to no final-state radiation), and $m = 1$ (for the collinear form factors, corresponding to the emission of the single particle created by the field).

At cross-section level, eikonal and collinear form factors must be appropriately squared, building up radiative soft and jet functions, which are fully local in the degrees of freedom of soft and collinear real radiation. Specifically, the radiative soft function, responsible for the emission of m soft particles by n resolved emitters, is defined by

$$S_{n, f_1 \dots f_m}(\{\beta_i\}; k_1, \dots, k_m) = \sum_{\{\lambda_j\}} \mathcal{S}_{n, f_1 \dots f_m}^\dagger(\{\beta_i\}; \{k_j, \lambda_j\}) \mathcal{S}_{n, f_1 \dots f_m}(\{\beta_i\}; \{k_j, \lambda_j\}), \quad (3.7)$$

where we summed over the polarisation of the final-state soft particles, regardless of their flavour⁴. Radiative jet functions must take into account the fact that hard-collinear emissions carry non-negligible momentum. At cross-section level one will therefore need a convolution rather than a simple product, with one of the two collinear form factors evaluated at a displaced location x , Fourier-conjugate to the total momentum ℓ carried by final-state particles. We thus define

$$J_{f,f_1\dots f_m}^{\alpha\beta}(\ell; n; k_1, \dots, k_m) = \sum_{\{\lambda_j\}} \int d^d x e^{i\ell \cdot x} \mathcal{J}_{f,f_1\dots f_m}^{\alpha,\dagger}(0; n; \{k_j, \lambda_j\}) \mathcal{J}_{f,f_1\dots f_m}^{\beta}(x; n; \{k_j, \lambda_j\}). \quad (3.8)$$

In eq. (3.8), f denotes the flavour of the parent particle, which can be either a quark or a gluon, and we have adopted a unified notation, where α and β are indices in the spin-1/2 or the spin-1 representations of the Lorentz group, depending on the flavour f . Performing the x integral will fix $\ell = \sum_j k_j$. To exemplify, for the discussion of NLO corrections we will need $J_{f,f_1 f_2}^{(0)}$, describing the tree-level splitting of type $f \rightarrow f_1 + f_2$; similarly, for tree-level triple-collinear emissions, relevant for NNLO corrections, we will need $J_{f,f_1 f_2 f_3}^{(0)}$, corresponding to the branching $f \rightarrow f_1 + f_2 + f_3$; finally, real-virtual corrections involving one-loop splittings will be described by the one-loop jet function $J_{f,f_1 f_2}^{(1)}$. We tested the definition of the radiative jet function at tree-level in the case of single and double radiation, and found agreement with known results (see for instance Ref. [84] for a comprehensive list of splitting functions). The single radiative jet functions are given explicitly in Appendix B. For cross-section-level radiative eikonal jets, the Fourier transform is not necessary, since they can be computed directly in the soft approximation⁵. We have

$$J_{\mathbb{E}_i, f_1\dots f_m}(\beta_i; n_i; k_1, \dots, k_m) = \sum_{\{\lambda_j\}} \mathcal{J}_{\mathbb{E}_i, f_1\dots f_m}^{\dagger}(\beta_i; n_i; \{k_j, \lambda_j\}) \mathcal{J}_{\mathbb{E}_i, f_1\dots f_m}(\beta_i; n_i; \{k_j, \lambda_j\}). \quad (3.9)$$

As argued in Ref. [102], the cross-section-level soft and jet functions thus defined provide natural candidates to build local soft and collinear counterterms for subtraction algorithms, to any order in perturbation theory. Indeed, integrating eq. (3.7) over the radiative m -particle phase space, summing over the number of particles, and using *completeness*, one finds

$$\sum_{m=0}^{\infty} \sum_{\{f_i\}} \int d\Phi_m S_{n, f_1\dots f_m}(\{\beta_i\}, k_1, \dots, k_m) = \langle 0 | \bar{T} \left[\prod_{i=1}^n \Phi_{\beta_i}(0, \infty) \right] T \left[\prod_{i=1}^n \Phi_{\beta_i}(\infty, 0) \right] | 0 \rangle, \quad (3.10)$$

where \bar{T} is the anti-time ordering. The *r.h.s.* of eq. (3.10) represents a total cross section in the presence of Wilson-line sources, and it is infrared finite order by order in perturbation theory. This implies that the phase-space integrals of the m -particle radiative soft functions defined in eq. (3.7) do indeed cancel the virtual poles arising from soft virtual corrections. Similarly, integrating eq. (3.8) over phase space, summing over the number of radiated particles, and using completeness, one finds (for quarks)

$$\begin{aligned} & \sum_{m=1}^{\infty} \sum_{\{f_i\}} \int d\Phi_m J_{q, f_1\dots f_m}^{\alpha\beta}(\ell; n; k_1, \dots, k_m) \\ &= \text{Disc} \left[\int d^d x e^{i\ell \cdot x} \langle 0 | T \left[\Phi_n(\infty, x) \psi^{\beta}(x) \bar{\psi}^{\alpha}(0) \Phi_n(0, \infty) \right] | 0 \rangle \right], \end{aligned} \quad (3.11)$$

and similarly for gluons. The *r.h.s.* of eq. (3.11) represents the discontinuity of a two-point function in the presence of Wilson lines, and it is infrared finite order by order, as was the case for eq. (3.10). This shows that the radiative jet functions in eq. (3.8) provide candidate local collinear counterterms to cancel virtual collinear singularities.

⁴Although Wilson lines only radiate gluons, those gluons can in turn produce $q\bar{q}$ pairs.

⁵Note that this convention is different from the one adopted in Ref. [102].

3.1 A top-down approach to subtraction at NLO

Before moving on to strongly-ordered soft and collinear limits, we illustrate how one can build and integrate local infrared counterterms within the framework presented in Section 3, and previously discussed in some detail in Ref. [102]. We begin at NLO, where some of the technical issues can be easily clarified. For the sake of notational simplicity, from now on we drop the n dependence from the argument of jet functions, and we expand all functions in perturbation theory using the same conventions as in eq. (2.1). With these definitions, the NLO virtual correction V_n can be obtained by expanding eq. (3.1) to NLO, and can be written as

$$\begin{aligned}
V_n &= \mathcal{H}_n^{(0)\dagger} S_n^{(1)}(\{\beta_i\}) \mathcal{H}_n^{(0)} - \mathcal{H}_n^{(0)\dagger} S_n^{(0)} \mathcal{H}_n^{(0)} \sum_{i=1}^n J_{E_i}^{(1)}(\beta_i) \\
&\quad + \sum_{i=1}^n \sum_{f_j} \int \frac{d^d \ell_i}{(2\pi)^d} \mathcal{H}_{n,\alpha_i}^{(0)\dagger}(\{p\}_i, \ell_i) J_{f_i, f_j}^{(1)\alpha_i \beta_i}(\ell_i; p_i) S_n^{(0)} \mathcal{H}_{n,\beta_i}^{(0)}(\{p\}_i, \ell_i) + \text{finite} \\
&\equiv V_n^{(s)} + \sum_{i=1}^n V_{n,i}^{(\text{hc})} + \text{finite}, \tag{3.12}
\end{aligned}$$

where we distinguish the soft singular contribution $V_n^{(s)}$, given by the first term in eq. (3.12), from hard-collinear contributions associated with each external particle, denoted by $V_{n,i}^{(\text{hc})}$ and given by the remaining two terms. The tree-level hard function $\mathcal{H}_n^{(0)}$ depends on the momentum and spin (as well as colour) of the partons in the Born process, while the tree-level soft function $S_n^{(0)}$ is just a colour tensor connecting the two hard functions. The notation $\mathcal{H}_{n,\alpha_i}^{(0)}(\{p\}_i, \ell_i)$ means that one needs to replace p_i with ℓ_i in the hard function, as well as remove the wave function of parton i (the spinor for quarks and the polarisation vector for gluons), uncovering the spin index α_i . Since $J_{f_i, f_j}^{(1)}(\ell_i; p_i) \sim \delta(\ell_i - p_i) \delta_{f_i, f_j}$, the ℓ_i integral and the flavour sum are trivial: we include them here in order to match the necessary notation when dealing with the case of real radiation, where the corresponding integrals will identify ℓ_i as the parent particle for collinear splittings, and the flavour sums will be non trivial.

We can now exploit the finiteness of eq. (3.10) and of eq. (3.11) (as well as the analogous relation for eikonal jets) to write the NLO *completeness relations*⁶

$$S_n^{(1)}(\{\beta_i\}) + \int d\Phi(k) S_{n,g}^{(0)}(\{\beta_i\}; k) = \text{finite}, \tag{3.13}$$

$$J_{E_i}^{(1)}(\beta_i) + \int d\Phi(k) J_{E_i, g}^{(0)}(\beta_i; k) = \text{finite}, \tag{3.14}$$

$$\sum_{f_1} \int d\Phi(k_1) J_{f, f_1}^{(1)\alpha\beta}(\ell; k_1) + \sum_{f_1, f_2} \varsigma_{f_1 f_2} \int d\Phi(k_1) d\Phi(k_2) J_{f, f_1 f_2}^{(0)\alpha\beta}(\ell; k_1, k_2) = \text{finite}, \tag{3.15}$$

where the flavour sum extends to all final-state flavour combinations compatible with the Feynman rules (with each combination counted only once: for example, if $\{f_1, f_2\} = \{g, g\}$ is included, then $\{f_1, f_2\} = \{g, q\}$ is excluded). Furthermore, $\varsigma_{f_1 f_2}$ is a phase-space symmetry factor, equal to 1/2 when $f_1 = f_2 = g$ and equal to one in all other cases at NLO. For single soft emissions, we have used the fact that only the radiation of a single gluon is allowed, which removes the need for a flavour sum in eq. (3.13) and in eq. (3.14). The finiteness conditions in eqs. (3.13-3.15) immediately suggest expressions for candidate soft and hard-collinear local infrared counterterms at NLO, which

⁶We defer to Appendix A a proper treatment of UV divergences associated with these relations.

are given by

$$K_{n+1}^{(\mathbf{1},s)}(\{p_i\}, k) = \mathcal{H}_n^{(0)\dagger}(\{p_i\}) S_{n,g}^{(0)}(\{\beta_i\}; k) \mathcal{H}_n^{(0)}(\{p_i\}), \quad (3.16)$$

$$\begin{aligned} K_{n+1,i}^{(\mathbf{1},\text{hc})}(\{p_i\}, k_1, k_2) &= \sum_{f_1, f_2} \left[\int \frac{d^d \ell_i}{(2\pi)^d} \mathcal{H}_{n,\alpha_i}^{(0)\dagger}(\{p\}_i, \ell_i) J_{f_i, f_1 f_2}^{(0)\alpha_i \beta_i}(\ell_i; k_1, k_2) S_n^{(0)} \mathcal{H}_{n,\beta_i}^{(0)}(\{p\}_i, \ell_i) \right. \\ &\quad \left. - \mathcal{H}_n^{(0)\dagger}(\{p_i\}) \left(\sum_{j=1}^2 J_{\mathbb{E}_i, f_j}^{(0)}(\beta_i; k_j) \right) S_n^{(0)} \mathcal{H}_n^{(0)}(\{p_i\}) \right] \\ &\equiv \mathcal{H}_n^{(0)\dagger} \sum_{f_1, f_2} \left(J_{f_i, f_1 f_2}^{(0)} - \sum_{j=1}^2 J_{\mathbb{E}_i, f_j}^{(0)} \right) S_n^{(0)} \mathcal{H}_n^{(0)}, \end{aligned} \quad (3.17)$$

where in the last line we have introduced a shorthand notation to denote the convolution of the hard function with the jet function over the total collinear momentum ℓ_i , including the spin sum. Note again that eikonal jets with a single final-state quark emission, $J_{\mathbb{E}_i, q}$, vanish: thus the sum on the second line of eq. (3.17) includes only one term, except in the case $f_1 = f_2 = g$. For all flavour combinations it is straightforward to check, using the results of Appendix B, that the jet combination in round brackets in the latter equation is completely free of soft phase-space singularities (*i.e.* both those associated to f_1 and to f_2). Hence we define the *hard-collinear* single-radiative jet at k loops as

$$J_{f_i, f_1 f_2}^{(k), \text{hc}} \equiv J_{f_i, f_1 f_2}^{(k)} - \sum_{j=1}^2 J_{\mathbb{E}_i, f_j}^{(k)}. \quad (3.18)$$

With these definitions, eq. (3.13) implies that the phase-space integral (over the gluon momentum k) of eq. (3.16) will cancel the explicit infrared poles of the first term in eq. (3.12); similarly, eq. (3.14) shows that the phase-space integration of momentum k_j in the last term in eq. (3.17) will cancel the explicit infrared poles of the second term in eq. (3.12); finally, eq. (3.15) shows that the phase-space integration of the first term in eq. (3.17) over momenta k_1 and k_2 will cancel the explicit infrared poles of the last term in eq. (3.12), after the (trivial) integration in $d\Phi(k_1)$.

It is important, at this stage, to emphasise that the candidate counterterms in (3.16) and (3.17) are not quite ready for implementation in a subtraction scheme. The first problem is that the phase-space integrals in eq. (3.13) and eq. (3.14) are affected by ultraviolet divergences, since the respective integrands correctly reproduce the amplitude only in the limit of soft k . Physically, we expect that infrared singularities will be independent of the choice of the ultraviolet regulator, but still a specific scheme needs to be devised. A second problem is that eq. (3.15) is valid as distribution identity, since the first term has support when ℓ is on-shell, while in the second term ℓ is off-shell, and divergences arise in the on-shell limit. In order to implement eq. (3.15) locally in the Born phase-space we will therefore need to introduce appropriate phase-space mappings, expressing ℓ in terms of an on-shell momentum in the real-radiation contribution. A detailed implementation of the soft and collinear cancellations in a form useful for subtraction is presented in Appendix A.

3.2 Factorisation structure at NNLO

Following the same procedure as at NLO, one can extract the poles of the two-loop amplitude by expanding all factors of eq. (3.1) at the proper order, and then organising them in terms of cross-section-level soft and jet functions. The final result for VV_n can be written as [102]

$$VV_n = VV_n^{(2s)} + VV_n^{(1s)} + \sum_{i=1}^n \left[VV_{n,i}^{(2\text{hc})} + \sum_{j=i+1}^n VV_{n,ij}^{(2\text{hc})} + VV_{n,i}^{(1\text{hc}, 1s)} + VV_{n,i}^{(1\text{hc})} \right] + \text{finite}, \quad (3.19)$$

where the superscripts identify the soft or hard-collinear nature of the poles collected in the different terms. Explicitly,

$$\begin{aligned}
VV_n^{(2s)} &= \mathcal{H}_n^{(0)\dagger} S_n^{(2)}(\{\beta_i\}) \mathcal{H}_n^{(0)}, \\
VV_n^{(1s)} &= \mathcal{H}_n^{(0)\dagger} S_n^{(1)}(\{\beta_i\}) \mathcal{H}_n^{(1)} + \mathcal{H}_n^{(1)\dagger} S_n^{(1)}(\{\beta_i\}) \mathcal{H}_n^{(0)}, \\
VV_{n,i}^{(2hc)} &= \mathcal{H}_n^{(0)\dagger} \left[J_{f_i, f_i}^{(2)}(p_i) - J_{E_i}^{(2)}(\beta_i) - J_{E_i}^{(1)}(\beta_i) J_{f_i, f_i}^{(1), hc} \right] S_n^{(0)} \mathcal{H}_n^{(0)}, \\
VV_{n,ij}^{(2hc)} &= \mathcal{H}_n^{(0)\dagger} J_{f_i, f_i}^{(1), hc} J_{f_j, f_j}^{(1), hc} S_n^{(0)} \mathcal{H}_n^{(0)}, \\
VV_{n,i}^{(1hc, 1s)} &= \mathcal{H}_n^{(0)\dagger} J_{f_i, f_i}^{(1), hc} S_n^{(1)}(\{\beta_j\}) \mathcal{H}_n^{(0)}, \\
VV_{n,i}^{(1hc)} &= \mathcal{H}_n^{(0)\dagger} J_{f_i, f_i}^{(1), hc} S_n^{(0)} \mathcal{H}_n^{(1)} + \mathcal{H}_n^{(1)\dagger} J_{f_i, f_i}^{(1), hc} S_n^{(0)} \mathcal{H}_n^{(0)},
\end{aligned} \tag{3.20}$$

where we slightly simplified the notation (as compared to eq. (3.12)), by performing, where needed, the trivial integration over the total jet momenta ℓ_i . We also introduced a symbol for the hard-collinear one-loop non-radiative jet

$$J_{f_i, f_i}^{(1), hc} \equiv J_{f_i, f_i}^{(1)}(p_i) - J_{E_i}^{(1)}(\beta_i), \tag{3.21}$$

which is free of ϵ poles of soft origin⁷.

Similarly to the double-virtual case, the explicit infrared poles of the real-virtual correction will be given by

$$\begin{aligned}
RV_{n+1} &= \mathcal{H}_{n+1}^{(0)\dagger} S_{n+1}^{(1)}(\{\beta_i\}) \mathcal{H}_{n+1}^{(0)} + \sum_{i=1}^{n+1} \mathcal{H}_{n+1}^{(0)\dagger} J_{f_i, f_i}^{(1), hc} S_{n+1}^{(0)} \mathcal{H}_{n+1}^{(0)} + \text{finite} \\
&\equiv RV_{n+1}^{(s)} + \sum_{i=1}^n RV_{n+1, i}^{(hc)} + \text{finite},
\end{aligned} \tag{3.22}$$

where, however, one must keep in mind that the finite contributions that we are not displaying in eq. (3.22) will be affected by phase-space singularities, when the radiated particle becomes soft or collinear. These singular contributions, as well as those stemming from the other terms in RV_{n+1} , are subtracted by introducing the local real-virtual counterterm $K_{n+1}^{(\mathbf{RV})}$.

Finding an explicit expression for $K_{n+1}^{(\mathbf{RV})}$ and $K_{n+2}^{(\mathbf{2})}$ requires extending the conditions given in

⁷For gluon jets, note that the subtraction of soft poles involves a single eikonal jet for virtual corrections, as in eq. (3.21), while for the real radiation of two gluons one needs to subtract two eikonal contributions, as in eq. (3.18), since both gluons can independently become soft. The symmetry factor $\varsigma_{f_1 f_2}$ multiplying the phase-space integral in eq. (3.15) is then crucial to compensate for this extra factor of two, ensuring the consistency of the two definitions in eq. (3.21) and in eq. (3.18).

eqs. (3.13-3.15) to two loops. They read

$$S_n^{(2)}(\{\beta_i\}) + \int d\Phi(k_1) S_{n,g}^{(1)}(\{\beta_i\}; k_1) \quad (3.23)$$

$$+ \sum_{f_1, f_2} \varsigma_{f_1 f_2} \int d\Phi(k_1) d\Phi(k_2) S_{n, f_1 f_2}^{(0)}(\{\beta_i\}; k_1, k_2) = \text{finite},$$

$$J_{E_i}^{(2)}(\beta_i) + \int d\Phi(k_1) J_{E_i, g}^{(1)}(\beta_i; k_1) \quad (3.24)$$

$$+ \sum_{f_1, f_2} \varsigma_{f_1 f_2} \int d\Phi(k_1) d\Phi(k_2) J_{E_i, f_1 f_2}^{(0)}(\beta_i; k_1, k_2) = \text{finite},$$

$$\sum_{f_1} \int d\Phi(k_1) J_{f, f_1}^{(2)\alpha\beta}(\ell; k_1) + \sum_{f_1, f_2} \varsigma_{f_1 f_2} \int d\Phi(k_1) d\Phi(k_2) J_{f, f_1 f_2}^{(1)\alpha\beta}(\ell; k_1, k_2) \quad (3.25)$$

$$+ \sum_{f_1, f_2, f_3} \varsigma_{f_1 f_2 f_3} \int d\Phi(k_1) d\Phi(k_2) d\Phi(k_3) J_{f, f_1 f_2 f_3}^{(0)\alpha\beta}(\ell; k_1, k_2, k_3) = \text{finite},$$

where again the flavour sums extend to all final-state flavour combinations compatible with the Feynman rules, as discussed in Section 3.1, and the symmetry factors differ from unity when identical particles are emitted in the final state, as expected. As was the case at NLO, eqs. (3.23-3.25) naturally provide tentative expressions for local counterterms at NNLO, following the logic outlined in Ref. [102]. More specifically, starting from eq. (3.20), and using eqs. (3.23-3.25), one can easily identify the contributions to the double-unresolved counterterm $K_{n+2}^{(2)}$. Such contributions live in the $(n+2)$ -particle phase space, and are thus proportional to a double-radiative jet or soft function, or to the product of a single-radiative soft function and a single-radiative jet function, properly combined into hard-collinear corrections. An example of the first configuration is given by the third term in eq. (3.23), which reproduces the singularities of two *uniformly soft* emissions. Pursuing this line of attack, the double-unresolved counterterm $K_{n+2}^{(2)}$ can be organised according to the soft or hard-collinear character of the radiated particles. We write

$$K_{n+2}^{(2)} = K_{n+2}^{(2, 2s)} + \sum_{i=1}^n \left[K_{n+2, i}^{(2, 2hc)} + \sum_{j=i+1}^n K_{n+2, ij}^{(2, 2hc)} + K_{n+2, i}^{(2, 1hc, 1s)} \right], \quad (3.26)$$

where each term, evaluated at tree level, is defined in a phase space with $n+2$ particles, two of which will become unresolved. As suggested by the notation in eq. (3.26), the two radiations can be both soft (including soft-collinear), or both hard and collinear, in which case they can be associated to either one or two detected particles, or, finally, one of them can be soft while the other one is hard and collinear to one of the Born-level particles⁸. Individual contributions read

$$K_{n+2}^{(2, 2s)}(\{p_i\}, k_1, k_2) = \mathcal{H}_n^{(0)\dagger} \sum_{f_1, f_2} S_{n, f_1 f_2}^{(0)}(\{\beta_i\}; k_1, k_2) \mathcal{H}_n^{(0)}, \quad (3.27)$$

for double-soft emission,

$$K_{n+2, i}^{(2, 2hc)}(\{p_i\}, k_1, k_2, k_3) = \mathcal{H}_n^{(0)\dagger} \sum_{f_1, f_2, f_3} \left[J_{f_i, f_1 f_2 f_3}^{(0), hc} - \sum_{jkl \in \{123, 312, 231\}} J_{E_i, f_j}^{(0)} J_{f_i, f_k f_l}^{(0), hc} \right] S_n^{(0)} \mathcal{H}_n^{(0)}, \quad (3.28)$$

⁸We note that the counterterm in eq. (3.26) is written, in the spirit of our top-down approach, for a fixed set of Born momenta, and with a specific assignment of unresolved momenta. When the subtraction is implemented on the full double-real matrix element, it will be necessary to perform a further sum over the possible assignments of unresolved momenta in the set of $n+2$ final-state particles, in order to account for all singular contributions. Note also that in Ref. [102] the counterterms in eq. (3.26) were written in compact form, keeping the flavour sums implicit, whereas here the flavour structure is given in detail, at the price of a slightly more cumbersome notation.

for double hard-collinear emission from a fixed Born-level particle i ,

$$K_{n+2, ij}^{(2, 2\text{hc})}(\{p_i\}, k_1, k_2, k_3, k_4) = \mathcal{H}_n^{(0)\dagger} \sum_{f_1, f_2, f_3, f_4} J_{f_i, f_1 f_2}^{(0), \text{hc}} J_{f_j, f_3 f_4}^{(0), \text{hc}} S_n^{(0)} \mathcal{H}_n^{(0)} + (i \leftrightarrow j), \quad (3.29)$$

for two hard-collinear emissions from two distinct Born-level particles i and j , and finally

$$K_{n+2, i}^{(2, 1\text{hc}, 1\text{s})}(\{p_i\}, k_1, k_2, k_3) = \mathcal{H}_n^{(0)\dagger} \sum_{f_1, f_2, f_3} \sum_{jkl \in \{123, 312, 231\}} J_{f_i, f_k f_l}^{(0), \text{hc}} S_{n, f_j}^{(0)} \mathcal{H}_n^{(0)}, \quad (3.30)$$

for the joint emission of a soft particle and a hard-collinear particle. Once again, flavour sums extend to all final-state flavour configurations allowed by the Feynman rules, and we introduced the necessary sums over assignments of soft and collinear momenta within the sets of radiated particles; furthermore, we have introduced the definition

$$J_{f_i, f_1 f_2 f_3}^{(0), \text{hc}} \equiv J_{f_i, f_1 f_2 f_3}^{(0)} - \sum_{j \in \{12, 13, 23\}} J_{E_i, f_j f_k}^{(0)}. \quad (3.31)$$

The most intricate case is clearly the double hard-collinear emission from a single Born-level parton, given in eq. (3.28). There, the first term, defined in eq. (3.31) gives the full collinear double emission, with the subtraction of configurations where two of the three final-state particles are soft (the only allowed flavour combinations in this case are $\{f_j, f_k\} = \{g, g\}$ and $\{f_j, f_k\} = \{q, \bar{q}\}$); the second term subtracts configurations where only one final-state particle is soft, while the remaining two particles form a hard-collinear pair: in this case, the soft emission factorises from the hard-collinear one, resulting in a single-radiative eikonal jet, so that f_j must be a gluon. We emphasise that symmetry factors for functions involving the radiation of identical particles, for example a factor of $1/6$ for the jet function $J_{g, ggg}$, must be included in the phase-space measure when the counterterm is integrated, according to eq. (3.25).

We turn next to the real-virtual counterterm $K_{n+1}^{(\text{RV})}$. In order to construct a candidate counterterm in this case, we need to collect all contributions arising from eqs. (3.23-3.25), which are defined in a phase space with n detected particles, involve a single extra unresolved radiation, and have one of the factor functions evaluated at one loop. Note that our goal here is to organise all phase-space singularities of the real-virtual contribution to the cross section, while retaining control of all explicit infrared poles arising in the loop. To this end, we write

$$K_{n+1}^{(\text{RV})} = K_{n+1}^{(\text{RV}, \text{s})} + \sum_{i=1}^n \left[K_{n+1, i}^{(\text{RV}, \text{hc})} + \sum_{j=i+1}^n K_{n+1, ij}^{(\text{RV}, \text{hc})} + K_{n+1, i}^{(\text{RV}, 1\text{hc}, 1\text{s})} + K_{n+1, i}^{(\text{RV}, 1\text{hc})} \right]. \quad (3.32)$$

Importantly, in eq. (3.32) the distinction between soft and hard-collinear radiation applies both to the single real radiation and to the loop correction. Thus, for example, $K_{n+1}^{(\text{RV}, \text{s})}$ collects all terms that have a soft phase-space singularity, possibly accompanied by a pole of soft origin. Therefore we define

$$K_{n+1}^{(\text{RV}, \text{s})} = \mathcal{H}_n^{(0)\dagger} S_{n, g}^{(0)} \mathcal{H}_n^{(1)} + \mathcal{H}_n^{(1)\dagger} S_{n, g}^{(0)} \mathcal{H}_n^{(0)} + \mathcal{H}_n^{(0)\dagger} S_{n, g}^{(1)} \mathcal{H}_n^{(0)}. \quad (3.33)$$

In eq. (3.33), the first two terms have soft singularities arising from soft-gluon emission, accompanied by finite one-loop corrections: thus, they have no explicit poles. The last term contains soft poles, accompanied by soft phase-space singularities. As customary in our approach, we include soft-collinear configurations in the soft sector, both for virtual and for real contributions. Next, we consider hard-collinear configurations associated with the i -th external leg. They are given by

$$\begin{aligned} K_{n+1, i}^{(\text{RV}, \text{hc})} &= \mathcal{H}_n^{(0)\dagger} \sum_{f_1, f_2} \left[J_{f_i, f_1 f_2}^{(1), \text{hc}} - \sum_{kl \in \{12, 21\}} \left(J_{f_i, f_k}^{(1)} - J_{E_i}^{(1)} \right) J_{E_i, f_l}^{(0)} - J_{E_i}^{(1)} J_{f_i, f_1 f_2}^{(0), \text{hc}} \right] S_n^{(0)} \mathcal{H}_n^{(0)}, \\ &= \mathcal{H}_n^{(0)\dagger} \sum_{f_1, f_2} \left[J_{f_i, f_1 f_2}^{(1), \text{hc}} - \sum_{kl \in \{12, 21\}} J_{f_i, f_k}^{(1), \text{hc}} J_{E_i, f_l}^{(0)} - J_{E_i}^{(1)} J_{f_i, f_1 f_2}^{(0), \text{hc}} \right] S_n^{(0)} \mathcal{H}_n^{(0)}, \end{aligned} \quad (3.34)$$

where the first term is defined in eq. (3.18), and we used the fact that $J_{f_i, f_k}^{(1)}$ carries momentum $k_k = k_i$, and is flavour-diagonal, $f_k = f_i$. In the second line of eq. (3.34), the first term in brackets contains the one-loop contributions to all relevant collinear splitting kernels (with a single unresolved radiation). This term is in fact affected by both collinear phase-space singularities and collinear poles, while it is free from singularities and poles of soft origin. The second term subtracts all hard-collinear one-loop virtual poles that are accompanied by soft-collinear phase-space singularities; finally, the third term subtracts hard-collinear phase-space singularities that are accompanied by soft-collinear one-loop poles.

Next, we need to consider the case in which collinear poles and collinear phase-space singularities are associated with different external legs: these contributions are given by

$$K_{n+1, ij}^{(\mathbf{RV}, \text{hc})} = \mathcal{H}_n^{(0)\dagger} J_{f_i, f_i}^{(1), \text{hc}} \sum_{f_1, f_2} J_{f_j, f_1 f_2}^{(0), \text{hc}} S_n^{(0)} \mathcal{H}_n^{(0)} + (i \leftrightarrow j). \quad (3.35)$$

A further contribution accounts for soft phase-space singularities accompanied by hard-collinear virtual poles on leg i , as well as hard-collinear phase-space singularities in emissions from leg i , accompanied by soft virtual poles. It is

$$K_{n+1, i}^{(\mathbf{RV}, \text{1hc}, \text{1s})} = \mathcal{H}_n^{(0)\dagger} \sum_{f_1, f_2} \left[\sum_{kl=\{12, 21\}} J_{f_k, f_k}^{(1), \text{hc}} S_{n, f_l}^{(0)} + J_{f_i, f_1 f_2}^{(0), \text{hc}} S_n^{(1)} \right] \mathcal{H}_n^{(0)}, \quad (3.36)$$

where we used again the fact that the virtual jet is flavour-diagonal, so that $J_{f_k, f_k}^{(1), \text{hc}} = J_{f_i, f_k}^{(1), \text{hc}}$.

Finally, one needs to account for hard-collinear phase-space singularities due to emissions from leg i , accompanied by the finite part of one-loop corrections. These give

$$K_{n+1, i}^{(\mathbf{RV}, \text{1hc})} = \mathcal{H}_n^{(0)\dagger} \sum_{f_1, f_2} J_{f_i, f_1 f_2}^{(0), \text{hc}} S_n^{(0)} \mathcal{H}_n^{(1)} + \mathcal{H}_n^{(1)\dagger} \sum_{f_1, f_2} J_{f_i, f_1 f_2}^{(0), \text{hc}} S_n^{(0)} \mathcal{H}_n^{(0)}. \quad (3.37)$$

The expressions given in eqs. (3.33-3.37) reproduce all the phase-space singularities of eq. (3.22), including those that are not accompanied by virtual poles. Note that only eq. (3.33) and eq. (3.37) contain non-universal one-loop ingredients, which must of course occur at this stage at NNLO. All other contributions are given by universal soft and collinear functions.

To conclude our discussion, the simplest required ingredient at NNLO is the single-unresolved counterterm in the $(n+2)$ -particle phase space, $K_{n+2}^{(1)}$. This has precisely the same form as its NLO counterpart, given in eq. (3.16) and in eq. (3.17), with the replacement $n \rightarrow (n+1)$. Our next goal is therefore to study the double-radiative local counterterms introduced in eqs. (3.27-3.30), in the hierarchical limit in which one of the two radiated particles becomes unresolved at a faster rate with respect to the second one. We expect, and verify below, that in these limits radiative functions *refactorise*, and this feature allows for an easy identification of the remaining local counterterm required for NNLO subtraction, namely $K_{n+2}^{(12)}$.

4 Factorisation of radiative functions in strongly-ordered limits at tree level

It is clear from our discussion in Section 2 that strongly-ordered soft and collinear limits play an increasingly important role for subtraction at higher perturbative orders. For practical purposes, the construction of strongly-ordered counterterms, starting from the corresponding ‘unordered’ ones, is not difficult: one simply needs to take suitable scaling limits on subsets of soft and collinear momenta. It is, however, very interesting to study these limits from an operator point of view, expressing strongly-ordered counterterms in terms of operator matrix elements related to those in

eqs. (3.7-3.9). This would be of significant help when attempting to prove the line-by-line finiteness of subtracted distributions, by means of completeness relations and power-counting arguments. Furthermore, a discussion of the factorisation properties of Wilson-line matrix elements including radiation is of intrinsic interest, and indeed issues of ‘refactorisation’ of soft and collinear cross sections have already arisen in the context of resummation for inclusive rates, for example in Ref. [106]. In this section, we will present a discussion of the factorisation properties of radiative functions, deriving general results at tree level.

To begin our discussion, we note that the jet and soft functions defined in eqs. (3.7-3.9) reproduce the relevant multiple singular configurations in the absence of any hierarchy among unresolved partons. Thus, for example, at NNLO the counterterms derived from these functions are naturally identified as contributions to the unordered counterterm $K_{n+2}^{(2)}$. A procedure is then necessary in order to extract the strongly-ordered configurations entering $K_{n+2}^{(12)}$, and similarly for higher-order counterterms.

4.1 Tree-level radiative soft functions

Consider, as a first example, the case of double-soft radiation at tree level. In the limit in which one of the two radiated soft gluons is much softer than the other, say $k_2 \ll k_1$, the strongly-ordered double-soft current is given by [84]

$$\left[J_{\text{CG}}^{(0), \text{s.o.}} \right]_{\mu_1 \mu_2}^{a_1 a_2} (\{\beta_i\}; k_1, k_2) = \left(J_{\mu_2}^{(0) a_2}(k_2) \delta^{a_1 a} + i g_s \mu^\epsilon f^{a_1 a_2 a} \frac{k_{1, \mu_2}}{k_1 \cdot k_2} \right) J_{\mu_1, a}^{(0)}(k_1), \quad (4.1)$$

where

$$J_\mu^{(0) a}(k) = g_s \mu^\epsilon \sum_{i=1}^n \frac{\beta_{i, \mu}}{\beta_i \cdot k} \mathbf{T}_i^a \quad (4.2)$$

is the single-gluon tree-level soft current. Notice that it is a colour matrix, so that the ordering in eq. (4.1) is fixed. This expression can of course be obtained from factorisation by considering the tree-level double-radiative soft function $\mathcal{S}_{n, gg}^{(0)}(\{\beta_i\}; k_1, k_2)$, stripping off the two gluon polarisation vectors, rescaling k_2 by a factor ξ_2 , and retaining only the leading power in the limit $\xi_2 \rightarrow 0$. As discussed above, however, it is desirable to give a definition of strongly-ordered soft operators without resorting to an *a posteriori* limit operation on unordered configurations: this can be achieved by applying soft factorisation in an iterative fashion.⁹

The key idea is that, in the limit $k_2 \ll k_1 \ll \mu$, with μ a typical hard scale of the process, gluon 1 (corresponding to momentum k_1) is soft with respect to the n hard Born partons, but, in turn, is seen as a hard parton if probed by gluon 2 (with momentum k_2). This implies that the soft emission of gluon 1 is described by a soft current featuring n Wilson lines, corresponding to the Born partons, while the emission of gluon 2 is represented by a soft current featuring $n + 1$ Wilson lines: one of these (in the adjoint representation) corresponds to gluon 1. In the language of factorisation, we may apply the standard techniques of the soft approximation to the matrix element $\mathcal{S}_{n, gg}^{(0)}(\beta_i; k_1, k_2)$, in the limit when gluon 2 is softer than all other particles. In this limit, such a matrix element factorises, and the resulting soft function is, as expected, a Wilson-line correlator, where gluon 2 is still treated as a final-state parton, while gluon 1 has been replaced by a Wilson line in the adjoint representation¹⁰. This factorisation leaves behind a ‘hard’ function which, consistently, is given by the Wilson line correlator for the radiation of gluon 1 from the n hard Born-level partons. This tree-level factorisation is represented pictorially in Fig. 1, in the simplified case with $n = 2$.

⁹We emphasise that strongly-ordered soft emission to leading IR accuracy was already investigated in Ref. [107, 108], where both real and virtual emission contributions are discussed.

¹⁰One could perhaps describe this factorisation by saying that the harder gluon has ‘Wilsonised’, becoming a classical source for all much softer radiation.

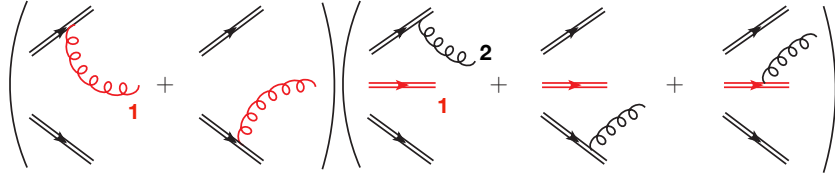


Figure 1: The factorisation of an eikonal form factor, illustrated for the case of two hard lines and strongly-ordered double-soft radiation.

In formulae, the natural definition for a strongly-ordered tree-level double-soft radiative function, which we denote by $\mathcal{S}_{n;g,g}^{(0)}$, is thus

$$\begin{aligned}
\left[\mathcal{S}_{n;g,g}^{(0)} \right]_{\{d_i e_i\}}^{a_1 a_2} (\{\beta_i\}; k_1, k_2) &\equiv \langle k_2, a_2 | T \left[\Phi_{\beta_{k_1}}^{a_1 b}(0, \infty) \prod_{i=1}^n \Phi_{\beta_i, d_i}^{c_i}(\infty, 0) \right] | 0 \rangle \\
&\quad \times \langle k_1, b | T \left[\prod_{i=1}^n \Phi_{\beta_i, c_i e_i}(\infty, 0) \right] | 0 \rangle \Big|_{\text{tree}} \\
&= \left[\mathcal{S}_{n+1,g}^{(0)} \right]_{\{d_i c_i\}}^{a_2, a_1 b} (\beta_{k_1}, \{\beta_i\}; k_2) \left[\mathcal{S}_{n,g}^{(0)} \right]_{b, \{c_i e_i\}} (\{\beta_i\}; k_1), \quad (4.3)
\end{aligned}$$

where, in the first line, one recognises the factorised emission amplitude of gluon 2 off $n+1$ Wilson lines, multiplied times the radiation of gluon 1 off n Born-level Wilson lines (the second line). For clarity, in eq. (4.3) we have written explicitly all colour indices: one sees that the first eikonal form factor, involving $n+1$ Wilson lines, acts as a colour operator on the second form factor, with the adjoint index b of the Wilson line associated with gluon 1 contracting with the index of the gluon state in the second line. It is straightforward to verify that Eq. (4.3) yields precisely

$$\left[\mathcal{S}_{n;g,g}^{(0)} \right]^{a_1 a_2} (\{\beta_i\}; k_1, k_2) = \epsilon^{* \mu_1}(k_1) \epsilon^{* \mu_2}(k_2) \left[J_{\text{CG}}^{(0), \text{s.o.}} \right]_{\mu_1 \mu_2}^{a_1 a_2} (\{\beta_i\}; k_1, k_2). \quad (4.4)$$

The strongly-ordered double-soft counterterm $K_{n+2}^{(\mathbf{12}, \text{s})}$ is then obtained by squaring eq. (4.3), in the spirit of eq. (3.16).

By iterating this factorisation procedure, one may define the strongly-ordered triple-soft current, in the kinematic limit $k_3 \ll k_2 \ll k_1 \ll \mu$, as

$$\begin{aligned}
\left[\mathcal{S}_{n;g,g,g}^{(0)} \right]_{\{f_i e_i\}}^{a_1 a_2 a_3} (\{\beta_i\}; k_1, k_2, k_3) &\equiv \left[\mathcal{S}_{n+2,g}^{(0)} \right]_{\{f_i d_i\}, a_1 b_1, a_2 b_2}^{a_3} \left[\mathcal{S}_{n+1,g}^{(0)} \right]_{\{d_i c_i\}, b_1 g_1}^{b_2} \left[\mathcal{S}_{n,g}^{(0)} \right]_{\{c_i e_i\}}^{g_1} \\
&= \langle k_3, a_3 | T \left[\Phi_{\beta_{k_1}}^{a_1 b_1}(\infty, 0) \Phi_{\beta_{k_2}}^{a_2 b_2}(\infty, 0) \prod_{i=1}^n \Phi_{\beta_i}^{f_i d_i}(\infty, 0) \right] | 0 \rangle \\
&\quad \times \langle k_2, b_2 | T \left[\Phi_{\beta_{k_1}}^{b_1 g_1}(0, \infty) \prod_{i=1}^n \Phi_{\beta_i}^{d_i c_i}(\infty, 0) \right] | 0 \rangle \\
&\quad \times \langle k_1, g_1 | T \left[\prod_{i=1}^n \Phi_{\beta_i}^{c_i e_i}(\infty, 0) \right] | 0 \rangle \Big|_{\text{tree}}, \quad (4.5)
\end{aligned}$$

where, on top of the double radiation already detailed in eq. (4.3), we recognise in second line the emission of the softest gluon 3 (with momentum k_3) from a set of $n+2$ Wilson lines, two of which are ‘Wilsonised’ versions of gluons 1 and 2. Eq. (4.5) yields a natural generalisation to the case of

triple radiation of the strongly-ordered two-gluon eikonal form factor given in eq. (4.4),

$$\begin{aligned}
\left[\mathcal{S}_{n;g,g,g}^{(0)} \right]^{a_1 a_2 a_3} &= \epsilon_{\mu_3}^*(k_3) \epsilon_{\mu_2}^*(k_2) \epsilon_{\mu_1}^*(k_1) \\
&\times \left[J_{a_3}^{\mu_3}(k_3) \delta^{a_1 b_1} \delta^{a_2 b_2} + i g_s \mu^\epsilon f^{a_1 a_3 b_1} \delta^{a_2 b_2} \frac{k_1^{\mu_3}}{k_1 \cdot k_3} + i g_s \mu^\epsilon f^{a_2 a_3 b_2} \delta^{a_1 b_1} \frac{k_2^{\mu_3}}{k_2 \cdot k_3} \right] \\
&\times \left[J_{b_2}^{\mu_2}(k_2) \delta^{b_1 c_1} + i g_s \mu^\epsilon f^{b_1 b_2 c_1} \frac{k_1^{\mu_2}}{k_1 \cdot k_2} \right] J_{c_1}^{\mu_1}(k_1), \tag{4.6}
\end{aligned}$$

in complete agreement with the strongly-ordered limit of the triple-soft current presented in Ref. [95]. Based on the above physically motivated discussion, and on the explicit form of the strongly-ordered currents for up to three soft radiations at tree-level, it is natural to build an ansatz for the strongly-ordered eikonal form factor for the radiation of m gluons with momenta $k_m \ll k_{m-1} \ll \dots \ll k_1 \ll \mu$. We write

$$\begin{aligned}
\left[\mathcal{S}_{n;g,\dots,g}^{(0)} \right]_{\{b_{1,\ell} b_{m+1,\ell}\}}^{a_{1,1} \dots a_{1,m}} &\equiv \prod_{i=1}^m \langle k_{m-i+1}, a_{i,m-i+1} | T \left[\prod_{p=1}^{m-i} \Phi_{\beta k_p}^{a_{i,p} a_{i+1,p}}(\infty, 0) \prod_{\ell=1}^n \Phi_{\beta \ell}^{b_{i,\ell} b_{i+1,\ell}}(\infty, 0) \right] | 0 \rangle \Big|_{\text{tree}} \\
&= \prod_{i=1}^m \left[\mathcal{S}_{n+m-i,g}^{(0)} \right]_{\{b_{i,\ell} b_{i+1,\ell}\}, a_{i,1} a_{i+1,1}, \dots, a_{i,m-i} a_{i+1,m-i}}^{a_{i,m-i+1}} \\
&= \prod_{i=1}^m \epsilon_{\mu_{m-i+1}}^*(k_{m-i+1}) \left[J_{a_{i,m-i+1}}^{\mu_{m-i+1}}(k_{m-i+1}) \prod_{p=1}^{m-i} \delta^{a_{i,p} a_{i+1,p}} \right. \\
&\quad \left. + i g_s \mu^\epsilon \sum_{r=1}^{m-i} \frac{k_r^{\mu_{m-i+1}}}{k_r \cdot k_{m-i+1}} f^{a_{i,r} a_{i,m-i+1} a_{i+1,r}} \prod_{\substack{j=1 \\ j \neq r}}^{m-i} \delta^{a_{i,j} a_{i+1,j}} \right], \tag{4.7}
\end{aligned}$$

which reduces to eq. (4.3) and eq. (4.5) for $m = 2$ and $m = 3$, respectively. We point out that the factorisation arguments presented for the totally ordered configuration $k_m \ll k_{m-1} \ll \dots \ll k_1 \ll \mu$ generalise to less hierarchical kinematics, in which for instance q among the radiated gluons have comparable softness: in such a case, the corresponding sequence of q single-radiative form factors is replaced by a single form factor radiating q gluons.

While the analysis above has focused on tree-level soft functions, the underlying physics, and the fact that the discussion can be phrased in terms of operator matrix elements, strongly suggests that the structure of the proposed factorisations can be extended to higher orders, upon retaining hard-collinear and finite loop contributions, as well as including renormalisation factors. Indeed, the fact that the softest radiation can be factorised from the remaining (harder) ones, in terms of a soft function, where harder radiated gluons have ‘Wilsonised’, follows from the standard rules of the soft approximation, and Ward identities could be applied, where appropriate, since the original eikonal form factor is gauge invariant. These qualitative arguments can be verified at one-loop by examining the strongly-ordered limit of the one-loop current for the radiation of two soft gluons [97, 99, 109], and indeed one recovers a natural generalisation of eq. (4.3), which we briefly discuss below in Section 5. Notwithstanding this strong check, a proper generalisation to all orders of a nested factorisation such as eq. (4.7) would require a thorough analysis, which is left for future work.

4.2 Tree-level radiative jet functions

Strongly-ordered collinear configurations need to be analysed next. Let us consider, for instance, the triple-collinear configuration corresponding to a kinematic situation in which three partons i , j , k become collinear, with relative angles $\theta_{ij}, \theta_{ik}, \theta_{jk} \rightarrow 0$, but with two partons displaying a dominant collinearity, say $\theta_{ij} \ll \theta_{ik}, \theta_{jk}$. It is known that the strongly-ordered collinear limit of

squared scattering amplitudes factorises into products of Altarelli-Parisi kernels, which are matrices in spin space. For instance, the NNLO strongly-ordered collinear configuration for a $q \rightarrow q'_1 \bar{q}'_2 q_3$ branching is given by

$$\lim_{\theta_{12} \ll \theta_{13} \rightarrow 0} RR_{n+2} = \frac{(8\pi\alpha_s)^2}{s_{12} s_{[12]3}} P_{q \rightarrow gq}^{\rho\sigma}(z_{[12]}, q_\perp) d_{\rho\mu}(k_{[12]}) P_{g \rightarrow q\bar{q}}^{\mu\nu}\left(\frac{z_1}{z_{[12]}}, k_\perp\right) d_{\sigma\nu}(k_{[12]}) B_n, \quad (4.8)$$

where the intermediate-particle momentum is $k_{[12]} \equiv k_1 + k_2$, its collinear energy fraction is $z_{[12]} \equiv z_1 + z_2 = 1 - z_3$, and $s_{[12]3} = 2 k_{[12]} \cdot k_3$. Finally,

$$d_{\mu\nu}(k_{[12]}) = -g_{\mu\nu} + \frac{k_{[12]\mu} n_\nu + k_{[12]\nu} n_\mu}{k_{[12]} \cdot n}, \quad (4.9)$$

with $n^2 = 0$, represents the gluon polarisation sum. The momenta q_\perp and k_\perp in the splitting kernels specify the transverse directions for the successive branchings, $q \rightarrow g_{[12]} q_3$ and $g_{[12]} \rightarrow q'_1 \bar{q}'_2$, respectively: their definitions follow from the Sudakov parametrisation of momenta k_i ($i = 1, 2, 3$), according to

$$k_i^\mu = z_i p^\mu + k_{\perp i} - \frac{k_{\perp i}^2}{z_i} \frac{n^\mu}{2p \cdot n}, \quad q_\perp = k_{\perp 3}, \quad k_\perp = z_2 k_{\perp 1} - z_1 k_{\perp 2}. \quad (4.10)$$

The kernel $P_{q \rightarrow gq}^{\rho\sigma}$ describes the first splitting of a parent quark into a quark-gluon pair, with gluon spin indices un-contracted. As such, it represents the spin matrix acting on the subsequent splitting of the virtual gluon in a quark-antiquark pair, described by $P_{g \rightarrow q\bar{q}}^{\mu\nu}$. The explicit form of the relevant kernels is

$$P_{g \rightarrow q\bar{q}}^{\mu\nu}(z, k) = T_R \left(-g^{\mu\nu} + 4z(1-z) \frac{k^\mu k^\nu}{k^2} \right), \quad P_{q \rightarrow gq}^{\rho\sigma}(z, k) = \frac{C_F}{2T_R} z P_{g \rightarrow q\bar{q}}^{\rho\sigma}(1/z, k). \quad (4.11)$$

Our goal is now to express such collinear refactorisations by means of radiative jet functions. This can be done without any loss of information, since the jet functions defined in eq. (3.8) retain full dependence on gluon (as well as quark) spin. As a first example, the strongly-ordered triple-collinear kernel in eq. (4.8) can be rewritten in the factorisation language as

$$\begin{aligned} \int \frac{d^d \ell}{(2\pi)^d} \left[\lim_{\theta_{12} \ll \theta_{13} \rightarrow 0} J_{q, q' \bar{q}'}^{(0)}(\ell; k_1, k_2, k_3) \right] &\equiv \int \frac{d^d \ell}{(2\pi)^d} J_{q, gq; g, q' \bar{q}'}^{(0)}(\ell; k_1, k_2, k_3) \\ &= \int \frac{d^d \ell}{(2\pi)^d} J_{q, gq}^{;\rho\sigma(0)}(\ell; k_{[12]}, k_3) \int \frac{d^d \ell'}{(2\pi)^d} J_{g, q' \bar{q}'}^{\rho\sigma(0)}(\ell'; k_1, k_2), \end{aligned} \quad (4.12)$$

where the first line sets up the notation for a strongly-ordered jet function, specifying the sequential splittings involved. The integrals over $d^d \ell$ and $d^d \ell'$ just serve the purpose of resolving the Dirac delta-function constraints contained in the definition of jet functions, which in turn fix the momentum of the splitting parton to equal the momentum sum of its decay products. Note also that in $J_{q, gq}^{;\rho\sigma(0)}$ we have left implicit the spin indices associated with the parent quark, to lighten the notation. The semicolon serves as a marker for this implicit dependence, and Lorentz spin indices after semicolon are associated to the daughter gluon created by the splitting. Conversely, in the secondary branching described by $J_{g, q' \bar{q}'}^{\rho\sigma(0)}$ the Lorentz indices are related to the splitting gluon. It is not difficult to verify that, upon retaining the leading-power contribution in the transverse momenta, the radiative quark jet $J_{q, gq}^{;\rho\sigma(0)}$ yields the $P_{q \rightarrow gq}^{\rho\sigma}$ kernel of (4.8), while the factor $J_{g, q' \bar{q}'}^{\rho\sigma(0)}$ reproduces the product $d_\mu^\rho P_{g \rightarrow q\bar{q}}^{\mu\nu} d_\nu^\sigma$.

The factorisation of other flavour combinations in strongly-ordered limits follows the same lines, upon keeping proper track of the relevant Dirac or Lorentz indices. As an example, we consider the case of the strongly-ordered splitting $q \rightarrow qgg$, which we display in the abelian limit for simplicity

(non-abelian terms follow the same kinematic pattern). This limit is described by the factorised formula

$$\begin{aligned} \int \frac{d^d \ell}{(2\pi)^d} \left[\lim_{\theta_{12} \ll \theta_{13} \rightarrow 0} J_{q,ggg}^{(\text{ab}) (0)}(\ell; k_1, k_2, k_3) \right] &\equiv \int \frac{d^d \ell}{(2\pi)^d} J_{q,gg;g,gg}^{(0)}(\ell; k_1, k_2, k_3) \\ &= \int \frac{d^d \ell}{(2\pi)^d} J_{q,gg}^{\alpha\beta (0)}(\ell; k_{[12]}, k_3) \int \frac{d^d \ell'}{(2\pi)^d} J_{q,gg}^{\alpha\beta (0)}(\ell'; k_1, k_2), \end{aligned} \quad (4.13)$$

where α and β are now Dirac indices. The only case featuring a further complication involves a gluon splitting into gluons: in fact, this requires keeping track of the Lorentz indices of both the parent and the sibling gluons. For instance we find

$$\begin{aligned} \int \frac{d^d \ell}{(2\pi)^d} \left[\lim_{\theta_{12} \ll \theta_{13} \rightarrow 0} J_{g,ggg}^{\mu\nu (0)}(\ell; k_1, k_2, k_3) \right] &\equiv \int \frac{d^d \ell}{(2\pi)^d} J_{g,gg;g,gg}^{\mu\nu (0)}(\ell; k_1, k_2, k_3) \\ &= \int \frac{d^d \ell}{(2\pi)^d} J_{g,gg}^{\mu\nu;\rho\sigma (0)}(\ell; k_{[12]}, k_3) \int \frac{d^d \ell'}{(2\pi)^d} J_{g,gg}^{\rho\sigma (0)}(\ell'; k_1, k_2), \end{aligned} \quad (4.14)$$

where the four-index jet $J_{g,gg}^{\mu\nu;\rho\sigma (0)}$ is defined by

$$J_{g,gg}^{\mu\nu;\rho\sigma (0)}(\ell; k_a, k_b) = \sum_{\lambda_a, \lambda_b} \int d^d x e^{i\ell \cdot x} \left(\mathcal{J}_{g,gg}^{\mu;\rho (0)}(0; \{k_j, \lambda_j\}) \right)^\dagger \mathcal{J}_{g,gg}^{\nu;\sigma (0)}(x; \{k_j, \lambda_j\}), \quad (4.15)$$

and $\mathcal{J}_{g,gg}^{\nu;\sigma (0)}$ satisfies

$$\mathcal{J}_{g,gg}^{\nu (0)}(x; k_a, k_b; \lambda_a, \lambda_b) = \mathcal{J}_{g,gg}^{\nu;\sigma (0)}(x; k_a, k_b; \lambda_a, \lambda_b) \epsilon_\sigma^{*(\lambda_a)}(k_a). \quad (4.16)$$

We emphasise that eqs. (4.12)-(4.14) have been found by explicitly computing the limits of the two-radiative jet functions.

This factorised structure can be generalised to the case of an arbitrary number of collinear emissions, all strongly ordered. Introducing appropriate notation, such limits can be described by the expression

$$\begin{aligned} \int \frac{d^d \ell}{(2\pi)^d} \left[\lim_{\theta_1 \ll \theta_2 \ll \dots \ll \theta_{m-1} \rightarrow 0} J_{f,f_1 \dots f_m}^{IJ (0)}(\ell; k_1, \dots, k_m) \right] \\ \equiv \int \frac{d^d \ell}{(2\pi)^d} J_{f,a_1 b_1, \dots, a_m b_m}^{IJ (0)}(\ell; k_1, \dots, k_m) \\ = \prod_{j=1}^{m-1} \int \frac{d^d \ell_j}{(2\pi)^d} J_{p_j, a_j b_j}^{I_{p_j} J_{p_j}; I_{a_j} J_{a_j}}^{(0)}(\ell_j; k_{a_j}, k_{b_j}). \end{aligned} \quad (4.17)$$

The labels in the previous equation are constructed as follows. Partons $a_1, b_1 \in \{1, \dots, m\}$, stemming from the splitting of parent particle p_1 , are those emitted with the smallest relative angle among all, θ_1 . If the next-to-smallest independent relative angle, θ_2 , is the one connecting partons $c, d \in \{1, \dots, \cancel{a}_1, \dots, \cancel{b}_1, \dots, m\}$, then $a_2 = c$ and $b_2 = d$. Otherwise, if θ_2 connects $c \in \{1, \dots, \cancel{a}_1, \dots, \cancel{b}_1, \dots, m\}$ with either a_1 or b_1 , then $a_2 = c$ and $b_2 = [a_1 b_1] = p_1$. Iteratively, proceeding by larger and larger relative angles θ_j , with $j \leq m-1$, a_j is assigned in the set $\{1, \dots, m\}$ deprived of all a_k, b_k with $k < j$; if θ_j connects a_j to a yet unassigned parton, the latter then gets labelled as b_j , otherwise b_j is labelled as the ancestor of the cluster of partons to which a_j is linked by θ_j . Parent p_j is $[a_j b_j]$, understanding the iterative rule $[a[bc]] = [abc]$ and so on. Finally, indices $I_{p_j} J_{p_j}$ ($I_{a_j} J_{a_j}$) are the Lorentz or Dirac indices of the j -th parent (first sibling), with the constraint $I_{p_1} J_{p_1} = IJ$. Once again, situations in which not all collinear splittings are strongly ordered, but rather successive clusters of $k > 2$ particles are produced with parametrically similar collinearities, can be described by analogous factorisations. This is not difficult to achieve case by case, while writing down a general formula for this would involve rather cumbersome notations.

5 Factorisation of single-radiative functions at one loop

Extending the discussion of Section 4 to loop level is non-trivial. Virtual corrections involve loop momenta which are unconstrained: thus they may, and do, carry soft, collinear and ultraviolet enhancements, which will eventually survive strongly-ordered limits. These enhancements will have to be properly identified and analysed, as they will impact the connection between strongly-ordered and real-virtual counterterms. Our strategy will be to treat the matrix elements defining radiative soft and jet functions as generalised scattering amplitudes: we will then conjecture natural expressions for their factorisations, and verify that they hold at one loop.

5.1 Single-radiative soft function at one loop

We consider first the single-radiative eikonal form factor defined by eq. (3.3) with $m = 1$. This amplitude-level radiative soft function is in fact, on its own accord, a scattering amplitude in the presence of Wilson lines acting as sources. As such, the following factorisation ansatz, along the lines set in eq. (3.1), is expected to hold:¹¹

$$\mathcal{S}_{n,g}(\{\beta_i\}; k) = \mathcal{S}_{n+1}(\{\beta_i\}, \beta_k) \frac{\mathcal{J}_{g,g}^\mu(0; k)}{\mathcal{J}_{E_g}(\beta_k)} \mathcal{S}_{n,g}^{\mathcal{H},\mu}(\{\beta_i\}; k). \quad (5.1)$$

Note that, at variance with previous sections, in eq. (5.1) we have dropped the dependence on the polarisation of the emitted gluon, since it is not relevant for the present discussion. This dependence is encoded on the *l.h.s.* in the definition of $\mathcal{S}_{n,g}$, and on the *r.h.s.* in the definition of $\mathcal{J}_{g,g}^\alpha$. The first factor in eq. (5.1) contains the virtual soft poles of an $(n+1)$ -point amplitude, while the jet ratio contains hard-collinear virtual poles associated with the radiated gluon. The factor $\mathcal{S}_{n,g}^{\mathcal{H},\mu}(\{\beta_i\}; k)$ encodes all loop contributions to the radiative soft function that are finite as $\epsilon \rightarrow 0$: thus, it describes hard wide-angle virtual contribution to the soft real radiation of gluon g off a set of n hard legs. Finally, observe that, starting from eq. (3.1), one might have expected further hard collinear factors in eq. (5.1), associated with the n Wilson lines along the directions β_i : these factors however are all equal to one, since the jet functions in the numerators coincide with their soft approximations, given by the eikonal jet functions in the denominators.

At NLO, the factorisation in eq. (5.1) leads to

$$\begin{aligned} \mathcal{S}_{n,g}^{(1)}(\{\beta_i\}; k) &= \left[\mathcal{S}_{n+1}^{(1)}(\{\beta_i\}, \beta_k) - \mathcal{J}_{E_g}^{(1)}(\beta_k) \right] \mathcal{S}_{n,g}^{(0)}(\{\beta_i\}; k) \\ &\quad + \mathcal{J}_{g,g}^{(1)\mu}(0; k) \mathcal{S}_{n,g}^{(0)\mu}(\{\beta_i\}; k) + \text{finite}, \end{aligned} \quad (5.2)$$

where we used the fact that at tree level $\mathcal{S}_{n,g}^{\mathcal{H},\mu}$ coincides with the full tree level radiative soft function $\mathcal{S}_{n,g}^{(0)}$ after contracting with the appropriate polarisation vector.

We can now proceed to verify eq. (5.2). We start with the known expressions for the relevant soft functions. At tree level, the radiative soft function gives

$$\left[\mathcal{S}_{n,g}^{(0)}(\{\beta_i\}; k) \right]^a = g_s \mu^\epsilon \sum_{i=1}^n \frac{\beta_i \cdot \epsilon_\lambda(k)}{\beta_i \cdot k} \mathbf{T}_i^a, \quad (5.3)$$

where μ is the $\overline{\text{MS}}$ renormalisation scale, including the appropriate correction for contributions proportional to γ_E and $\ln 4\pi$, and g_s is the bare strong coupling. The one-loop contribution to the

¹¹The jet functions, defined in eqs.(3.4-3.5), can be evaluated at $x = 0$ in this case, without loss of generality.

virtual soft function for $(n + 1)$ particles, on the other hand, reads (see for instance [69])

$$\begin{aligned} \left[\mathcal{S}_{n+1}^{(1)}(\{\beta_i\}, \beta_k) \right]^{ab} &= \frac{\alpha_s}{4\pi} \sum_{\substack{i,j=1 \\ i \neq j}}^n \mathbf{T}_i \cdot \mathbf{T}_j \delta^{ab} \left[\frac{1}{\epsilon^2} - \frac{1}{\epsilon} \ln \frac{2p_i \cdot p_j}{\mu^2} \right] \\ &+ \frac{\alpha_s}{2\pi} \sum_{i=1}^n \mathbf{T}_i \cdot (\mathbf{T}_k)^{ab} \left[\frac{1}{\epsilon^2} - \frac{1}{\epsilon} \ln \frac{2p_i \cdot k}{\mu^2} \right], \end{aligned} \quad (5.4)$$

where $p_i = \mu/\sqrt{2}\beta_i$, and we have understood the gluon with momentum k to be at position $n + 1$, *i.e.* $p_{n+1} = k$, we wrote explicitly the colour indices of the Wilson line associated with that gluon, and all poles in ϵ are of purely soft origin. Since eq. (5.4) is the leading-order term for the virtual soft function, the coupling α_s can equivalently be taken to be bare or renormalised, without affecting the argument below.

The first term of eq. (5.2) is found by multiplying eq. (5.3) to the right of eq. (5.4). Importantly, one can show that

$$\mathcal{S}_{n+1}^{(1)}(\{\beta_i\}, \beta_k) \mathcal{S}_{n,g}^{(0)}(\{\beta_i\}; k) = \mathcal{S}_{n,g}^{(0)}(\{\beta_i\}; k) \mathcal{S}_n^{(1)}(\{\beta_i\}) + \varepsilon_\lambda(k) \cdot J_{\text{CG}}^{(1),b}(\{\beta_i\}; k), \quad (5.5)$$

where $J_{\text{CG}}^{(1),b}$ is the bare one-loop Catani-Grazzini (CG) soft-gluon current for final-state radiation [87], given by

$$J_{\text{CG}}^{(1),b,\mu}(\{\beta_i\}; k) = -\frac{\alpha_s}{4\pi} g_s \mu^\epsilon i f^{abc} \sum_{i,j=1}^n \mathbf{T}_i^b \mathbf{T}_j^c \frac{1}{\epsilon^2} \left(\frac{\beta_i^\mu}{\beta_i \cdot k} - \frac{\beta_j^\mu}{\beta_j \cdot k} \right) \left(\frac{\mu^2 p_i \cdot p_j}{2 p_i \cdot k p_j \cdot k} \right)^\epsilon. \quad (5.6)$$

Eq. (5.4) is useful because the combination $\mathcal{S}_{n,g}^{(0)} \mathcal{S}_n^{(1)}$ appears in the one-loop renormalised radiative amplitude $\mathcal{A}_{n,1}^{(1)}$

$$\begin{aligned} \mathcal{A}_{n,1}^{(1)}(\{p_i\}; k) &= \mathcal{S}_{n,g}^{(0)}(\{\beta_i\}; k) \sum_{i=1}^n \left[\mathcal{J}_i^{(1)}(\{p_i\}) - \mathcal{J}_{E_i}^{(1)}(\{\beta_i\}) \right] \mathcal{H}_n^{(0)}(\{p_i\}) \\ &+ \mathcal{S}_{n,g}^{(0)}(\{\beta_i\}; k) \mathcal{H}_n^{(1)}(\{p_i\}) + \mathcal{S}_{n,g}^{(1)}(\{\beta_i\}; k) \mathcal{H}_n^{(0)}(\{p_i\}) \\ &= \mathcal{S}_{n,g}^{(0)}(\{\beta_i\}; k) \mathcal{A}_n^{(1)}(\{p_i\}) \\ &+ \left[\mathcal{S}_{n,g}^{(1)}(\{\beta_i\}; k) - \mathcal{S}_{n,g}^{(0)}(\{\beta_i\}; k) \mathcal{S}_n^{(1)}(\{\beta_i\}) \right] \mathcal{A}_n^{(0)}(\{p_i\}), \end{aligned} \quad (5.7)$$

where $\mathcal{A}_n^{(0)} = \mathcal{H}_n^{(0)}$. We can now compare eq. (5.7) to the equivalent formulation from [87]: in that approach one writes

$$\mathcal{A}_{n,1}^{(1)}(\{p_i\}; k) = \varepsilon_\lambda(k) \cdot \left[J_{\text{CG}}^{(0)}(\{\beta_i\}; k) \mathcal{A}_n^{(1)}(\{p_i\}) + J_{\text{CG}}^{(1),r}(\{\beta_i\}; k) \mathcal{A}_n^{(0)}(\{p_i\}) \right], \quad (5.8)$$

where $J_{\text{CG}}^{(0)}$ is equal to the expression in eq. (5.3). We note that all quantities in eq. (5.8) are renormalised, and in particular we now feature the *renormalised* CG current $J_{\text{CG}}^{(1),r}$. Thus we can identify

$$\varepsilon_\lambda(k) \cdot J_{\text{CG}}^{(1),r}(\{\beta_i\}; k) = \mathcal{S}_{n,g}^{(1)}(\{\beta_i\}; k) - \mathcal{S}_{n,g}^{(0)}(\{\beta_i\}; k) \mathcal{S}_n^{(1)}(\{\beta_i\}). \quad (5.9)$$

Then, using (5.5), we have

$$\begin{aligned} \mathcal{S}_{n,g}^{(1)}(\{\beta_i\}; k) &= \mathcal{S}_{n+1}^{(1)}(\{\beta_i\}, \beta_k) \mathcal{S}_{n,g}^{(0)}(\{\beta_i\}; k) + \left[J_{\text{CG}}^{(1),r}(\{\beta_i\}; k) - J_{\text{CG}}^{(1),b}(\{\beta_i\}; k) \right] \cdot \varepsilon_\lambda(k) \\ &= \mathcal{S}_{n+1}^{(1)}(\{\beta_i\}, \beta_k) \mathcal{S}_{n,g}^{(0)}(\{\beta_i\}; k) - \frac{\alpha_s}{4\pi} \frac{b_0}{2\epsilon} J_{\text{CG}}^{(0)}(\{\beta_i\}; k) \cdot \varepsilon_\lambda(k) \\ &= \left[\mathcal{S}_{n+1}^{(1)}(\{\beta_i\}, \beta_k) - \frac{\alpha_s}{4\pi} \frac{b_0}{2\epsilon} \right] \mathcal{S}_{n,g}^{(0)}(\{\beta_i\}; k), \end{aligned} \quad (5.10)$$

where $b_0 = (11C_A - 4T_R n_f)/3$ in our normalisation, with n_f being the number of active flavours in the process. Eq. (5.10) is actually equivalent to eq. (5.2), which we set out to prove: indeed, the second term in the last line is the hard-collinear contribution from the radiated gluon, *i.e.* the contribution arising from the ratio of the two jet functions in eq. (5.2). Such a ratio is computed for instance in Ref. [110] (see eqs. (2.21) and (2.26) there). The β -function coefficient b_0 arises in this context as the anomalous dimension of the gluon jet function.¹² We note that the result in eq. (5.10) is compatible with the soft factorisation displayed in eq. (4.3) upon converting the softer real gluon into a soft virtual radiation, namely selecting soft loops only.

In order to apply these ideas to subtraction, we need to explore what happens at cross-section level. In order to do this, we begin by examining the general expression of the real-virtual contribution to the cross section, RV_{n+1} , in the limit in which the emitted gluon k becomes soft. The corresponding kernel features explicit soft and hard-collinear poles relevant to all $n+1$ external legs. When comparing it with the cross-section-level version of eq. (5.2), we then expect the two expressions to differ by the hard-collinear poles associated with all particles but the radiated gluon. This expectation is verified in the following.

The soft limit of RV_{n+1} in the $\overline{\text{MS}}$ scheme can be found in Refs. [15, 86, 87, 111, 112], and reads¹³

$$\mathbf{S}_k RV_{n+1} = -\mathcal{N}_1 \delta_{f_k g} \sum_{\substack{i \neq k \\ j \neq i, k}} \mathcal{I}_{ij}^{(k)} \left[V_{n,ij} - \left(\mathcal{N}_1 c_\Gamma \frac{C_A}{\epsilon} \pi \cot(\pi\epsilon) \left(\mathcal{I}_{ij}^{(k)} \right)^\epsilon + \frac{\alpha_s}{4\pi} \frac{b_0}{\epsilon} \right) B_{n,ij} \right. \\ \left. + \mathcal{N}_1 c_\Gamma \frac{2\pi}{\epsilon} \sum_{p \neq i, j, k} \left(\mathcal{I}_{jp}^{(k)} \right)^\epsilon B_{n,ijp} \right], \quad (5.11)$$

where the colour-correlated Born and virtual contributions are defined by $B_{n,ij} = \mathcal{A}_n^{(0)\dagger}(\mathbf{T}_i \cdot \mathbf{T}_j) \mathcal{A}_n^{(0)}$ and by $V_{n,ij} = 2\text{Re}[\mathcal{A}_n^{(0)\dagger}(\mathbf{T}_i \cdot \mathbf{T}_j) \mathcal{A}_n^{(1)}]$, respectively. Furthermore, we introduced the notations

$$\mathcal{I}_{ab}^{(i)} = \frac{s_{ab}}{s_{ai} s_{bi}}, \quad B_{n,ijp} = f_{abc} \mathcal{A}_n^{(0)\dagger} \mathbf{T}_i^a \mathbf{T}_j^b \mathbf{T}_p^c \mathcal{A}_n^{(0)}, \\ \mathcal{N}_1 = 8\pi\alpha_s \mu^{2\epsilon}, \quad c_\Gamma = \frac{1}{(4\pi)^{2-\epsilon}} \frac{\Gamma(1+\epsilon)\Gamma^2(1-\epsilon)}{\Gamma(1-2\epsilon)}, \quad (5.12)$$

where $s_{ab} = 2p_a \cdot p_b$. In order to make the pole content of eq. (5.11) explicit, we need to extract the divergent contributions to the colour-correlated virtual matrix element $V_{n,ij}$. This can be written as

$$V_{n,ij} \Big|_{\text{poles}} = -\frac{\alpha_s}{2\pi} \left\{ B_{n,ij} \sum_{m \neq k} \left[\delta_{f_m g} \left(\frac{C_A}{\epsilon^2} + \frac{b_0}{2\epsilon} \right) + \delta_{f_m \{q, \bar{q}\}} C_F \left(\frac{1}{\epsilon^2} + \frac{3}{2} \frac{1}{\epsilon} \right) \right] \right. \\ \left. + \frac{1}{2\epsilon} \sum_{\substack{r \neq k \\ s \neq k, r}} B_{n,ijrs} \ln \frac{s_{rs}}{\mu^2} \right\}, \quad (5.13)$$

where $B_{n,ijrs} = \mathcal{A}_n^{(0)\dagger} \{ \mathbf{T}_i \cdot \mathbf{T}_j, \mathbf{T}_r \cdot \mathbf{T}_s \} \mathcal{A}_n^{(0)}$. The flavour Kronecker delta functions are defined as follows: if f_i is the flavour of parton i , then $\delta_{f_i g} = 1$ if parton i is a gluon, and $\delta_{f_i g} = 0$ otherwise. Similarly, we define $\delta_{f_i \{q, \bar{q}\}} \equiv \delta_{f_i q} + \delta_{f_i \bar{q}}$. Next, we expand in ϵ the curly bracket in eq. (5.11): one can then use colour conservation to show that $\sum_{p \neq i, j, k} B_{ijp} = 0$. The explicit pole content of

¹²Note that in Ref. [110] different conventions are used for the normalisation of the β -function coefficients.

¹³This is the \mathbf{S}_k limit defined in Section 2. Note that, with a slight abuse of notation, we are using k both for the ordering number of the gluon in the set of radiated particles, and for its momentum.

eq. (5.11) can then be presented as follows

$$\begin{aligned} \mathbf{S}_k RV_{n+1} \Big|_{\text{poles}} &= \mathcal{N}_1 \frac{\alpha_s}{2\pi} \sum_{\substack{i \neq k \\ j \neq i, k}} \mathcal{I}_{ij}^{(k)} \left\{ B_{n,ij} \sum_{m \neq k} \left[\delta_{f_m g} \left(\frac{C_A}{\epsilon^2} + \frac{b_0}{2} \frac{1}{\epsilon} \right) + \delta_{f_m \{q, \bar{q}\}} C_F \left(\frac{1}{\epsilon^2} + \frac{3}{2} \frac{1}{\epsilon} \right) \right] \right. \\ &\quad \left. + \frac{1}{2\epsilon} \sum_{\substack{r \neq k \\ s \neq r, k}} B_{n,ijrs} \ln \frac{s_{rs}}{\mu^2} + \left[C_A \left(\frac{1}{\epsilon^2} + \frac{1}{\epsilon} \ln \frac{\mu^2 s_{ij}}{s_{ik} s_{jk}} \right) + \frac{b_0}{2\epsilon} \right] B_{n,ij} \right\}. \end{aligned} \quad (5.14)$$

One can then express the equation above in the language of factorisation, and find

$$\begin{aligned} \mathbf{S}_k RV_{n+1} &= \alpha_s^2 \mu^{2\epsilon} \sum_{\substack{i, j=1 \\ j \neq i}}^n \frac{2\beta_i \cdot \beta_j}{\beta_i \cdot k \beta_j \cdot k} \mathcal{H}_n^{(0)\dagger} \left\{ \mathbf{T}_i \cdot \mathbf{T}_j \sum_{m=1}^n \left(\frac{C_m}{\epsilon^2} + \frac{\gamma_m^{(1)}}{\epsilon} \right) \right. \\ &\quad \left. + \mathbf{T}_i \cdot \mathbf{T}_j \left[C_A \left(\frac{1}{\epsilon^2} + \frac{1}{\epsilon} \ln \frac{\mu^2 \beta_i \cdot \beta_j}{2\beta_i \cdot k \beta_j \cdot k} \right) + \frac{b_0}{2\epsilon} \right] \right. \\ &\quad \left. + \frac{1}{2\epsilon} \sum_{\substack{r, s=1 \\ r \neq s}}^n \left\{ \mathbf{T}_i \cdot \mathbf{T}_j, \mathbf{T}_r \cdot \mathbf{T}_s \right\} \ln \frac{2p_r \cdot p_s}{\mu^2} \right\} \mathcal{H}_n^{(0)} + \text{finite}, \end{aligned} \quad (5.15)$$

where $C_m = C_F$ and $\gamma_m^{(1)} = 3C_F/2$ for (anti-)quarks, while $C_m = C_A$ and $\gamma_m^{(1)} = b_0/2$ for gluons. The contributions proportional to quadratic Casimir eigenvalues are of soft origin, while the ones proportional to $\gamma_m^{(1)}$ are hard-collinear single poles, and the b_0 term is due to renormalisation. After performing the relevant colour algebra, eq. (5.15) can be shown to satisfy

$$\begin{aligned} \mathbf{S}_k RV_{n+1} &= \mathcal{H}_n^{(0)\dagger} \left(\mathcal{S}_{n,g}^{(0)}(\{\beta_i\}; k) \right)^\dagger S_{n+1}^{(1)}(\{\beta_i\}, \beta_k) \mathcal{S}_{n,g}^{(0)}(\{\beta_i\}; k) \mathcal{H}_n^{(0)} \\ &\quad + \alpha_s^2 \mu^{2\epsilon} \sum_{\substack{i, j=1 \\ j \neq i}}^n \frac{2\beta_i \cdot \beta_j}{\beta_i \cdot k \beta_j \cdot k} \mathcal{H}_n^{(0)\dagger} \mathbf{T}_i \cdot \mathbf{T}_j \mathcal{H}_n^{(0)} \left[\sum_{m=1}^n \frac{\gamma_m^{(1)}}{\epsilon} + \frac{b_0}{2\epsilon} \right], \end{aligned} \quad (5.16)$$

where $S_{n+1}^{(1)} = 2 \text{Re}[\mathcal{S}_{n+1}^{(1)} \mathcal{S}_{n+1}^{(0)\dagger}]$, and, for brevity, we are henceforth omitting the mention of finite contributions. Eq. (5.16) is an example of the issues outlined in the introduction of this Section. RV_{n+1} is a cross section involving $(n+1)$ outgoing particles, one of which is gluon k ; upon taking the soft limit for k , the first term on the *r.h.s.* provides a natural generalisation of the tree-level soft refactorisation discussed in Section 4. At loop level, as expected, we find poles in ϵ of hard-collinear origin, that correct a purely soft refactorisation picture: this is given by the second term on the right-hand side. In particular, $\gamma_m^{(1)}$ comes from the loop momentum being collinear to leg m , while b_0 comes from the loop momentum being collinear to the extra gluon, $k = n+1$. This can be further clarified by rewriting the second term using the cross-section-level version of eq. (5.10), found by multiplying it times the tree-level complex conjugate and summing over the polarisations of the radiated gluon. Writing $\mathbf{S}_k RV_{n+1}$ in terms of $S_{n,g}^{(1)}$ cancels the term involving b_0 in eq. (5.16), with the result

$$\mathbf{S}_k RV_{n+1} = \mathcal{H}_n^{(0)\dagger} \left[S_{n,g}^{(1)}(\{\beta_i\}; k) + S_{n,g}^{(0)}(\{\beta_i\}; k) \frac{\alpha_s}{2\pi} \sum_{m=1}^n \frac{\gamma_m^{(1)}}{\epsilon} \right] \mathcal{H}_n^{(0)}. \quad (5.17)$$

One can then further rewrite the remaining hard-collinear term as a difference of jet functions for each external particle of the Born process, in the form

$$\mathbf{S}_k RV_{n+1} = \mathcal{H}_n^{(0)\dagger} \left[S_{n,g}^{(1)}(\{\beta_i\}; k) + \sum_{i=1}^n J_{f_i, f_i}^{(1), \text{hc}} S_{n,g}^{(0)}(\{\beta_i\}; k) \right] \mathcal{H}_n^{(0)}, \quad (5.18)$$

where we have adopted the notation of eq. (3.20) for the jet function multiplying the hard function $\mathcal{H}_n^{(0)}$. Eq. (5.18) thus confirms the argument presented above eq. (5.11): the one-loop radiative soft function $S_{n,g}^{(1)}$ captures all the soft-virtual poles of $\mathbf{S}_k RV$, while there are still collinear poles from hard momenta circulating in the loop, which are correctly reproduced by the appropriate combination of jet functions.

We emphasise that the expressions presented in eq. (5.18) are particularly suitable for verifying explicitly that the pole content of the soft limit $\mathbf{S}_k RV_{n+1}$ coincides (up to a sign) with the pole structure of the soft component of $I_{n+1}^{(12)}$. This is a crucial validation of the arguments presented below eq. (2.18), and will be discussed in Section 6. We now proceed to the analysis of the collinear limit of the real-virtual correction.

5.2 Single-radiative jet functions at one loop

By the same reasoning that was applied to the radiative soft function in Section 5.1, the radiative jet function is also expected to factorise as a scattering amplitude in the presence of Wilson lines, in the form¹⁴

$$\mathcal{J}_{f_i, f_1 f_2}(0; k_1, k_2) = \mathcal{S}_3(\beta_1, \beta_2, n) \frac{\mathcal{J}_{f_1, f_1}(0; k_1)}{\mathcal{J}_{E_1}(\beta_1)} \frac{\mathcal{J}_{f_2, f_2}(0; k_2)}{\mathcal{J}_{E_2}(\beta_2)} \mathcal{J}_{f_i, f_1 f_2}^{\mathcal{H}}(0; k_1, k_2), \quad (5.19)$$

with one hard-collinear jet combination, $\mathcal{J}_{f_m, f_m}(0; k_m)/\mathcal{J}_{E_m}(\beta_m)$ for each outgoing parton, $m = 1, 2$, a three-line soft function $\mathcal{S}_3(\beta_1, \beta_2, n)$ defined by Wilson lines in the directions of k_1 , k_2 and n , and finally a hard function $\mathcal{J}_{f_i, f_1 f_2}^{\mathcal{H}}(0; k_1, k_2)$ responsible for finite corrections, due to hard virtual particles not collinear to either f_1 or f_2 . Note that there is no hard-collinear behaviour associated to the Wilson-line in direction n (provided $n^2 \neq 0$), only soft singularities. Spin indices connecting the two outgoing jet functions to the hard jet function are implicit in eq. (5.19).

Squaring the factorised expression in eq. (5.19) and evaluating the result at one loop gives the cross-section level jet function $J_{f_i, f_1 f_2}^{(1)}$, which appears in the collinear sector of $K_{n+1}^{(\mathbf{RV})}$. This factorisation reads

$$\begin{aligned} J_{f_i, f_1 f_2}^{(1)\alpha_i \beta_i}(\ell_i; k_1, k_2) &= \quad (5.20) \\ &= \int d^d x e^{i\ell_i \cdot x} \left\{ \left(\mathcal{J}_{f_i, f_1 f_2}^{(0)\alpha_i} (0; k_1, k_2) \right)^\dagger \left[S_3^{(1)}(\beta_1, \beta_2, n) - \sum_{j \in \{1, 2\}} J_{E_j}^{(1)}(\beta_j) \right] \mathcal{J}_{f_i, f_1 f_2}^{(0)\beta_i}(x; k_1, k_2) \right. \\ &\quad + \int \frac{d^d q}{(2\pi)^d} \left(\mathcal{J}_{f_i, f_1 f_2}^{(0)\alpha_i; \bar{\alpha}_1} (0; q, k_2) \right)^\dagger J_{f_1, f_1}^{(1)\bar{\alpha}_1 \bar{\beta}_1}(q; k_1) \mathcal{J}_{f_i, f_1 f_2}^{(0)\beta_i; \bar{\beta}_1}(x; q, k_2) \\ &\quad \left. + \int \frac{d^d q}{(2\pi)^d} \left(\mathcal{J}_{f_i, f_1 f_2}^{(0)\alpha_i; \bar{\alpha}_2} (0; k_1, q) \right)^\dagger J_{f_2, f_2}^{(1)\bar{\alpha}_2 \bar{\beta}_2}(q; k_2) \mathcal{J}_{f_i, f_1 f_2}^{(0)\beta_i; \bar{\beta}_2}(x; k_1, q) \right\} + \text{finite}, \end{aligned}$$

where the spin indices undergo the conventions explained below eq. (4.12). The integrals over the parent momentum q are trivial in eq. (5.20), since the cross-section-level jet functions $J_{f_m, f_m}^{(1)}$ are proportional to $\delta(q - k_m)$. However we will see later, in Section 6, that in the strongly-ordered limit for double-radiative jet function the corresponding momentum q will play an important role. The cross-section-level soft function S_3 in eq. (5.20) is defined as usual by squaring the vacuum expectation value of the appropriate Wilson lines. In this case

$$S_3(\beta_1, \beta_2, n) = \left| \langle 0 | T \left[\Phi_n(0, \infty) \Phi_{\beta_1}(0, \infty) \Phi_{\beta_2}(0, \infty) \right] | 0 \rangle \right|^2. \quad (5.21)$$

In order for S_3 to be gauge invariant, we require colour conservation, in the form $\mathbf{T}_n + \mathbf{T}_1 + \mathbf{T}_2 = 0$, whenever the soft function operates within an on-shell amplitude. This implies that the Wilson

¹⁴As before, we evaluate the jet functions at $x = 0$, and we do not display the dependence on the polarisation vectors.

line in direction n carries the total colour charge of all the Born-level particles, excluding the colour charge of the parent momentum ℓ_i .

We note that an equivalent factorisation exists for the eikonal radiative jet. At cross-section level we write

$$J_{\mathbb{E}_i, g}^{(1)}(\beta_i; k) = \left[S_3^{(1)}(\beta_i, \beta_k, n) - J_{\mathbb{E}_g}^{(1)}(\beta_k) \right] J_{\mathbb{E}_i, g}^{(0)}(\beta_i; k) + \int \frac{d^d q}{(2\pi)^d} \mathcal{J}_{\mathbb{E}_i, g}^{(0)\bar{\alpha}}(\beta_i; q) J_{g; g}^{(1)\bar{\alpha}\bar{\beta}}(q; k) \mathcal{J}_{\mathbb{E}_i, g}^{(0)\bar{\beta}}(\beta_i; q). \quad (5.22)$$

Here we can specify that the radiated particle is a gluon since one cannot radiate a single quark from a Wilson line. We will now show that eqs. (5.20) and (5.22) hold, by explicit computation of the one-loop radiative jet.

5.3 Computing radiative jet functions at one loop

In Section 5.2 we have introduced factorisation formulas for jet and eikonal-jet functions at the one-loop level. In order to test such formulas, it is necessary to compute these functions at order α_s . This is non-trivial, since different scales enter the relevant diagrams, and the corresponding Feynman rules involve denominators that are linear in the loop momentum.

Often, an axial gauge ($n \cdot A = 0$) is chosen when computing jet functions, since the Wilson line Φ_n in eqs. (3.4), (3.5) and (3.6) becomes unity in that gauge. This choice prevents the proliferation of diagrams involving the interaction of gluons with the auxiliary Wilson line, and also avoids diagrams with ghosts. At loop-level, however, there are complications that arise from the denominators of the axial-gauge gluon propagator [113]: it is therefore practical to work in Feynman gauge. Another convenient choice would be to set $n^2 = 0$, which makes the integrals easier to compute, as there is no additional variable, proportional to n^2 , that they could depend upon. One difficulty in this selection, however, is that it introduces a set of unphysical collinear divergences associated with the Wilson line in the direction n , which would need to be removed. To be on the safe side and to avoid confusion, we choose $n^2 \neq 0$.

The computation of the (bare) jet functions proceeds in a standard way. The necessary Dirac and colour algebra for the Feynman diagrams can be performed with the software `FeynCalc` [114–116]. The results are then passed to the program `LiteRed` [117, 118] to reduce them to a set of basis integrals using integration-by-parts identities. Some details of the calculation are presented in Appendix C. In particular, given the results for the relevant master integrals, presented in eqs. (C.2), (C.8) and (C.9), it is easy to obtain compact expressions for the bare jet functions at one loop. The quark radiative jet function with a single gluon emission reads

$$J_{q, qg}^{(1), b}(\ell; k_1, k_2) = -\frac{\alpha_s}{2\pi} J_{q, qg}^{(0)}(\ell; k_1, k_2) \times \left[C_A \left(\frac{1}{\epsilon^2} + \frac{1}{\epsilon} \log \frac{\mu^2 k_1 \cdot n}{2k_2 \cdot n k_1 \cdot k_2} \right) + C_F \left(\frac{1}{\epsilon^2} + \frac{1}{\epsilon} \left(1 + \log \frac{\mu^2 n^2}{(2k_1 \cdot n)^2} \right) \right) \right] + \text{finite}, \quad (5.23)$$

where the superscript b denotes a bare function. The gluon radiative jet function with the emission of a quark-antiquark pair reads

$$J_{g, q\bar{q}}^{(1), b, \mu\nu}(\ell; k_1, k_2) = -\frac{\alpha_s}{2\pi} J_{g, q\bar{q}}^{(0), \mu\nu}(\ell; k_1, k_2) \times \left[\frac{C_A}{\epsilon} \left(\log \frac{n^2 k_1 \cdot k_2}{2k_1 \cdot n k_2 \cdot n} - \frac{8}{3} \right) + C_F \left(\frac{2}{\epsilon^2} + \frac{1}{\epsilon} \left(3 + 2 \log \frac{\mu^2}{2k_1 \cdot k_2} \right) \right) + \frac{2n_f}{3\epsilon} \right] + \text{finite}. \quad (5.24)$$

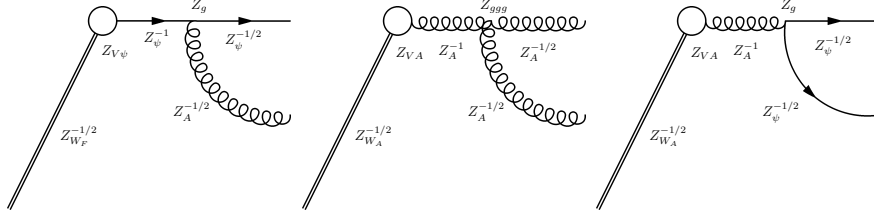


Figure 2: Assigning renormalisation constants to different factors in the radiative jet functions: radiation from the field line.

Similarly, the gluon radiative jet function with the emission of a gluon pair reads

$$J_{g,gg}^{(1),b,\mu\nu}(\ell; k_1, k_2) = -\frac{\alpha_s}{2\pi} J_{g,gg}^{(0),\mu\nu}(\ell; k_1, k_2) \times C_A \left[\frac{2}{\epsilon^2} + \frac{1}{\epsilon} \left(1 + \log \frac{\mu^2 n^2}{2k_1 \cdot n k_2 \cdot n} + \log \frac{\mu^2}{2k_1 \cdot k_2} \right) \right] + \text{finite}. \quad (5.25)$$

Finally, the radiative eikonal jet function with the emission of a gluon reads

$$J_{E,g}^{(1),b}(\beta; k) = -\frac{\alpha_s}{2\pi} J_{E,g}^{(0)}(\beta; k) C_A \left[\frac{1}{\epsilon^2} + \frac{1}{\epsilon} \log \left(\frac{\mu^2 \beta \cdot n}{2k \cdot n k \cdot \beta} \right) \right] + \text{finite}. \quad (5.26)$$

In eqs. (5.23)-(5.26) we extracted the tree-level results, given in Appendix B, and α_s is the bare coupling. It is worthwhile to discuss the renormalisation of the jet functions in detail. As we have chosen to regulate the infrared and ultraviolet both in dimensional regularisation, we cannot readily distinguish between them in the calculation (note that radiative functions are not pure counterterms even in the eikonal limit, since the radiated momentum provides a scale). As a consequence, the renormalisation factors need to be determined separately. We will do so by examining the tree-level diagrams and dressing each component with a renormalisation factor. All relevant factors are known or can be easily computed. Upon renormalisation we will find a universal and transparent expression for single-radiative jet functions at one loop.

The tree-level diagrams where the radiated particle is emitted from the field line are displayed in Fig. 2. Each internal vertex carries a Z factor for the corresponding coupling (these are $Z_{V\psi}$, Z_{V_A} , Z_g , Z_{ggg}). Similarly, each internal propagator carries a factor Z^{-1} for the corresponding field (in the case at hand, Z_{ψ}^{-1} and Z_A^{-1}). Finally, each external leg carries a factor of $Z^{-1/2}$ for the corresponding wave function (here $Z_{W_F}^{-1/2}$, $Z_{W_A}^{-1/2}$, $Z_A^{-1/2}$, $Z_{\psi}^{-1/2}$). Altogether, the renormalisation takes the form

$$\begin{aligned} J_{q,qq}(\ell; k_1, k_2) &= J_{q,qq}^b(\ell; k_1, k_2) \left(Z_{V\psi} Z_g Z_{\psi}^{-3/2} Z_A^{-1/2} Z_{W_F}^{-1/2} \right)^2, \\ J_{g,gg}^{\mu\nu}(\ell; k_1, k_2) &= J_{g,gg}^{b,\mu\nu}(\ell; k_1, k_2) \left(Z_{V_A} Z_{ggg} Z_A^{-2} Z_{W_A}^{-1/2} \right)^2, \\ J_{g,qq}^{\mu\nu}(\ell; k_1, k_2) &= J_{g,qq}^{b,\mu\nu}(\ell; k_1, k_2) \left(Z_{V_A} Z_g Z_{\psi}^{-1} Z_A^{-1} Z_{W_A}^{-1/2} \right)^2, \end{aligned} \quad (5.27)$$

and the relevant renormalisation factors Z_i are collected in Appendix C.

Furthermore, there is another type of graph at tree-level, where a gluon is radiated from the Wilson line, as shown in Fig. 3. The corresponding renormalisation factors can be consistently determined by demanding that these diagrams renormalise in the same way as those in Fig. 2. The results are also given in Appendix C. Finally, the single-radiative eikonal jet renormalisation factors are presented in Fig. 4, showing one of the two tree-level diagrams. The eikonal jet thus

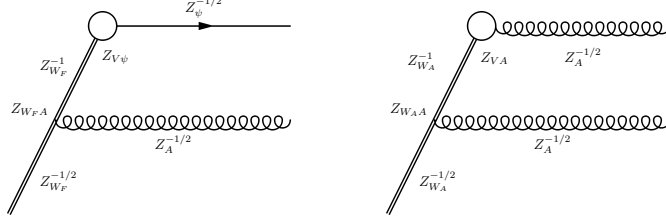


Figure 3: Assigning renormalisation constants to different factors in the radiative jet functions: radiation from the Wilson line.

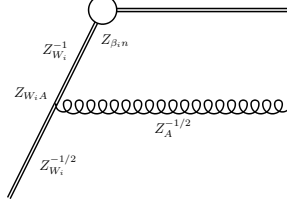


Figure 4: Assigning renormalisation constants for the eikonal radiative jet function.

renormalises as

$$J_{E_i}(\beta_i; k) = J_{E_i}^b(\beta_i; k) \left(Z_{\beta_i, n} Z_{W_{iA}} Z_{W_i}^{-3/2} Z_A^{-1/2} \right)^2, \quad (5.28)$$

where $Z_{\beta_i, n}$ is the renormalisation of the vertex connecting the Wilson lines in directions β_i and n (see eq. (C.13)). On the other hand, light-like Wilson lines do not carry a ‘wave function renormalisation’, as all self-energy diagrams vanish, since they are proportional to $\beta_i^2 = 0$. Once renormalised in the $\overline{\text{MS}}$ scheme, single-radiative jet functions can be written universally in the form

$$J_{f_i, f_1, f_2}^{(1)}(\ell_i; k_1, k_2) = -\frac{\alpha_s}{2\pi} J_{f_i, f_1, f_2}^{(0)}(\ell_i; k_1, k_2) \left[\frac{\gamma_1^{(1)}}{\epsilon} + \frac{\gamma_2^{(1)}}{\epsilon} + \frac{C_1 + C_2}{\epsilon^2} + \frac{1}{\epsilon} \left(C_i + 2\mathbf{T}_1 \cdot \mathbf{T}_2 \log \frac{(k_1 \cdot k_2)n^2}{2k_1 \cdot n k_2 \cdot n} + C_1 \log \frac{n^2 \mu^2}{4(k_1 \cdot n)^2} + C_2 \log \frac{n^2 \mu^2}{4(k_2 \cdot n)^2} \right) + \mathcal{O}(\epsilon^0) \right], \quad (5.29)$$

where $\gamma_i^{(1)}$ is the one-loop collinear anomalous dimension for parton i , given below eq. (5.15): the terms involving these anomalous dimensions are of hard-collinear origin and feature in the difference between radiative jet and eikonal jet functions arising from eq. (5.20).

To complete the proof of factorisation at one-loop, we need to show that the remaining terms build the soft function $S_3^{(1)}(\beta_1, \beta_2, n)$. To this end, recall that $S_3^{(1)}(\beta_1, \beta_2, n)$ is a Wilson-line correlator defined with lines β_1 , β_2 and n , as in eq. (5.21). In particular, at one-loop, it is the sum of three terms, given by

$$S_3^{(1)}(\beta_1, \beta_2, n) = \frac{\alpha_s}{\pi} \mathbf{T}_1 \cdot \mathbf{T}_2 \left(\frac{1}{\epsilon^2} - \frac{1}{\epsilon} \log \beta_1 \cdot \beta_2 \right) + \frac{\alpha_s}{2\pi} \mathbf{T}_1 \cdot \mathbf{T}_n \left[\frac{1}{\epsilon^2} + \frac{1}{\epsilon} \left(1 + \log \frac{n^2}{2(\beta_1 \cdot n)^2} \right) \right] + \frac{\alpha_s}{2\pi} \mathbf{T}_2 \cdot \mathbf{T}_n \left[\frac{1}{\epsilon^2} + \frac{1}{\epsilon} \left(1 + \log \frac{n^2}{2(\beta_2 \cdot n)^2} \right) \right], \quad (5.30)$$

where the first term captures the correlation between the two light-like Wilson lines in directions β_1 and β_2 , and can be borrowed directly from eq. (3.9) in Ref. [69] up to taking twice its real part. The next two terms in eq. (5.30) connect one of the light-like lines to the line along n , which is

off the light cone. The corresponding expression can be derived from eq. (3.11) in Ref. [69]. Using colour conservation in the form $\mathbf{T}_n = -\mathbf{T}_1 - \mathbf{T}_2$ we find then

$$S_3^{(1)}(\beta_1, \beta_2, n) = -\frac{\alpha_s}{2\pi} \left[\frac{C_1 + C_2}{\epsilon^2} + \frac{1}{\epsilon} \left(C_{[12]} + 2\mathbf{T}_1 \cdot \mathbf{T}_2 \log \frac{(\beta_1 \cdot \beta_2) n^2}{2\beta_1 \cdot n \beta_2 \cdot n} + C_1 \log \frac{n^2}{2(\beta_1 \cdot n)^2} + C_2 \log \frac{n^2}{2(\beta_2 \cdot n)^2} \right) \right], \quad (5.31)$$

where $C_{[12]} \equiv (\mathbf{T}_1 + \mathbf{T}_2)^2$ is the quadratic Casimir of the parent particle radiating 1 and 2. Using eq. (5.31) in eq. (5.29), with $\beta_i = \sqrt{2} k_i / \mu$, we finally find

$$J_{f_i, f_1 f_2}^{(1)}(\ell_i; k_1, k_2) = J_{f_i, f_1 f_2}^{(0)}(\ell_i; k_1, k_2) \left[-\frac{\alpha_s}{2\pi} \frac{1}{\epsilon} (\gamma_1^{(1)} + \gamma_2^{(1)}) + S_3^{(1)}(\beta_1, \beta_2, n) + \mathcal{O}(\epsilon^0) \right]. \quad (5.32)$$

Thus, identifying, as before, $\gamma_i^{(1)}$ as the difference between the one-loop jet function and its eikonal counterpart, we have indeed obtained the factorisation of the radiative one-loop jet function, as given in eq. (5.20). One can similarly verify that eq. (5.22) also holds.

6 A top-down approach to strongly-ordered counterterms

Before proceeding, we find it useful to summarise what we have achieved so far. In Section 4 we obtained expressions for strongly-ordered radiative functions at tree level, by applying soft and collinear factorisation in an iterative fashion: we conjectured the form of such hierarchical configurations to all orders, and we verified *a posteriori* their correspondence with known results. On the other hand, in Section 5 we derived the form of soft and collinear limits of squared matrix elements at one loop, starting from factorisation concepts: in doing so, we treated soft and jet functions as generalised scattering amplitudes featuring Wilson lines as sources. These two constructions may seem unrelated, and based on different principles. However, soft and collinear limits of real-virtual contributions, and strongly-ordered limits of double-real contributions, must be intertwined. Indeed, the corresponding counterterms $K_{n+1}^{(\mathbf{RV})}$ and $K_{n+2}^{(\mathbf{12})}$ (or, more precisely, its integral $I_{n+1}^{(\mathbf{12})}$) have to combine appropriately in order to ensure the cancellation of explicit poles in the second line of eq. (2.18), similarly to what happens with the combination of V_n and $I_n^{(\mathbf{1})}$ at NLO. One can thus expect $K_{n+1}^{(\mathbf{RV})}$ and $K_{n+2}^{(\mathbf{12})}$ to be connected by NLO-like completeness relations, analogous to those presented in eqs. (3.13-3.15). This reasoning suggests that, by following the *top-down approach* introduced in Section 3.1, one can obtain explicit expression for double-real strongly-ordered counterterms, directly from the factorised form of real-virtual counterterms: this is the goal of this Section.

To proceed, we insert the factorised real-virtual functions found in Section 5.1 and in Section 5.2 in the expression for $K_{n+1}^{(\mathbf{RV})}$. We then apply the NLO completeness relations in eqs. (3.13-3.15), and we arrive at the factorised strongly-ordered terms discussed in Section 4. From these expressions, after a preliminary analysis in Section 6.1 and in Section 6.2, we proceed to derive, in Section 6.3, the expression for the complete counterterm $K_{n+2}^{(\mathbf{12})}$ responsible for strongly-ordered configurations. In Appendix D, we will verify that indeed our result coincides with the single-unresolved limit $\mathbf{L}^{(\mathbf{1})}$ of $K_{n+2}^{(\mathbf{2})}$, defined in eq. (2.12).

6.1 Soft sector

In this section we show that, by applying the NLO-like completeness relations in eqs. (3.13-3.15) to the factorised one-loop radiative soft function $S_{n,g}^{(\mathbf{1})}$, we arrive at NNLO finiteness conditions linking the real-virtual contribution to double-real strongly-ordered configurations.

We start by considering the factorised one-loop soft function given in eq. (5.2). Constructing the corresponding cross-section level expression, we obtain

$$\begin{aligned} S_{n,g}^{(1)}(\{\beta_i\}; k) &= S_{n,g}^{(0)\dagger}(\{\beta_i\}; k) \left[S_{n+1}^{(1)}(\{\beta_i\}, \beta_k) - J_{E_g}^{(1)}(\beta_k) \right] S_{n,g}^{(0)}(\{\beta_i\}; k) \\ &+ \int \frac{d^d \ell}{(2\pi)^d} \left(S_{n,g}^{(0)\mu}(\{\beta_i\}; \ell) \right)^\dagger J_{g,g}^{(1)\mu\nu}(\ell; k) S_{n,g}^{(0)\nu}(\{\beta_i\}; \ell), \end{aligned} \quad (6.1)$$

where β_k is the velocity of the radiated gluon with momentum k . In this form, we can readily apply the relations in eqs. (3.13-3.15) to the inner one-loop functions on the right-hand side. Effectively, this means exchanging a loop function with an integrated radiative function. This gives

$$\begin{aligned} S_{n,g}^{(1)}(\{\beta_i\}; k_1) &+ \int d\Phi(k_2) \left\{ \left(S_{n,g}^{(0)}(\{\beta_i\}; k_1) \right)^\dagger \left[S_{n+1,g}^{(0)}(\{\beta_i\}, \beta_{k_1}; k_2) - J_{E_g,g}^{(0)}(\beta_{k_1}; k_2) \right] S_{n,g}^{(0)}(\{\beta_i\}; k_1) \right. \\ &+ \left. \int \frac{d^d \ell}{(2\pi)^d} \left(S_{n,g}^{(0)\mu}(\{\beta_i\}; \ell) \right)^\dagger \sum_{f_1, f_2} J_{g, f_1 f_2}^{(0)\mu\nu}(\ell; k_1, k_2) S_{n,g}^{(0)\nu}(\{\beta_i\}; \ell) \right\} = \text{finite}. \end{aligned} \quad (6.2)$$

Eq. (6.2) can be slightly refined by replacing momentum k_1 with the combination $k_1 + k_2$ in the tree-level soft function responsible for the harder emission. This makes no difference in the soft limit for k_2 , but it proves useful to maintain consistency in collinear limits, as discussed in Appendix D. With this understanding, we can now identify the strongly-ordered soft function, defined in eq. (4.3), as the first term in the integrand of eq. (6.2). We can then write

$$\begin{aligned} S_{n,g}^{(1)}(\{\beta_i\}; k_1) &+ \int d\Phi(k_2) \left\{ S_{n,g}^{(0)}(\{\beta_i\}; k_{[12]}; k_2) - \left(S_{n,g}^{(0)}(\{\beta_i\}; k_{[12]}) \right)^\dagger J_{E_g,g}^{(0)}(\beta_{k_1}; k_2) S_{n,g}^{(0)}(\{\beta_i\}; k_{[12]}) \right. \\ &+ \left. \int \frac{d^d \ell}{(2\pi)^d} \left(S_{n,g}^{(0)\mu}(\{\beta_i\}; \ell) \right)^\dagger \sum_{f_1, f_2} J_{g, f_1 f_2}^{(0)\mu\nu}(\ell; k_1, k_2) S_{n,g}^{(0)\nu}(\{\beta_i\}; \ell) \right\} = \text{finite}. \end{aligned} \quad (6.3)$$

As usual, the k_2 phase-space integration in the first line cancels the poles of $S_{n,g}^{(1)}$ originating from soft radiation at wide angles from the directions $\{\beta_i, k_1\}$, while the convolution on the second line cancels collinear poles (including soft-collinear ones, which were subtracted in the first line) associated with the emitted gluon. As discussed below eq. (5.1), there are no hard-collinear poles associated with the directions of the n Wilson lines.

6.2 Collinear sector

We can similarly apply the NLO finiteness conditions in eqs. (3.13-3.15) to the factorised one-loop single-radiative jet function $J_{f_i, f_1 f_2}^{(1)}$, which will lead to a finite relation between the latter and the strongly-ordered double-radiative jet function. We start with the factorised one-loop radiative jet in eq. (5.20). Applying the NLO completeness relations to the inner one-loop functions of that equation we find

$$\begin{aligned} J_{f_i, f_1 f_2}^{(1)\alpha_i \beta_i}(\ell_i; k_1, k_2) &+ \int d\Phi(k_3) \int d^d x e^{i\ell_i \cdot x} \quad (6.4) \\ &\left\{ \left(\mathcal{J}_{f_i, f_1 f_2}^{(0)\alpha_i} (0; k_1, k_2) \right)^\dagger \left[S_{3, f_3}^{(0)}(\beta_1, \beta_2, n; k_3) - \sum_{j \in \{1, 2\}} J_{E_j, f_3}^{(0)}(\beta_j; k_3) \right] \mathcal{J}_{f_i, f_1 f_2}^{(0)\beta_i} (x; k_1, k_2) \right. \\ &+ \int \frac{d^d q}{(2\pi)^d} \left(\mathcal{J}_{f_i, f_1 f_2}^{(0)\alpha_i \bar{\alpha}_1} (0; q, k_2) \right)^\dagger J_{f_q, f_1 f_3}^{(0)\bar{\alpha}_1 \bar{\beta}_1} (q; k_1, k_3) \mathcal{J}_{f_i, f_1 f_2}^{(0)\bar{\beta}_1 \beta_i} (x; q, k_2) \\ &+ \left. \int \frac{d^d q}{(2\pi)^d} \left(\mathcal{J}_{f_i, f_1 f_2}^{(0)\alpha_i \bar{\alpha}_2} (0; k_1, q) \right)^\dagger J_{f_q, f_2 f_3}^{(0)\bar{\alpha}_2 \bar{\beta}_2} (q; k_2, k_3) \mathcal{J}_{f_i, f_1 f_2}^{(0)\bar{\beta}_2 \beta_i} (x; k_1, q) \right\} = \text{finite}. \end{aligned}$$

In the last two lines of the integrand of eq. (6.4) one recognises the expressions for strongly-ordered jet functions discussed in Section 4.2, specifically $J_{f_i; f_q f_2; f_1 f_3, f_2}^{(0)\alpha_i \beta_i}$ and $J_{f_i; f_1 f_q; f_1, f_2 f_3}^{(0)\alpha_i \beta_i}$. In the same way as for the soft function in Section 6.1, collinear poles of $J_{f_i, f_1 f_2}^{(1)}$ are cancelled by integrating the strongly-ordered jet functions, while soft non-collinear poles are cancelled by integrating the radiative soft function in the second line, where the soft-collinear region has been subtracted to avoid double counting.

6.3 Extracting strongly-ordered counterterms

After working out soft and collinear finiteness conditions, we are ready to derive in this section a complete, explicit expression for the strongly-ordered counterterm $K_{n+2}^{(\mathbf{12})}$, in a top-down approach. In order to do so, we first write $K_{n+1}^{(\mathbf{RV})}$ in eq. (3.32) using the factorised expressions we have derived. Then, applying the finiteness relations derived in the previous sections, we can arrive at the integrated counterterm $I_{n+1}^{(\mathbf{12})}$, whose integrand is $K_{n+2}^{(\mathbf{12})}$.

We begin by focusing on the explicit poles of the soft component $K_{n+1}^{(\mathbf{RV}, s)}$. They are entirely encoded in the third and last term on the right-hand side of eq. (3.33), and, in particular, in the radiative, one-loop soft function $S_{n,g}^{(1)}$. Therefore we can write

$$K_{n+1}^{(\mathbf{RV}, s)} = \mathcal{H}_n^{(0)\dagger} S_{n,g}^{(1)} \mathcal{H}_n^{(0)} + \text{finite}. \quad (6.5)$$

Using the finiteness condition in eq. (6.2), or equivalently in eq. (6.3), we can identify the integrals on the left-hand sides of these equations as the integrated strongly-ordered counterterm, $I_{n+1}^{(\mathbf{12}, s)}$. This provides an ansatz for the corresponding integrand functions as $K_{n+2}^{(\mathbf{12}, s)}$. In Appendix D we will verify that this ansatz indeed corresponds to the single-soft limit of the double-unresolved counterterm $K_{n+2}^{(2, s)}$. We get

$$K_{n+2}^{(\mathbf{12}, s)} = \mathcal{H}_n^{(0)\dagger} \sum_{f_1, f_2} \left[S_{n; f_{[12]}, f_2}^{(0)}(k_{[12]}, k_2) + S_{n, f_{[12]}}^{(0)} \left(J_{f_{[12]}, f_1 f_2}^{(0)} - J_{E_{[12]}, f_2}^{(0)} \right) \right] \mathcal{H}_n^{(0)}, \quad (6.6)$$

where we have understood spin indices and, as discussed in Section 6.1, we have included a set of non-singular contributions by attributing the total soft momentum to the harder gluon emission. In writing eq. (6.6), starting from eq. (6.2), we have used the fact that jet functions are colour singlets, and thus they commute with soft functions, which carry colour structure; furthermore, for simplicity, we are understanding the convolution in the parent gluon momentum $k_{[12]}$ that was explicitly written in eq. (6.2).

We now turn to the hard-collinear component, and examine $K_{n+1, i}^{(\mathbf{RV}, \text{hc})}$ in eq. (3.34). To manipulate this term, it is convenient to use the factorised expressions for jet and eikonal jet functions derived in Section 5.2. In particular, we can consider eq. (5.20), and then obtain the corresponding result at cross-section level. For the one-loop radiative eikonal jet function we can directly use the result in eq. (5.22). Exploiting the definition in eq. (3.18), we can write the real-virtual counterterm for the hard-collinear sector associated with particle i as

$$K_{n+1, i}^{(\mathbf{RV}, \text{hc})} = \mathcal{H}_n^{(0)\dagger} \sum_{f_1, f_2} J_{f_i, f_1 f_2}^{(0), \text{hc}} \left[S_3^{(1)} - J_{E_i}^{(1)} + \sum_{k=1}^2 J_{f_k, f_k}^{(1), \text{hc}} \right] \mathcal{H}_n^{(0)}, \quad (6.7)$$

where for simplicity, we have understood the necessary convolution, as before, as well as the spin structure, which was displayed in detail in eq. (5.22) and in eq. (6.4). Recall that eq. (6.7) describes the one-loop correction to the hard-collinear splitting of Born-level particle i into two particles of flavours f_1 and f_2 , summed over the consistent flavour channels: thus the soft function S_3 involves the Wilson lines associated with external legs 1 and 2, and the Wilson line for the reference vector

n_i of the jets along the direction of leg i . Now, using the finiteness conditions, we can derive the corresponding counterterm for the strongly-ordered hard-collinear configuration. It can be written as

$$K_{n+2,i}^{(\mathbf{12}, \text{hc})} = \mathcal{H}_n^{(0)\dagger} \sum_{f_1, f_2, f_3} \left[J_{f_i, f_1 f_2}^{(0), \text{hc}}(\bar{k}_1, \bar{k}_2) S_{3, f_3}^{(0)} - J_{f_i, f_1 f_2}^{(0), \text{hc}}(k_1, k_2) J_{E_i, f_3}^{(0)} \right. \\ \left. + \sum_{kl=\{12, 21\}} J_{f_i, f_{[k3]} f_l}^{(0), \text{hc}} \left(J_{f_{[k3]}, f_k f_3}^{(0)} - J_{E_k, f_3}^{(0)} \right) \right] \mathcal{H}_n^{(0)}. \quad (6.8)$$

In analogy to what was done in the soft sector, we have introduced a shift of the collinear momenta, so that the hardest splitting carries the total radiated momentum, according to $\bar{k}_1 + \bar{k}_2 = k_1 + k_2 + k_3$, while the soft function S_3 is built with $\bar{\beta}_1$, $\bar{\beta}_2$, and n_i . This reparametrisation does not affect singular contributions.

We now turn to the hard-collinear real-virtual counterterm $K_{n+1,ij}^{(\mathbf{RV}, \text{hc})}$ in eq. (3.35), featuring the hard-collinear radiation from two distinct Born-level partons. In this case, loop corrections and real radiation affect separately parton i and j , and they are not intertwined. Then we can simply apply the completeness relations to the one-loop jet function following eq. (3.15), to obtain

$$K_{n+2,ij}^{(\mathbf{12}, \text{hc})} = \mathcal{H}_n^{(0)\dagger} \sum_{f_1, f_2, f_3, f_4} J_{f_i, f_1 f_2}^{(0), \text{hc}} J_{f_j, f_3 f_4}^{(0), \text{hc}} \mathcal{H}_n^{(0)} + (i \leftrightarrow j). \quad (6.9)$$

which is the same as eq. (3.29). The final expression is simple, since for two uncorrelated limits ‘democratic’ and strongly-ordered counterterms coincide. Note however that, in a concrete implementation, one needs to complement eq. (6.9) with appropriate phase-space mappings, as discussed in Appendix A. For example, when checking that collinear limits of $K^{(\mathbf{2})}$ coincide with those of $K^{(\mathbf{12})}$, one must assume the corresponding mappings to behave in the same way. A similar structure emerges in the case of $K_{n+1,i}^{(\mathbf{RV}, \text{1hc}, \text{1s})}$, presented in eq. (3.36), describing singular configurations involving one soft and one collinear limit. Also in this case, the contributions of virtual and real origin are factorised, leading to a particularly simple expression, which is expected as a consequence of QCD colour coherence: soft emissions do not resolve individual colour charges of the decay products, just the total colour charge of the emitters. Applying completeness to eq. (3.36) we obtain

$$K_{n+2,i}^{(\mathbf{12}, \text{1hc}, \text{1s})} = \mathcal{H}_n^{(0)\dagger} \sum_{f_1, f_2, f_3} \sum_{jkl \in \{123, 312, 231\}} J_{f_i, f_k f_l}^{(0), \text{hc}} S_{n, f_j}^{(0)} \mathcal{H}_n^{(0)}, \quad (6.10)$$

reproducing eq. (3.30), which is factorised, and thus effectively strongly ordered. The last term of eq. (3.32), $K_{n+1,i}^{(\mathbf{RV}, \text{1hc})}$, is presented in eq. (3.37): its loop content is entirely carried by the one-loop resolved amplitude $\mathcal{H}_n^{(1)}$, which is finite in $d = 4$ dimensions. As a consequence, there is no $K_{n+2}^{(\mathbf{12})}$ contribution stemming from this term.

We are now in a position to assemble the different contributions and arrive at the final expression of the strongly-ordered double-unresolved counterterm. This reads

$$K_{n+2}^{(\mathbf{12})} = K_{n+2}^{(\mathbf{12}, \text{s})} + \sum_{i=1}^n \left[K_{n+2,i}^{(\mathbf{12}, \text{hc})} + \sum_{j=i+1}^n K_{n+2,ij}^{(\mathbf{12}, \text{hc})} + K_{n+1,i}^{(\mathbf{12}, \text{1hc}, \text{1s})} \right], \quad (6.11)$$

which is structurally analogous to eq. (3.26) and eq. (3.32). The results given above for individual contributions to eq. (6.11) are obtained by exploiting completeness relations, starting from the factorised form of the real-virtual counterterm. This represents an alternative approach with respect to the one in Section 4, which is based on the iterative factorisation of subsequent emissions. As a crucial validation of our arguments, we need to verify that the two results agree. In particular,

we have to check that eq. (6.11) reproduces the iterative limits of double-real matrix elements, constructed by taking single-unresolved soft and collinear limits of the double-real counterterm. In formulae, we have to prove the relation $\mathbf{L}_1[K_{n+2}^{(2)}] = \mathbf{L}_1[K_{n+2}^{(12)}]$, given the definition of \mathbf{L}_1 in eq. (2.5), the expression for $K_{n+2}^{(2)}$ reported in eq. (3.26), and the results in eq. (6.11). The required calculation is successfully carried out in Appendix D.

7 Summary and future prospects

In this paper we have outlined a general procedure to identify local counterterms capturing the singular behaviour of real-radiation squared matrix elements, including the case of strongly-ordered and nested limits. The organisation of the relevant counterterms has been presented at NNLO, and sketched at N³LO in Section 2, following the spirit of previous studies performed in the context of the *local analytic sector subtraction* [30, 31, 102]. The general structure of this subtraction algorithm turns out to be remarkably transparent, and allows for a straightforward generalisation to higher orders, at least so far as a formal analysis is concerned. We note also that the number and complexity of independent counterterms grow exponentially with the perturbative order (see eq. (2.27)), but remain reasonably limited for the perturbative orders that are expected to be of phenomenological interest.

Having established the subtraction framework, in Section 3 we went on to construct all the local counterterms that are needed for the NNLO subtraction procedure, relying on the established factorised structure of infrared poles of virtual corrections to scattering amplitudes. This approach was first exploited in Ref. [102], and it builds on the cancellation of infrared singularities between real and virtual corrections, ensured by general cancellation theorems. At cross-section level, soft and collinear functions responsible for virtual poles are used as building blocks for inclusive cross-section-like quantities that can be shown to be infrared finite by power counting: throughout the paper, we have referred to these constructions as *completeness relations*, since finiteness is achieved by performing an inclusive sum over a complete set of radiation states. These soft and collinear cross sections then contain integrated real-radiation contributions that cancel virtual poles by construction: their integrands are thus readily understood as local soft and collinear counterterms.

We note that our approach essentially reverses the standard logic guiding the construction of most established infrared subtraction schemes. Typically, these schemes are based on three main steps: *i*) the identification of the real-emission subtraction terms, *ii*) the analytic integration of the counterterms over the unresolved phase space, leading to explicit poles, and *iii*) the proof of pole cancellation between integrated counterterms and virtual corrections. The idea of starting from the infrared structure of virtual corrections to infer the form of the counterterms has been recently considered by other groups, in the context of *nested soft-collinear subtraction* [33] and *antenna subtraction* [34]. We stress that in this paper we have moved a further step forward with respect to simply using the singularity structure of virtual amplitudes as a guideline. We have, indeed, taken advantage of the detailed infrared factorisation properties of fixed-angle massless amplitudes, and we have derived expressions for all relevant real-radiation counterterms, in a fully general fashion. As explained in Section 2, and noted above, we derive expressions for local counterterms as matrix elements of fields and Wilson lines by “completing” the corresponding soft, collinear and soft-collinear building blocks that appear in the factorisation formula for virtual amplitudes. This approach to the definition of counterterms is, by construction, valid to all orders in perturbation theory and can accommodate an arbitrary number of real emissions.

Starting from Section 4, we focused on the issue of disentangling and modelling strongly-ordered configurations, that are not directly manifest in the expressions for multiple real-radiation counterterms, which are based on uniform infrared limits. Strongly-ordered counterterms are very important, not only because they proliferate as the perturbative order increases, as noted in Section 2,

but also because their integrals play the delicate role of cancelling the poles of mixed real-virtual contributions, without upsetting the balance of singular phase space limits for the remaining un-integrated radiation. In all existing approaches, this subtle cancellation has been engineered on a case-by-case basis, fine-tuning the structure of individual counterterms. Our aim in this paper has been to provide a systematic method to secure this cancellation in full generality. To this end, we first made educated guesses to conjecture expressions for the relevant hierarchical configurations, to all orders, in terms of expectation values of appropriate combinations of fields and Wilson lines. Then we checked for agreement with results known from the literature. Next, in Section 5, we derived factorised expressions for soft and collinear limits of squared matrix elements involving both real radiation and virtual corrections. With these expressions in hand, as explained in Section 6, one can exploit NLO-like completeness relations to connect real-virtual counterterms to integrals involving multiple real radiations. These integrals are, in turn, identified with contributions to the integrated strongly-ordered counterterm $I_{n+1}^{(\mathbf{12})}$. Completeness relations thus link the real-virtual counterterm $K_{n+1}^{(\mathbf{RV})}$ with the strongly-ordered double-real counterterm $K_{n+2}^{(\mathbf{12})}$, in a way that automatically ensures the cancellations foreseen in our approach. We have explicitly checked that the results obtain by means of the “completeness procedure” (applied to the real-virtual counterterm) agree with direct iterated limits of double-real matrix elements.

We emphasise that our results do not immediately translate into a concrete subtraction algorithm, because we have assumed, but not concretely implemented, the phase-space mappings that are necessary for all singular limits involving collinear splittings, and that must be chosen in a consistent way when multiple nested limits are considered. These issues are discussed in detail in Ref. [31]: we believe that the approach presented in this paper can lead to a significant simplification of the intricate structure of the mappings employed there.

The method we have introduced naturally lends itself to various extensions. First of all, the inclusion of initial-state radiation can be devised without posing, in principle, new theoretical challenges: indeed, there are no significant conceptual differences between soft and jet functions involving initial and final state particles. Similarly, the extension of the method to massive quarks (which is of considerable interest in phenomena related to top-quark observables, and in connection with b -quark mass effects) does not pose new conceptual issues at the level of the definition of local counterterms. However, in the case of massive partons, defining phase-space mappings related to their branchings [119] and performing the corresponding integrations, will necessitate further work. Finally, we emphasise that the approach we have presented is likely to significantly influence the structuring of general N³LO subtraction algorithms. Work is underway to explore these generalisations.

Acknowledgements

We are grateful to Sandro Uccirati for participating in the initial stages of this project and for many useful discussions. PT has been partially supported by the Italian Ministry of University and Research (MUR) through grant PRIN 2022BCXSW9, and by Compagnia di San Paolo through grant TORP_S1921_EX-POST_21_01.

A Soft and collinear cancellations at NLO

In this appendix we present a detailed calculation verifying the cancellations implied by the NLO completeness relation in eqs. (3.13-3.15). As we will see, this requires the introduction of an appropriate regulator to cure the (unphysical) UV divergences of the relevant matrix elements, and a

choice of phase-space mapping in the collinear case. We discuss soft and collinear cancellations in Appendices A.1 and A.2 respectively.

A.1 Soft cancellation

The cancellation stated in eq. (3.13) occurs, as usual, between a virtual term, the one-loop soft function $S_n^{(1)}$, and a real-radiation term, the integrated radiative soft function $\int d\Phi(k)S_{n,g}^{(0)}$. The virtual contribution is understood to be renormalised, so it is affected only by infrared (soft and collinear) divergences (indeed, the bare Wilson-line correlator vanishes beyond tree level, since it is constructed out of scale-less integrals). The phase-space integral of the real-radiation contribution, on the other hand, diverges at large values of the radiated momentum, since the soft gluon energy is not constrained by momentum conservation in the eikonal approximation.

In order to regulate this UV singularity, we introduce a soft cross section at *fixed total final-state energy*, following [106], and then we integrate over this energy up to a finite cutoff, matching the scale of the virtual correction. Concretely, we displace one of the two Wilson line correlators defining the soft cross section by a finite timelike vector $y^\mu = \{y, \mathbf{0}\}$, and we introduce the finite quantity

$$\int_0^\lambda d\xi \int \frac{dy}{2\pi} e^{i\xi y} \langle 0 | \bar{T} \left[\prod_{i=1}^n \Phi_{\beta_i}(0, \infty) \right] T \left[\prod_{i=1}^n \Phi_{\beta_i}(\infty, y) \right] | 0 \rangle = \text{finite}. \quad (\text{A.1})$$

The timelike displacement y corresponds to the Fourier conjugate of a cutoff on the energy of the final state, represented here by λ . By letting $y \rightarrow 0$ in the correlator, or by letting the ξ integration run unconstrained, one recovers the *r.h.s.* of eq. (3.10). Expanding eq. (A.1) to NLO (see also the *l.h.s.* of eq. (3.10)), we obtain the completeness relation

$$\int_0^\lambda d\xi \int \frac{dy}{2\pi} e^{i\xi y} \left\{ \langle 0 | \bar{T} \left[\prod_{i=1}^n \Phi_{\beta_i}(0, \infty) \right] | 0 \rangle \langle 0 | T \left[\prod_{i=1}^n \Phi_{\beta_i}(\infty, y) \right] | 0 \rangle \Big|_{\text{one-loop}} \right. \\ \left. + \int d\Phi(k) \langle 0 | \bar{T} \left[\prod_{i=1}^n \Phi_{\beta_i}(0, \infty) \right] | k \rangle \langle k | T \left[\prod_{i=1}^n \Phi_{\beta_i}(\infty, y) \right] | 0 \rangle \Big|_{\text{tree}} \right\} = \text{finite}, \quad (\text{A.2})$$

where $d\Phi(k)$ is the phase-space measure of the radiated gluon. Using translational invariance of the vacuum, which implies

$$\langle 0 | T \left[\prod_{i=1}^n \Phi_{\beta_i}(\infty, y) \right] | 0 \rangle = \langle 0 | T \left[\prod_{i=1}^n \Phi_{\beta_i}(\infty, 0) \right] | 0 \rangle, \quad (\text{A.3})$$

the first term can be shown to equal $S_n^{(1)}$. The second term, on the other hand, evaluates to $\int d\Phi(k) \Theta(\lambda - k^0) S_{n,g}^{(0)}$, where k^0 is the energy component of the total final-state momentum. This modified version of the completeness relation in eq. (3.13) makes the dependence on the energy cutoff λ manifest, as we can write

$$S_n^{(1)} + \int d\Phi(k) \Theta(\lambda - k^0) S_{n,g}^{(0)} = \text{finite}. \quad (\text{A.4})$$

We can now proceed with the explicit validation of eq. (A.4). First we need to obtain a cross-section-level expression for the single-radiative soft function. This can be easily achieved by squaring the result in eq. (5.3), and summing over the polarisation and colour degrees of freedom relevant for the emission of momentum k . We obtain, as expected, the well-known result

$$S_{n,g}^{(0)} = -g_s^2 \mu^{2\epsilon} \sum_{i \neq j=1}^n \mathbf{T}_i \cdot \mathbf{T}_j \frac{\beta_i \cdot \beta_j}{(\beta_i \cdot k)(\beta_j \cdot k)}. \quad (\text{A.5})$$

Next, we perform the phase-space integration over $d\Phi(k)$ by parametrising the momentum of the radiated gluon as $k^\mu = x\beta_i^\mu + y\beta_j^\mu + k_\perp^\mu$. The integrand and the measure in eq. (A.4) become then

$$d\Phi(k) \Theta(\lambda - k^0) S_{n,g}^{(0)} = -2\alpha_s \mu^{2\epsilon} \sum_{i \neq j=1}^n \mathbf{T}_i \cdot \mathbf{T}_j \frac{dx}{x} \frac{dy}{y} \frac{d^{d-2}k_\perp}{(2\pi)^{d-2}} \delta(2xy \beta_i \cdot \beta_j + k_\perp \cdot k_\perp) \\ \times \Theta(x\beta_i^0 + y\beta_j^0) \Theta(\lambda - x\beta_i^0 - y\beta_j^0). \quad (\text{A.6})$$

The integrals over x , y and k_\perp can be performed to arrive at

$$\int d\Phi(k) \Theta(\lambda - k^0) S_{n,g}^{(0)} = -\frac{\alpha_s}{2\pi} \sum_{i \neq j=1}^n \mathbf{T}_i \cdot \mathbf{T}_j \left[\frac{1}{\epsilon^2} - \frac{1}{\epsilon} \ln \frac{4\lambda^2}{\mu^2} + \mathcal{O}(\epsilon^0) \right]. \quad (\text{A.7})$$

The virtual soft function $S_n^{(1)}$ is given by the first line on the *r.h.s.* of eq. (5.4),

$$S_n^{(1)} = \frac{\alpha_s}{2\pi} \sum_{i \neq j=1}^n \mathbf{T}_i \cdot \mathbf{T}_j \left[\frac{1}{\epsilon^2} - \frac{1}{\epsilon} \ln \frac{2p_i \cdot p_j}{\mu^2} \right]. \quad (\text{A.8})$$

After identifying $\lambda^2 = p_i \cdot p_j/2$, we have satisfied eq. (A.4). Note that the choice of the cutoff λ is arbitrary: indeed, the numerical factor in the argument of the logarithm in eq. (A.8) can be freely chosen by rescaling the momenta p_i and p_j . This ambiguity is cancelled by an equivalent calculation for the eikonal jet function in eq. (3.14), where the hard momentum can be similarly rescaled [69, 70].

A.2 Collinear cancellation

The cancellation of collinear poles in eq. (3.15) has a different subtlety with respect to the soft cancellation discussed in Section A.1. Indeed, eq. (3.15) understands an explicit mapping to go from the $(n+1)$ -particle phase space of the real-radiation matrix element to the n -particle phase space of the virtual matrix element. In particular, we seek an expression that is locally finite in the n -body phase space: to be precise, we will prove a condition of the form

$$d\Phi(\bar{k}_r) d\Phi(k_{12}) J_{f,f_1}^{(1)}(\bar{\ell}; k_{12}) + d\Phi(k_r) d\Phi(k_1) \int d\Phi(k_2) J_{f,f_1 f_2}^{(0)}(\ell; k_1, k_2) = \text{finite}. \quad (\text{A.9})$$

This describes the splitting $k_{12} \rightarrow k_1 + k_2$, with momentum k_r acting as a spectator. Note that all the momenta in eq. (A.9) are on-shell and massless, except the ‘parent’ momenta ℓ and $\bar{\ell}$, which are fixed by the δ functions implicit in the jet definitions. The advantage of eq. (A.9), as compared to eq. (3.15), is that it is local in k_{12} and k_1 , *i.e.* we only integrate the momentum of the radiated parton, k_2 . We will now show that eq. (A.9) holds, using as an example the splitting $q \rightarrow qg$.

We start with the second term, where the integrand (discussed in Appendix B) is given by [102]

$$J_{q,qg}^{(0)}(\ell; k_1, k_2) = \frac{4\pi\alpha_s C_F}{(k_1 \cdot k_2)} (2\pi)^d \delta^d(\ell - k_1 - k_2) \left\{ \left[1 + \frac{2(k_1 \cdot n)}{(k_2 \cdot n)} - \frac{(k_1 \cdot k_2)}{(k_2 \cdot n)^2} n^2 \right] \not{k}_1 \right. \\ \left. + \left[1 - \epsilon + \frac{(k_1 \cdot n)}{(k_2 \cdot n)} \right] \not{k}_2 - \frac{(k_1 \cdot k_2)}{(k_2 \cdot n)} \not{n} \right\}, \quad (\text{A.10})$$

where we keep $n^2 \neq 0$ to regulate spurious collinear singularities. We note that the above expression reduces to the usual Altarelli-Parisi splitting kernel P_{qg} upon taking the collinear $k_1 || k_2$ limit. Next, we apply the Catani-Seymour mapping $(k_1, k_2, k_r) \rightarrow (k_{12}, \bar{k}_r)$ [7],

$$k_{12} = k_1 + k_2 - \frac{s_{12}}{s_{1r} + s_{2r}} k_r, \\ \bar{k}_r = \frac{s_{12} + s_{1r} + s_{2r}}{s_{1r} + s_{2r}} k_r, \\ \delta^{(d)}(\ell - k_1 - k_2) = \delta^{(d)}(\bar{\ell} - k_{12}), \quad (\text{A.11})$$

where $s_{ir} = 2k_i \cdot k_r$ for $i = 1, 2$, and ℓ is mapped to $\bar{\ell}$ so that the δ functions align in eq. (A.9). The jacobian of this change of variables is

$$d\Phi(k_r) d\Phi(k_1) d\Phi(k_2) = d\Phi(\bar{k}_r) d\Phi(k_{12}) d\Phi(k_2) \times \left(\frac{s_{1r} + s_{2r}}{s_{12} + s_{1r} + s_{2r}} \right)^{d-3} \left(\frac{s_{1r} + s_{2r}}{s_{1r}} \right) \Theta \left(\frac{s_{1r}}{s_{1r} + s_{2r}} \right) \Theta \left(\frac{s_{1r} + s_{2r}}{s_{12} + s_{1r} + s_{2r}} \right). \quad (\text{A.12})$$

As the vector n in the jet function definition is arbitrary, we simplify the integration by choosing $n = k_{12} + \bar{k}_r$, so that $n^2 \neq 0$. The integration then depends on only two light-like momenta, \bar{k}_r and k_{12} , instead of three. We use them to parameterise k_2 as

$$k_2 = z k_{12} + y (1 - z) \bar{k}_r + k_{2\perp}. \quad (\text{A.13})$$

Our phase space is then

$$d\Phi(k_r) d\Phi(k_1) d\Phi(k_2) = d\Phi(\bar{k}_r) d\Phi(k_{12}) d\Phi(k_2) \frac{(1-y)^{1-2\epsilon}}{1-z} \Theta(1-z) \Theta(1-y). \quad (\text{A.14})$$

Integrating eq. (A.10) over z, y and $k_{2\perp}$ we arrive at

$$d\Phi(k_r) d\Phi(k_1) \int d\Phi(k_2) J_{f,f_1 f_2}^{(0)}(\ell; k_1, k_2) = (2\pi)^d \delta^{(d)}(\bar{\ell} - k_{12}) d\Phi(k_{12}) d\Phi(\bar{k}_r) \times \frac{\alpha_s C_F}{2\pi} \left\{ \left[\frac{1}{\epsilon^2} + \frac{1}{\epsilon} \left(\frac{5}{2} - \log \frac{\mu^2}{2k_{12} \cdot k_r} \right) \right] k_{12} + \mathcal{O}(\epsilon^0) \right\}. \quad (\text{A.15})$$

Reinstating the dependence on an arbitrary n by writing $k_{12} \cdot \bar{k}_r = 2(k_{12} \cdot n)^2/n^2$, we recognise in the second line the structure of the one-loop virtual jet function $J_{q,q}^{(1)}$, which is given by [69]

$$J_{q,q}^{(1)}(\bar{\ell}; k_{12}) = -(2\pi)^d \delta^{(d)}(\bar{\ell} - k_{12}) \frac{\alpha_s C_F}{2\pi} \left[\frac{1}{\epsilon^2} + \frac{1}{\epsilon} \left(\frac{5}{2} - \log \frac{n^2 \mu^2}{(2k_{12} \cdot n)^2} \right) + \mathcal{O}(\epsilon^0) \right] k_{12}, \quad (\text{A.16})$$

which completes the proof of the cancellation of collinear poles according to eq. (A.9).

B Tree-level radiative jet functions for different partonic processes

In this Appendix we give explicit expressions for tree-level single-radiative jet functions for QCD partonic processes. In the process, we recover the Altarelli-Parisi splitting functions by considering the collinear limit of the results, expressed as the limit $k_\perp \rightarrow 0$ in the Sudakov parametrisation of radiative momenta,

$$k_1^\mu = z p^\mu + k_\perp^\mu - A n^\mu, \quad k_2^\mu = (1-z) p^\mu - k_\perp^\mu - B n^\mu, \quad (\text{B.1})$$

where p is the collinear light-like direction, and

$$A = -\frac{z p \cdot n}{n^2} \left(1 - \sqrt{1 - \frac{n^2 k_\perp^2}{(z p \cdot n)^2}} \right), \quad B = A|_{z \rightarrow 1-z}. \quad (\text{B.2})$$

We have checked that a similar, lengthier calculation for double-radiative process yields the Catani-Grazzini [84] double splitting kernels for all the relevant partonic processes.

For the $q \rightarrow qg$ process the calculation yields eq. (A.10), which we reproduce here for convenience:

$$J_{q,qg}^{(0)}(\ell; k_1, k_2) = \frac{4\pi\alpha_s C_F}{(k_1 \cdot k_2)} (2\pi)^d \delta^d(\ell - k_1 - k_2) \left\{ \left[1 + \frac{2(k_1 \cdot n)}{(k_2 \cdot n)} - \frac{(k_1 \cdot k_2)n^2}{(k_2 \cdot n)^2} \right] k_1 + \left[1 - \epsilon + \frac{(k_1 \cdot n)}{(k_2 \cdot n)} \right] k_2 - \frac{(k_1 \cdot k_2)}{(k_2 \cdot n)} \not{n} \right\}. \quad (\text{B.3})$$

In the limit $k_\perp \rightarrow 0$ one recovers the P_{qg} splitting function:

$$\begin{aligned} J_{q,gg}^{(0)}(\ell; k_1, k_2) &= \frac{4\pi\alpha_s}{(k_1 \cdot k_2)} C_F \left[\frac{1+z^2}{1-z} - \epsilon(1-z) \right] \not{p} (2\pi)^d \delta^{(d)}(\ell-p) + \mathcal{O}(k_\perp^0) \\ &= \frac{4\pi\alpha_s}{(k_1 \cdot k_2)} P_{qg}(z) \not{p} (2\pi)^d \delta^{(d)}(\ell-p) + \mathcal{O}(k_\perp^0). \end{aligned} \quad (\text{B.4})$$

For a gluon radiating a quark-antiquark pair, summing over massless flavours, we find

$$\begin{aligned} J_{g,q\bar{q}}^{(0)}(\ell; k_1, k_2) &= \frac{4\pi\alpha_s n_f T_R}{(k_1 \cdot k_2)} \left[-g^{\mu\nu} + \frac{2(k_1 \cdot n)(k_2 \cdot n) - n^2(k_1 \cdot k_2)}{(k_1 \cdot k_2)(\ell \cdot n)^2} (k_1^\mu k_2^\nu + k_1^\nu k_2^\mu) \right. \\ &\quad - \frac{n^2(k_1 \cdot k_2)(k_1^\mu k_1^\nu + k_2^\mu k_2^\nu) + 2(k_2 \cdot n)^2 k_1^\mu k_1^\nu + 2(k_1 \cdot n)^2 k_2^\mu k_2^\nu}{(k_1 \cdot k_2)(\ell \cdot n)^2} \\ &\quad \left. + \frac{1}{(\ell \cdot n)} (k_1^\nu n^\mu + k_2^\nu n^\mu + k_1^\mu n^\nu + k_2^\mu n^\nu) \right] (2\pi)^d \delta^{(d)}(\ell - k_1 - k_2). \end{aligned} \quad (\text{B.5})$$

In the collinear limit, we recover the $P_{q\bar{q}}$ splitting function:

$$\begin{aligned} J_{g,q\bar{q}}^{(0)\mu\nu}(\ell; k_1, k_2) &= \frac{4\pi\alpha_s}{(k_1 \cdot k_2)} d_\rho^\mu(p, n) n_f T_R \left(-g^{\rho\sigma} + 4z(1-z) \frac{k_\perp^\rho k_\perp^\sigma}{k_\perp^2} \right) \\ &\quad \times d_\sigma^\nu(p, n) (2\pi)^d \delta^{(d)}(\ell-p) + \mathcal{O}(k_\perp^0) \\ &= \frac{4\pi\alpha_s}{(k_1 \cdot k_2)} d_\rho^\mu(p, n) n_f P_{q\bar{q}}^{\rho\sigma}(z) d_\sigma^\nu(p, n) (2\pi)^d \delta^{(d)}(\ell-p) + \mathcal{O}(k_\perp^0), \end{aligned} \quad (\text{B.6})$$

where $d^{\mu\nu}(p, n)$ is the gluon polarisation tensor for non-light-like reference momenta,

$$d^{\mu\nu}(p, n) = -g^{\mu\nu} + \frac{p^\mu n^\nu + p^\nu n^\mu}{p \cdot n} - n^2 \frac{p^\mu p^\nu}{(p \cdot n)^2}. \quad (\text{B.7})$$

For a gluon radiating to two gluons the full result is somewhat lengthier, and we find

$$\begin{aligned} J_{g,gg}^{(0)\mu\nu}(\ell; k_1, k_2) &= \frac{4\pi\alpha_s C_A}{(k_1 \cdot k_2)} \left\{ g^{\mu\nu} \left[\frac{n^2(k_1 \cdot k_2)}{(k_2 \cdot n)^2} - \frac{2(k_1 \cdot n)}{(k_2 \cdot n)} \right] - \frac{k_1^\mu k_2^\nu}{(\ell \cdot n)^2} \left[\frac{2(1-\epsilon)(k_1 \cdot n)(k_2 \cdot n)}{(k_1 \cdot k_2)} \right. \right. \\ &\quad \left. \left. + \frac{n^2}{(k_1 \cdot n)(k_2 \cdot n)} (n^2(k_1 \cdot k_2) + (k_1 \cdot n)^2 + (k_2 \cdot n)^2) \right] \right. \\ &\quad \left. + \frac{k_1^\mu k_1^\nu}{(\ell \cdot n)^2} \left[\frac{2(1-\epsilon)(k_2 \cdot n)^2}{(k_1 \cdot k_2)} - 2n^2 \left(1 + \frac{(k_1 \cdot n)}{(k_2 \cdot n)} + \frac{(k_2 \cdot n)}{(k_1 \cdot n)} \right) + \frac{(n^2)^2(k_1 \cdot k_2)}{(k_2 \cdot n)^2} \right] \right. \\ &\quad \left. + \frac{k_1^\mu n^\nu + k_1^\nu n^\mu}{(\ell \cdot n)} \left[1 + 2 \frac{(k_1 \cdot n)}{(k_2 \cdot n)} + \frac{(k_2 \cdot n)}{(k_1 \cdot n)} + \frac{n^2(k_1 \cdot k_2)((k_2 \cdot n) - (k_1 \cdot n))}{(k_1 \cdot n)(k_2 \cdot n)^2} \right] \right. \\ &\quad \left. - \frac{(k_1 \cdot k_2)}{(k_1 \cdot n)(k_2 \cdot n)} n^\mu n^\nu + (k_1 \leftrightarrow k_2) \right\} (2\pi)^d \delta^{(d)}(\ell - k_1 - k_2). \end{aligned} \quad (\text{B.8})$$

In the collinear limit, eq. (B.8) reproduces the P_{gg} splitting function:

$$\begin{aligned} J_{g,gg}^{(0)\mu\nu}(\ell; k_1, k_2) &= \frac{4\pi\alpha_s}{(k_1 \cdot k_2)} d_\rho^\mu(p, n) 2C_A \left[-g^{\rho\sigma} \left(\frac{z}{1-z} + \frac{1-z}{z} \right) - 2(1-\epsilon)z(1-z) \frac{k_\perp^\rho k_\perp^\sigma}{k_\perp^2} \right] \\ &\quad \times d_\sigma^\nu(p, n) (2\pi)^d \delta^{(d)}(\ell-p) + \mathcal{O}(k_\perp^0) \\ &= \frac{4\pi\alpha_s}{(k_1 \cdot k_2)} d_\rho^\mu(p, n) P_{gg}^{\rho\sigma}(z) d_\sigma^\nu(p, n) (2\pi)^d \delta^{(d)}(\ell-p) + \mathcal{O}(k_\perp^0). \end{aligned} \quad (\text{B.9})$$

Finally, the single-radiative eikonal jet function is given by

$$J_{E_f,g}^{(0)}(\beta; k) = 4\pi\alpha_s C_f \left[\frac{2(\beta \cdot n)}{(\beta \cdot k)(k \cdot n)} - \frac{n^2}{(k \cdot n)^2} \right], \quad (\text{B.10})$$

and can be obtained both by direct calculation, or by taking the soft limit of either eq. (B.3) or eq. (B.8): as expected, it is spin-independent.

C On the computation of radiative jet functions at one loop

In this Appendix we summarise the techniques relevant for the calculation of one-loop single-radiative jet functions for the required flavour structures, and we give some details about their renormalisation. For all the relevant processes, the underlying integrals can be written in terms of the family

$$T_{a_1 a_2 a_3 a_4} = \int \frac{d^d k}{i\pi^{d/2}} \frac{e^{\epsilon\gamma_E}}{(k^2)^{a_1} ((p_i - k)^2)^{a_2} ((p_i + p_j - k)^2)^{a_3} (k \cdot n)^{a_4}}, \quad (\text{C.1})$$

with a_i being non-negative integers, $p_i^2 = p_j^2 = 0$, and we can set $p_i \cdot p_j = -1$ (a negative value is useful to simplify numerical tests); furthermore, as mentioned in the main text, in order to avoid unphysical collinear divergences, we set $n^2 = 1$. The numerical values for the invariants $p_i \cdot p_j$ and n^2 are chosen so as to simplify the calculation: the dependence on such invariants can be fully reconstructed using the mass dimension of the integral and its scaling with respect to n , respectively. In the case of partonic jet functions, the momenta p_i and p_j are the outgoing partonic momenta, whereas, for the eikonal, jet one of them should be thought of as the light-like Wilson-line velocity. The integral family in eq. (C.1) can be computed from the basis integrals T_{0011} , T_{0101} , T_{1010} , T_{1011} and T_{1111} . In particular, the integrals T_{0011} , T_{0101} and T_{1010} can be easily evaluated to all orders in ϵ by Feynman parameterisation. For instance,

$$T_{0101} = 2 (-2p_i \cdot n)^{1-2\epsilon} e^{\epsilon\gamma_E} \Gamma(1-\epsilon)\Gamma(2\epsilon-1), \quad T_{1010} = \frac{2^{-\epsilon} e^{\epsilon\gamma_E} \Gamma(1-\epsilon)^2 \Gamma(\epsilon)}{\Gamma(2-2\epsilon)}, \quad (\text{C.2})$$

and similarly for $T_{0011} = T_{0101}|_{p_i \rightarrow p_i + p_j}$. We note that the integral T_{1011} is finite in ϵ and, therefore, is not needed for the present analysis. On the other hand, there is one non-standard integral we have to evaluate, namely the IR divergent box integral T_{1111} . To tackle this calculation we exploit the method of differential equations.

As a first step, we assemble the integral basis

$$\mathbf{f} = \left\{ \frac{\epsilon(1-2\epsilon)}{(p_i + p_j) \cdot n} T_{0011}, \frac{\epsilon(1-2\epsilon)}{p_i \cdot n} T_{0101}, \epsilon(1-2\epsilon) T_{1010}, \epsilon^2 \sqrt{2 + ((p_i + p_j) \cdot n)^2} T_{1011}, \right. \\ \left. \epsilon^2 (p_i \cdot n) T_{1111} \right\}. \quad (\text{C.3})$$

Then, we define new variables, t_1 and t_2 , to remove any square roots that may appear in the integral basis \mathbf{f} . They are implicitly defined by

$$p_i \cdot n = \frac{2\sqrt{2} t_1 t_2}{t_1^2 - (1+t_2)^2}, \quad p_j \cdot n = \frac{2\sqrt{2} t_1}{t_1^2 - (1+t_2)^2}. \quad (\text{C.4})$$

Using this basis and these variables has the advantage that the differential equations take the canonical form [120]

$$d\mathbf{f}(\epsilon, t_1, t_2) = \epsilon \left[\sum_{l \in \mathcal{A}} A_l d \log(l) \right] \cdot \mathbf{f}(\epsilon, t_1, t_2), \quad (\text{C.5})$$

where the A_l are constant 5×5 matrices, each associated to a letter l in the alphabet

$$\mathcal{A} = \left\{ t_1, t_2 + 1, t_2, \frac{t_1 + t_2 + 1}{1 - t_1 + t_2}, t_1^2 + t_2^2 + 2t_2 + 1, 1 - t_1^2 + t_2^2 + 2t_2, \right. \\ \left. t_1^2 - 2t_1 t_2 + 2t_1 + t_2^2 + 2t_2 + 1, t_1^2 + 2t_1 t_2 - 2t_1 + t_2^2 + 2t_2 + 1 \right\}. \quad (\text{C.6})$$

The overall ϵ factor in eq. (C.3) is chosen so that \mathbf{f} admits an expansion in ϵ starting at $\mathcal{O}(\epsilon^0)$. We can then integrate eq. (C.5) in terms of iterated integrals. In principle, one can compute the integrals to arbitrary order in ϵ , assuming the appropriate boundary conditions are known. In our case, however, as we are only interested in the poles of the jet functions, one iteration of the differential equations is sufficient. This corresponds to functions that have a transcendental weight of one, which is the highest possible weight that can appear. Notice that f_1, f_2 and f_3 are given by eq. (C.2), and the first non-vanishing term of f_4 will be of weight two. We can then focus directly on f_5 : upon solving eq. (C.5), without specifying the boundary conditions, we get an expression of the form

$$f_5 = c_0 + \epsilon \left[c_1 + \log g(t_1, t_2) \right] + \mathcal{O}(\epsilon^2), \quad (\text{C.7})$$

where $g(t_1, t_2)$ is a known polynomial built from the letters in the alphabet \mathcal{A} , c_0 is of weight zero, and c_1 is of weight one, ensuring that eq. (C.7) is of uniform weight. The values of the coefficients can be found by computing f_5 numerically, for example using `pySecDec` [121, 122], and then fitting the result: it turns out that $c_0 = -\frac{3}{4}$, and $c_1 = \frac{7}{4} \log 2$. Inverting eq. (C.3) for T_{1111} , and reinstating the Mandelstam invariants, we finally find

$$T_{1111} = \frac{(-p_i \cdot p_j)^{-1-\epsilon}}{2p_i \cdot n} \left[-\frac{3}{2} \frac{1}{\epsilon^2} + \frac{1}{2} \frac{1}{\epsilon} \log \left(\frac{-2(p_i \cdot n)^2}{(p_i + p_j) \cdot n \sqrt{n^2} \sqrt{-p_i \cdot p_j}} \right) + \mathcal{O}(\epsilon^0) \right]. \quad (\text{C.8})$$

A similar calculation leads to the eikonal version of eq. (C.8), which we compute using $p^2 = \beta^2 = 0$. Up to $\mathcal{O}(\epsilon^0)$ corrections, we find

$$\int \frac{d^d k}{i\pi^{d/2}} \frac{e^{\epsilon\gamma_E}}{k^2(p-k)^2((k-p)\cdot\beta)k\cdot n} = \frac{1}{(p\cdot n)(p\cdot\beta)} \left[\frac{3}{2} \frac{1}{\epsilon^2} + \frac{1}{2} \frac{1}{\epsilon} \log \left(\frac{n^2(2\beta\cdot n)^2}{(2p\cdot n)^4(2p\cdot\beta)^2} \right) \right]. \quad (\text{C.9})$$

In order to complete our discussion about one-loop radiative jet functions, we report below the renormalisation factors in the $\overline{\text{MS}}$ scheme that were used in Section 5.3. They are given by

$$Z_\psi = 1 - \frac{\alpha_s}{4\pi} \frac{1}{\epsilon} C_F + \mathcal{O}(\alpha_s^2), \quad \text{quark field}, \quad (\text{C.10a})$$

$$Z_A = 1 + \frac{\alpha_s}{4\pi} \frac{1}{\epsilon} \left(\frac{5}{3} C_A - \frac{2}{3} n_f \right) + \mathcal{O}(\alpha_s^2), \quad \text{gluon field}, \quad (\text{C.10b})$$

$$Z_g = 1 - \frac{\alpha_s}{4\pi} \frac{1}{\epsilon} (C_F + C_A) + \mathcal{O}(\alpha_s^2), \quad q\bar{q}g \text{ vertex}, \quad (\text{C.10c})$$

$$Z_{ggg} = 1 + \frac{\alpha_s}{4\pi} \frac{1}{\epsilon} \frac{2}{3} (C_A - n_f) + \mathcal{O}(\alpha_s^2), \quad ggg \text{ vertex}, \quad (\text{C.10d})$$

$$Z_{W_i} = 1 + \frac{\alpha_s}{4\pi} \frac{2}{\epsilon} C_{f_i} + \mathcal{O}(\alpha_s^2), \quad \text{Wilson line}, \quad (\text{C.10e})$$

$$Z_{V\psi} = 1 - \frac{\alpha_s}{4\pi} \frac{1}{\epsilon} C_F + \mathcal{O}(\alpha_s^2), \quad q - \text{Wilson-line vertex}, \quad (\text{C.10f})$$

$$Z_{VA} = 1 + \mathcal{O}(\alpha_s^2), \quad g - \text{Wilson-line vertex}. \quad (\text{C.10g})$$

Eqs. (C.10a)-(C.10d) are standard textbook QCD results. Eq. (C.10e) can be found for instance in [69]. Eqs. (C.10f) and (C.10g) were found by explicit computation of the diagrams involved. We also derive the renormalisation factors for the coupling of a Wilson line radiating a gluon, see figure 3: they are given by

$$Z_{W_{FA}} = Z_g Z_\psi^{-1} Z_{W_F} = 1 + \frac{\alpha_s}{2\pi} \frac{1}{\epsilon} \left(C_F - \frac{C_A}{2} \right), \quad \text{fundamental Wilson line} \quad (\text{C.11a})$$

$$Z_{W_{AA}} = Z_{ggg} Z_A^{-1} Z_{W_A} = 1 + \frac{\alpha_s}{2\pi} \frac{1}{\epsilon} \frac{C_A}{2}, \quad \text{adjoint Wilson line}. \quad (\text{C.11b})$$

Note that both colour factors in eq. (C.11) are of the form $(C_{f_i} - N_c/2)$ expected for vertex graphs. Since also

$$Z_g Z_\psi^{-1} Z_A^{-1/2} = Z_{ggg} Z_A^{-3/2} \equiv Z_{\alpha_s} = 1 - \frac{\alpha_s}{4\pi} \frac{1}{\epsilon} \frac{b_0}{2} + \mathcal{O}(\alpha_s^2), \quad (\text{C.12})$$

the jets $J_{g,gg}^{\mu\nu}(\ell; k_1, k_2)$ and $J_{g,qq}^{\mu\nu}(\ell; k_1, k_2)$ renormalise in the same way.

Finally, the renormalisation factor related to the vertex connecting the Wilson lines in directions β_i and n is given by the usual cusp renormalisation, involving an extra collinear pole. It is given by

$$Z_{\beta_i n} = 1 - \frac{\alpha_s}{4\pi} C_{f_i} \left(\frac{1}{\epsilon^2} + \frac{1}{\epsilon} \log \frac{n^2}{4(\beta_i \cdot n)^2} \right). \quad (\text{C.13})$$

D Consistency relations

In Section 6.3 we mentioned the necessity to verify the relation $\mathbf{L}_1[K_{n+2}^{(2)}] = \mathbf{L}_1[K_{n+2}^{(12)}]$ in order to confirm the consistency of the strongly-ordered counterterm we derived. Here we report the relevant details of the calculation. We note once again that, when hard-collinear configurations are involved, factorised matrix elements involve convolutions (which are understood in our notation). In these cases the tests we perform below rely on the assumption that the necessary phase-space mappings are chosen consistently, ensuring that they behave properly under iterated limits.

We start by acting on $K_{n+2}^{(2)}$ with the soft limit \mathbf{S}_1 , *i.e.* considering the $k_1 \rightarrow 0$ limit of each of the constituent counterterms in eqs. (3.27) to (3.30). As for the double-soft counterterm in eq. (3.27), accounting for two uniform soft emissions, we get

$$\mathbf{S}_1 \left[K_{n+2}^{(2,2s)} \right] = \mathcal{H}_n^{(0)\dagger} S_{n;g_2,g_1}^{(0)} \mathcal{H}_n^{(0)} = \mathcal{H}_n^{(0)\dagger} S_{n,g_2}^{(0)\dagger} S_{n+1,g_1}^{(0)} S_{n,g_2}^{(0)} \mathcal{H}_n^{(0)}, \quad (\text{D.1})$$

where we have used eq. (4.3). In order to compare this expression with the soft limit of $K_{n+2}^{(12,s)}$, we note that eq. (6.6) is written assuming k_2 , as opposed to k_1 , to be the unresolved momentum, hence a meaningful comparison with eq. (D.1) needs a $1 \leftrightarrow 2$ relabelling of eq. (6.6). We get then

$$\begin{aligned} \mathbf{S}_1 \left[K_{n+2}^{(12,s)} \right] &= \mathcal{H}_n^{(0)\dagger} \sum_{f_1, f_2} \mathbf{S}_1 \left[S_{n;f_{[12]},f_1}^{(0)} + S_{n,f_{[12]}}^{(0)} \left(J_{f_{[12]},f_1 f_2}^{(0)} - J_{E_{[12]},f_1}^{(0)} \right) \right] \mathcal{H}_n^{(0)} \\ &= \mathcal{H}_n^{(0)\dagger} S_{n;g_2,g_1}^{(0)} \mathcal{H}_n^{(0)} = \mathbf{S}_1 \left[K_{n+2}^{(2,2s)} \right], \end{aligned} \quad (\text{D.2})$$

where we have used $\mathbf{S}_1 J_{f_{[12]},f_1 f_2}^{(0)} = J_{E_{[12]},f_1}^{(0)}$. Next we consider the hard-collinear counterterm associated with a single leg, given by $K_{n+2,i}^{(2,2hc)}$ in eq. (3.28). The single-soft limit of the various contributions to this counterterm read

$$\begin{aligned} \mathbf{S}_1 \left[J_{f_i, f_1 f_2 f_3}^{(0)} \right] &= J_{f_i, f_2 f_3}^{(0)} S_{3, f_1}^{(0)}, \\ \mathbf{S}_1 \left[J_{E_i, f_1 f_k}^{(0)} \right] &= J_{E_i, f_k}^{(0)} S_{3, f_1}^{(0)}, \quad k = 2, 3, \\ \mathbf{S}_1 \left[J_{E_i, f_2 f_3}^{(0)} \right] &= 0, \\ \mathbf{S}_1 \left[J_{E_i, f_1}^{(0)} J_{f_i, f_2 f_3}^{(0), hc} \right] &= J_{E_i, f_1}^{(0)} J_{f_i, f_2 f_3}^{(0), hc}, \\ \mathbf{S}_1 \left[J_{E_i, f_j}^{(0)} J_{f_i, f_1 f_k}^{(0), hc} \right] &= 0, \quad j, k = 2, 3, \end{aligned} \quad (\text{D.3})$$

where $S_{3, f_1}^{(0)}$ is the same object appearing in eq. (6.4), namely a soft function formed from three Wilson lines in the directions β_2 , β_3 and n (the latter being the auxiliary vector used in the definition

of the jet functions), radiating a gluon with momentum k_1 . Plugging these limits into eq. (3.28), we can assemble

$$\mathbf{S}_1 \left[K_{n+2,i}^{(2,2\text{hc})} \right] = \mathcal{H}_n^{(0)\dagger} \sum_{f_1, f_2, f_3} J_{f_i, f_2 f_3}^{(0), \text{hc}} \left(S_{3, f_1}^{(0)} - J_{E_i, f_1}^{(0)} \right) \mathcal{H}_n^{(0)}. \quad (\text{D.4})$$

We can compare this expression with the single-soft limit of eq. (6.8). For this purpose, we note that in eq. (6.8) the unresolved momentum is k_3 , hence a $1 \leftrightarrow 3$ relabelling is necessary. This gives

$$\begin{aligned} \mathbf{S}_1 \left[K_{n+2,i}^{(12, \text{hc})} \right] &= \mathcal{H}_n^{(0)\dagger} \sum_{f_1, f_2, f_3} \left[J_{f_i, f_2 f_3}^{(0), \text{hc}} \left(S_{3, f_1}^{(0)} - J_{E_i, f_1}^{(0)} \right) \right. \\ &\quad \left. + \mathbf{S}_1 \sum_{kl=\{23, 32\}} J_{f_i, f_{[1k]} f_l}^{(0), \text{hc}} \left(J_{f_{[1k]}, f_1 f_k}^{(0)} - J_{E_{[1k]}, f_1}^{(0)} \right) \right] \mathcal{H}_n^{(0)} \\ &= \mathcal{H}_n^{(0)\dagger} \sum_{f_1, f_2, f_3} J_{f_i, f_2 f_3}^{(0), \text{hc}} \left(S_{3, f_1}^{(0)} - J_{E_i, f_1}^{(0)} \right) \mathcal{H}_n^{(0)} = \mathbf{S}_1 \left[K_{n+2,i}^{(2, 2\text{hc})} \right]. \end{aligned} \quad (\text{D.5})$$

One can similarly show that $\mathbf{S}_1 \left[K_{n+2,ij}^{(2, 2\text{hc})} \right] = 0$, and furthermore one sees that $K_{n+2,i}^{(2, 1\text{hc}, 1\text{s})} = K_{n+2,i}^{(12, 1\text{hc}, 1\text{s})}$ before taking any limits. Therefore, the consistency test for the soft limit, $\mathbf{S}_1 \left[K_{n+2,i}^{(2)} \right] = \mathbf{S}_1 \left[K_{n+2,i}^{(12)} \right]$, is completed.

Next, we analyse the collinear \mathbf{C}_{12} limit of the double-unresolved counterterm. Beginning, as above, with the double-soft counterterm in eq. (3.27), we find

$$\mathbf{C}_{12} \left[K_{n+2}^{(2, 2\text{s})} \right] = \mathcal{H}_n^{(0)\dagger} \sum_{f_1, f_2} \mathbf{C}_{12} S_{n, f_1 f_2}^{(0)} \mathcal{H}_n^{(0)} = \mathcal{H}_n^{(0)\dagger} \sum_{f_1, f_2} S_{n, f_{[12]}}^{(0)} J_{f_{[12]}, f_1 f_2}^{(0)} \mathcal{H}_n^{(0)}. \quad (\text{D.6})$$

On the other hand, from eq. (6.6) we get

$$\begin{aligned} \mathbf{C}_{12} \left[K_{n+2}^{(12, \text{s})} \right] &= \mathcal{H}_n^{(0)\dagger} \sum_{f_1, f_2} \left[\mathbf{C}_{12} S_{n; f_{[12]}, f_2}^{(0)} (k_{[12]}, k_2) + S_{n, f_{[12]}}^{(0)} \left(J_{f_{[12]}, f_1 f_2}^{(0)} - J_{E_{[12]}, f_2}^{(0)} \right) \right] \mathcal{H}_n^{(0)} \\ &= \mathcal{H}_n^{(0)\dagger} \sum_{f_1, f_2} S_{n, f_{[12]}}^{(0)} J_{f_{[12]}, f_1 f_2}^{(0)} \mathcal{H}_n^{(0)} = \mathbf{C}_{12} \left[K_{n+2}^{(2, 2\text{s})} \right], \end{aligned} \quad (\text{D.7})$$

where we have used $\mathbf{C}_{12} S_{n; f_{[12]}, f_2}^{(0)} (k_{[12]}, k_2) = S_{n, f_{[12]}}^{(0)} J_{E_{[12]}, f_2}^{(0)}$. Moving on to the contributions of $K_{n+2,i}^{(2, 2\text{hc})}$ in eq. (3.28), we find

$$\begin{aligned} \mathbf{C}_{12} \left[J_{f_i, f_1 f_2 f_3}^{(0)} \right] &= J_{f_i, f_3 f_{[12]}}^{(0)} J_{f_{[12]}, f_1 f_2}^{(0)}, \\ \mathbf{C}_{12} \left[J_{E_i, f_1 f_2}^{(0)} \right] &= J_{E_i, f_{[12]}}^{(0)} J_{f_{[12]}, f_1 f_2}^{(0)}, \\ \mathbf{C}_{12} \left[J_{E_i, f_k f_3}^{(0)} \right] &= J_{E_{[12]}, f_k}^{(0)} J_{E_i, f_3}^{(0)}, \quad k = 1, 2, \\ \mathbf{C}_{12} \left[J_{E_i, f_j}^{(0)} J_{f_i, f_k f_3}^{(0), \text{hc}} \right] &= 0, \quad j, k = 1, 2, \\ \mathbf{C}_{12} \left[J_{E_i, f_3}^{(0)} J_{f_i, f_1 f_2}^{(0), \text{hc}} \right] &= J_{E_i, f_3}^{(0)} J_{f_i, f_1 f_2}^{(0), \text{hc}} = J_{E_i, f_3}^{(0)} J_{f_{[12]}, f_1 f_2}^{(0), \text{hc}}, \end{aligned} \quad (\text{D.8})$$

where spin indices have been understood. Combining these contributions we obtain the simple result

$$\mathbf{C}_{12} \left[K_{n+2,i}^{(2, 2\text{hc})} \right] = \mathcal{H}_n^{(0)\dagger} \sum_{f_1, f_2, f_3} J_{f_i, f_{[12]} f_3}^{(0), \text{hc}} J_{f_{[12]}, f_1 f_2}^{(0)} \mathcal{H}_n^{(0)}. \quad (\text{D.9})$$

This expression must be compared with the collinear limit of eq. (6.8), after the necessary $1 \leftrightarrow 3$ relabelling. We get

$$\begin{aligned} \mathbf{C}_{12} \left[K_{n+2,i}^{(\mathbf{12}, \text{hc})} \right] &= \mathcal{H}_n^{(0)\dagger} \mathbf{C}_{12} \sum_{f_1, f_2, f_3} \left[J_{f_i, f_2 f_3}^{(0), \text{hc}}(\bar{k}_2, \bar{k}_3) S_{3, f_1}^{(0)} - J_{f_i, f_2 f_3}^{(0), \text{hc}}(k_2, k_3) J_{\mathbb{E}_i, f_1}^{(0)} \right. \\ &\quad \left. + \sum_{kl=\{23, 32\}} J_{f_i, f_{[1k]} f_l}^{(0), \text{hc}} \left(J_{f_{[1k]}, f_1 f_k}^{(0)} - J_{\mathbb{E}_{[1k]}, f_1}^{(0)} \right) \right] \mathcal{H}_n^{(0)} \\ &= \mathcal{H}_n^{(0)\dagger} \mathbf{C}_{12} \sum_{f_1, f_2, f_3} J_{f_i, f_{[12]} f_3}^{(0), \text{hc}} \left[S_{3, f_1}^{(0)} + J_{f_{[12]}, f_1 f_2}^{(0)} - J_{\mathbb{E}_{[12]}, f_1}^{(0)} \right] \mathcal{H}_n^{(0)}. \end{aligned} \quad (\text{D.10})$$

Noting that $\mathbf{C}_{12} S_{3, f_1}^{(0)}(\beta_{[12]}, \beta_3, n) = J_{\mathbb{E}_{[12]}, f_1}^{(0)}(\beta_2, n)$, we finally get

$$\mathbf{C}_{12} \left[K_{n+2,i}^{(\mathbf{12}, \text{hc})} \right] = \mathcal{H}_n^{(0)\dagger} \sum_{f_1, f_2, f_3} J_{f_i, f_{[12]} f_3}^{(0), \text{hc}} J_{f_{[12]}, f_1 f_2}^{(0)} \mathcal{H}_n^{(0)} = \mathbf{C}_{12} \left[K_{n+2,i}^{(\mathbf{2}, \text{2hc})} \right]. \quad (\text{D.11})$$

The remaining counterterms do not cause any difficulties, since $K_{n+2,ij}^{(\mathbf{2}, \text{2hc})} = K_{n+2,ij}^{(\mathbf{12}, \text{2hc})}$, and similarly $K_{n+2,i}^{(\mathbf{2}, \text{1hc}, \text{1s})} = K_{n+2,i}^{(\mathbf{12}, \text{1hc}, \text{1s})}$. The collinear consistency check $\mathbf{C}_{12} [K_{n+2,i}^{(\mathbf{2})}] = \mathbf{C}_{12} [K_{n+2,i}^{(\mathbf{12})}]$ is thus completed. This, in turn, concludes the proof that $\mathbf{L}_1 [K_{n+2}^{(\mathbf{2})}] = \mathbf{L}_1 [K_{n+2}^{(\mathbf{12})}]$.

References

- [1] G. Heinrich, *Collider Physics at the Precision Frontier*, *Phys. Rept.* **922** (2021) 1 [2009.00516].
- [2] N. Agarwal, L. Magnea, C. Signorile-Signorile and A. Tripathi, *The infrared structure of perturbative gauge theories*, *Phys. Rept.* **994** (2023) 1 [2112.07099].
- [3] S. Badger, J. Henn, J. Plefka and S. Zoia, *Scattering Amplitudes in Quantum Field Theory*, **2306.05976**.
- [4] W.T. Giele, E.W.N. Glover and D.A. Kosower, *Higher order corrections to jet cross-sections in hadron colliders*, *Nucl. Phys. B* **403** (1993) 633 [hep-ph/9302225].
- [5] W.T. Giele, E.W.N. Glover and D.A. Kosower, *The inclusive two jet triply differential cross-section*, *Phys. Rev.* **D52** (1995) 1486 [hep-ph/9412338].
- [6] S. Frixione, Z. Kunszt and A. Signer, *Three jet cross-sections to next-to-leading order*, *Nucl. Phys.* **B467** (1996) 399 [hep-ph/9512328].
- [7] S. Catani and M.H. Seymour, *A General algorithm for calculating jet cross-sections in NLO QCD*, *Nucl. Phys.* **B485** (1997) 291 [hep-ph/9605323].
- [8] Z. Nagy and D.E. Soper, *General subtraction method for numerical calculation of one loop QCD matrix elements*, *JHEP* **09** (2003) 055 [hep-ph/0308127].
- [9] G. Bevilacqua, M. Czakon, M. Kubocz and M. Worek, *Complete Nagy-Soper subtraction for next-to-leading order calculations in QCD*, *JHEP* **10** (2013) 204 [1308.5605].
- [10] R.M. Prisco and F. Tramontano, *Dual subtractions*, *JHEP* **06** (2021) 089 [2012.05012].
- [11] S. Frixione and M. Grazzini, *Subtraction at NNLO*, *JHEP* **06** (2005) 010 [hep-ph/0411399].
- [12] A. Gehrmann-De Ridder, T. Gehrmann and E.W.N. Glover, *Antenna subtraction at NNLO*, *JHEP* **09** (2005) 056 [hep-ph/0505111].
- [13] J. Currie, E.W.N. Glover and S. Wells, *Infrared Structure at NNLO Using Antenna Subtraction*, *JHEP* **04** (2013) 066 [1301.4693].
- [14] G. Somogyi, Z. Trócsányi and V. Del Duca, *Matching of singly- and doubly-unresolved limits of tree-level QCD squared matrix elements*, *JHEP* **06** (2005) 024 [hep-ph/0502226].

- [15] G. Somogyi and Z. Trocsanyi, *A Subtraction scheme for computing QCD jet cross sections at NNLO: Regularization of real-virtual emission*, *JHEP* **01** (2007) 052 [[hep-ph/0609043](#)].
- [16] V. Del Duca, C. Duhr, A. Kardos, G. Somogyi and Z. Trócsányi, *Three-Jet Production in Electron-Positron Collisions at Next-to-Next-to-Leading Order Accuracy*, *Phys. Rev. Lett.* **117** (2016) 152004 [[1603.08927](#)].
- [17] V. Del Duca, C. Duhr, A. Kardos, G. Somogyi, Z. Ször, Z. Trócsányi et al., *Jet production in the CoLoRFulNNLO method: event shapes in electron-positron collisions*, *Phys. Rev.* **D94** (2016) 074019 [[1606.03453](#)].
- [18] M. Czakon, *A novel subtraction scheme for double-real radiation at NNLO*, *Phys. Lett.* **B693** (2010) 259 [[1005.0274](#)].
- [19] M. Czakon, *Double-real radiation in hadronic top quark pair production as a proof of a certain concept*, *Nucl. Phys.* **B849** (2011) 250 [[1101.0642](#)].
- [20] M. Czakon and D. Heymes, *Four-dimensional formulation of the sector-improved residue subtraction scheme*, *Nucl. Phys. B* **890** (2014) 152 [[1408.2500](#)].
- [21] C. Anastasiou, K. Melnikov and F. Petriello, *A new method for real radiation at NNLO*, *Phys. Rev. D* **69** (2004) 076010 [[hep-ph/0311311](#)].
- [22] F. Caola, K. Melnikov and R. Röntsch, *Nested soft-collinear subtractions in NNLO QCD computations*, *Eur. Phys. J.* **C77** (2017) 248 [[1702.01352](#)].
- [23] S. Catani and M. Grazzini, *An NNLO subtraction formalism in hadron collisions and its application to Higgs boson production at the LHC*, *Phys. Rev. Lett.* **98** (2007) 222002 [[hep-ph/0703012](#)].
- [24] M. Grazzini, S. Kallweit and M. Wiesemann, *Fully differential NNLO computations with MATRIX*, *Eur. Phys. J. C* **78** (2018) 537 [[1711.06631](#)].
- [25] R. Boughezal, K. Melnikov and F. Petriello, *A subtraction scheme for NNLO computations*, *Phys. Rev.* **D85** (2012) 034025 [[1111.7041](#)].
- [26] J. Gaunt, M. Stahlhofen, F.J. Tackmann and J.R. Walsh, *N-jettiness Subtractions for NNLO QCD Calculations*, *JHEP* **09** (2015) 058 [[1505.04794](#)].
- [27] R. Boughezal, C. Focke, X. Liu and F. Petriello, *W-boson production in association with a jet at next-to-next-to-leading order in perturbative QCD*, *Phys. Rev. Lett.* **115** (2015) 062002 [[1504.02131](#)].
- [28] G.F.R. Sborlini, F. Driencourt-Mangin and G. Rodrigo, *Four-dimensional unsubtraction with massive particles*, *JHEP* **10** (2016) 162 [[1608.01584](#)].
- [29] F. Herzog, *Geometric IR subtraction for final state real radiation*, *JHEP* **08** (2018) 006 [[1804.07949](#)].
- [30] L. Magnea, E. Maina, G. Pelliccioli, C. Signorile-Signorile, P. Torrielli and S. Uccirati, *Local analytic sector subtraction at NNLO*, *JHEP* **12** (2018) 107 [[1806.09570](#)].
- [31] G. Bertolotti, L. Magnea, G. Pelliccioli, A. Ratti, C. Signorile-Signorile, P. Torrielli et al., *NNLO subtraction for any massless final state: a complete analytic expression*, *JHEP* **07** (2023) 140 [[2212.11190](#)].
- [32] Z. Capatti, V. Hirschi, D. Kermanschah and B. Ruijl, *Loop-Tree Duality for Multiloop Numerical Integration*, *Phys. Rev. Lett.* **123** (2019) 151602 [[1906.06138](#)].
- [33] F. Devoto, K. Melnikov, R. Röntsch, C. Signorile-Signorile and D.M. Tagliabue, *A fresh look at the nested soft-collinear subtraction scheme: NNLO QCD corrections to N-gluon final states in $q\bar{q}$ annihilation*, *JHEP* **02** (2024) 016 [[2310.17598](#)].
- [34] T. Gehrmann, E.W.N. Glover and M. Marcoli, *The colourful antenna subtraction method*, [2310.19757](#).

- [35] W.J. Torres Bobadilla et al., *May the four be with you: Novel IR-subtraction methods to tackle NNLO calculations*, *Eur. Phys. J. C* **81** (2021) 250 [[2012.02567](#)].
- [36] X. Chen, T. Gehrmann, E.W.N. Glover and M. Jaquier, *Precise QCD predictions for the production of Higgs + jet final states*, *Phys. Lett. B* **740** (2015) 147 [[1408.5325](#)].
- [37] R. Boughezal, F. Caola, K. Melnikov, F. Petriello and M. Schulze, *Higgs boson production in association with a jet at next-to-next-to-leading order*, *Phys. Rev. Lett.* **115** (2015) 082003 [[1504.07922](#)].
- [38] F. Caola, K. Melnikov and M. Schulze, *Fiducial cross sections for Higgs boson production in association with a jet at next-to-next-to-leading order in QCD*, *Phys. Rev. D* **92** (2015) 074032 [[1508.02684](#)].
- [39] X. Chen, J. Cruz-Martinez, T. Gehrmann, E.W.N. Glover and M. Jaquier, *NNLO QCD corrections to Higgs boson production at large transverse momentum*, *JHEP* **10** (2016) 066 [[1607.08817](#)].
- [40] J.M. Campbell, R.K. Ellis and S. Seth, *H + 1 jet production revisited*, *JHEP* **10** (2019) 136 [[1906.01020](#)].
- [41] M. Cacciari, F.A. Dreyer, A. Karlberg, G.P. Salam and G. Zanderighi, *Fully Differential Vector-Boson-Fusion Higgs Production at Next-to-Next-to-Leading Order*, *Phys. Rev. Lett.* **115** (2015) 082002 [[1506.02660](#)].
- [42] J. Cruz-Martinez, T. Gehrmann, E.W.N. Glover and A. Huss, *Second-order QCD effects in Higgs boson production through vector boson fusion*, *Phys. Lett. B* **781** (2018) 672 [[1802.02445](#)].
- [43] R. Gauld, A. Gehrmann-De Ridder, E.W.N. Glover, A. Huss and I. Majer, *VH + jet production in hadron-hadron collisions up to order α_s^3 in perturbative QCD*, *JHEP* **03** (2022) 008 [[2110.12992](#)].
- [44] S. Catani, S. Devoto, M. Grazzini, S. Kallweit, J. Mazzitelli and C. Savoini, *Higgs Boson Production in Association with a Top-Antitop Quark Pair in Next-to-Next-to-Leading Order QCD*, *Phys. Rev. Lett.* **130** (2023) 111902 [[2210.07846](#)].
- [45] H.A. Chawdhry, M.L. Czakon, A. Mitov and R. Poncelet, *NNLO QCD corrections to three-photon production at the LHC*, *JHEP* **02** (2020) 057 [[1911.00479](#)].
- [46] H.A. Chawdhry, M. Czakon, A. Mitov and R. Poncelet, *NNLO QCD corrections to diphoton production with an additional jet at the LHC*, *JHEP* **09** (2021) 093 [[2105.06940](#)].
- [47] M. Czakon, A. Mitov, M. Pellen and R. Poncelet, *NNLO QCD predictions for W+c-jet production at the LHC*, *JHEP* **06** (2021) 100 [[2011.01011](#)].
- [48] R. Gauld, A. Gehrmann-De Ridder, E.W.N. Glover, A. Huss, A.R. Garcia and G. Stagnitto, *NNLO QCD predictions for Z-boson production in association with a charm jet within the LHCb fiducial region*, *Eur. Phys. J. C* **83** (2023) 336 [[2302.12844](#)].
- [49] J. Currie, A. Gehrmann-De Ridder, T. Gehrmann, E.W.N. Glover, A. Huss and J. Pires, *Precise predictions for dijet production at the LHC*, *Phys. Rev. Lett.* **119** (2017) 152001 [[1705.10271](#)].
- [50] X. Chen, T. Gehrmann, E.W.N. Glover, A. Huss and J. Mo, *NNLO QCD corrections in full colour for jet production observables at the LHC*, *JHEP* **09** (2022) 025 [[2204.10173](#)].
- [51] S. Badger, M. Czakon, H.B. Hartanto, R. Moodie, T. Peraro, R. Poncelet et al., *Isolated photon production in association with a jet pair through next-to-next-to-leading order in QCD*, *JHEP* **10** (2023) 071 [[2304.06682](#)].
- [52] M. Czakon, A. Mitov and R. Poncelet, *Next-to-Next-to-Leading Order Study of Three-Jet Production at the LHC*, *Phys. Rev. Lett.* **127** (2021) 152001 [[2106.05331](#)].
- [53] M. Czakon, D. Heymes and A. Mitov, *High-precision differential predictions for top-quark pairs at the LHC*, *Phys. Rev. Lett.* **116** (2016) 082003 [[1511.00549](#)].

- [54] S. Catani, S. Devoto, M. Grazzini, S. Kallweit and J. Mazzitelli, *Top-quark pair production at the LHC: Fully differential QCD predictions at NNLO*, *JHEP* **07** (2019) 100 [[1906.06535](#)].
- [55] L. Buoncore, S. Devoto, M. Grazzini, S. Kallweit, J. Mazzitelli, L. Rottoli et al., *Precise Predictions for the Associated Production of a W Boson with a Top-Antitop Quark Pair at the LHC*, *Phys. Rev. Lett.* **131** (2023) 231901 [[2306.16311](#)].
- [56] M. Brucherseifer, F. Caola and K. Melnikov, *On the NNLO QCD corrections to single-top production at the LHC*, *Phys. Lett. B* **736** (2014) 58 [[1404.7116](#)].
- [57] E.L. Berger, J. Gao, C.P. Yuan and H.X. Zhu, *NNLO QCD Corrections to t-channel Single Top-Quark Production and Decay*, *Phys. Rev. D* **94** (2016) 071501 [[1606.08463](#)].
- [58] J. Campbell, T. Neumann and Z. Sullivan, *Single-top-quark production in the t-channel at NNLO*, *JHEP* **02** (2021) 040 [[2012.01574](#)].
- [59] C. Brønnum-Hansen, K. Melnikov, J. Quarroz, C. Signorile-Signorile and C.-Y. Wang, *Non-factorisable contribution to t-channel single-top production*, *JHEP* **06** (2022) 061 [[2204.05770](#)].
- [60] M. Alvarez, J. Cantero, M. Czakon, J. Llorente, A. Mitov and R. Poncelet, *NNLO QCD corrections to event shapes at the LHC*, *JHEP* **03** (2023) 129 [[2301.01086](#)].
- [61] X. Chen, T. Gehrmann, E.W.N. Glover, A. Huss and M. Marcoli, *Automation of antenna subtraction in colour space: gluonic processes*, *JHEP* **10** (2022) 099 [[2203.13531](#)].
- [62] L. Magnea, G. Pelliccioli, C. Signorile-Signorile, P. Torrielli and S. Uccirati, *Analytic integration of soft and collinear radiation in factorised QCD cross sections at NNLO*, *JHEP* **02** (2021) 037 [[2010.14493](#)].
- [63] A. Sen, *Asymptotic Behavior of the Wide Angle On-Shell Quark Scattering Amplitudes in Nonabelian Gauge Theories*, *Phys. Rev.* **D28** (1983) 860.
- [64] J.C. Collins, *Sudakov form-factors*, *Adv. Ser. Direct. High Energy Phys.* **5** (1989) 573 [[hep-ph/0312336](#)].
- [65] L. Magnea and G.F. Sterman, *Analytic continuation of the Sudakov form-factor in QCD*, *Phys.Rev.* **D42** (1990) 4222.
- [66] G.F. Sterman, *Partons, factorization and resummation*, *TASI 95*, in *Theoretical Advanced Study Institute in Elementary Particle Physics (TASI 95): QCD and Beyond*, pp. 327–408, 6, 1995 [[hep-ph/9606312](#)].
- [67] S. Catani, *The Singular behavior of QCD amplitudes at two loop order*, *Phys. Lett.* **B427** (1998) 161 [[hep-ph/9802439](#)].
- [68] G.F. Sterman and M.E. Tejeda-Yeomans, *Multiloop amplitudes and resummation*, *Phys. Lett.* **B552** (2003) 48 [[hep-ph/0210130](#)].
- [69] L.J. Dixon, L. Magnea and G.F. Sterman, *Universal structure of subleading infrared poles in gauge theory amplitudes*, *JHEP* **0808** (2008) 022 [[0805.3515](#)].
- [70] E. Gardi and L. Magnea, *Factorization constraints for soft anomalous dimensions in QCD scattering amplitudes*, *JHEP* **0903** (2009) 079 [[0901.1091](#)].
- [71] E. Gardi and L. Magnea, *Infrared singularities in QCD amplitudes*, *Nuovo Cim.* **C32N5-6** (2009) 137 [[0908.3273](#)].
- [72] T. Becher and M. Neubert, *Infrared singularities of scattering amplitudes in perturbative QCD*, *Phys.Rev.Lett.* **102** (2009) 162001 [[0901.0722](#)].
- [73] T. Becher and M. Neubert, *On the Structure of Infrared Singularities of Gauge-Theory Amplitudes*, *JHEP* **06** (2009) 081 [[0903.1126](#)].
- [74] I. Feige and M.D. Schwartz, *Hard-Soft-Collinear Factorization to All Orders*, *Phys. Rev. D* **90** (2014) 105020 [[1403.6472](#)].

- [75] Ø. Almeliid, C. Duhr and E. Gardi, *Three-loop corrections to the soft anomalous dimension in multileg scattering*, *Phys. Rev. Lett.* **117** (2016) 172002 [[1507.00047](#)].
- [76] Ø. Almeliid, C. Duhr, E. Gardi, A. McLeod and C.D. White, *Bootstrapping the QCD soft anomalous dimension*, *JHEP* **09** (2017) 073 [[1706.10162](#)].
- [77] J.M. Henn and B. Mistlberger, *Four-Gluon Scattering at Three Loops, Infrared Structure, and the Regge Limit*, *Phys. Rev. Lett.* **117** (2016) 171601 [[1608.00850](#)].
- [78] C. Duhr, B. Mistlberger and G. Vita, *Soft integrals and soft anomalous dimensions at N^3LO and beyond*, *JHEP* **09** (2022) 155 [[2205.04493](#)].
- [79] J.M. Henn, G.P. Korchemsky and B. Mistlberger, *The full four-loop cusp anomalous dimension in $\mathcal{N} = 4$ super Yang-Mills and QCD*, *JHEP* **04** (2020) 018 [[1911.10174](#)].
- [80] A. von Manteuffel, E. Panzer and R.M. Schabinger, *Cusp and collinear anomalous dimensions in four-loop QCD from form factors*, *Phys. Rev. Lett.* **124** (2020) 162001 [[2002.04617](#)].
- [81] B. Agarwal, A. von Manteuffel, E. Panzer and R.M. Schabinger, *Four-loop collinear anomalous dimensions in QCD and $N=4$ super Yang-Mills*, *Phys. Lett. B* **820** (2021) 136503 [[2102.09725](#)].
- [82] D.A. Kosower, *All order collinear behavior in gauge theories*, *Nucl. Phys.* **B552** (1999) 319 [[hep-ph/9901201](#)].
- [83] S. Catani and M. Grazzini, *Collinear factorization and splitting functions for next-to-next-to-leading order QCD calculations*, *Phys. Lett.* **B446** (1999) 143 [[hep-ph/9810389](#)].
- [84] S. Catani and M. Grazzini, *Infrared factorization of tree level QCD amplitudes at the next-to-next-to-leading order and beyond*, *Nucl. Phys.* **B570** (2000) 287 [[hep-ph/9908523](#)].
- [85] J.M. Campbell and E.W.N. Glover, *Double unresolved approximations to multiparton scattering amplitudes*, *Nucl. Phys.* **B527** (1998) 264 [[hep-ph/9710255](#)].
- [86] Z. Bern, V. Del Duca, W.B. Kilgore and C.R. Schmidt, *The infrared behavior of one loop QCD amplitudes at next-to-next-to leading order*, *Phys. Rev. D* **60** (1999) 116001 [[hep-ph/9903516](#)].
- [87] S. Catani and M. Grazzini, *The soft gluon current at one loop order*, *Nucl. Phys.* **B591** (2000) 435 [[hep-ph/0007142](#)].
- [88] V. Del Duca, A. Frizzo and F. Maltoni, *Factorization of tree QCD amplitudes in the high-energy limit and in the collinear limit*, *Nucl. Phys.* **B568** (2000) 211 [[hep-ph/9909464](#)].
- [89] S.D. Badger and E.W.N. Glover, *Two loop splitting functions in QCD*, *JHEP* **07** (2004) 040 [[hep-ph/0405236](#)].
- [90] C. Duhr and T. Gehrmann, *The two-loop soft current in dimensional regularization*, *Phys. Lett.* **B727** (2013) 452 [[1309.4393](#)].
- [91] Y. Li and H.X. Zhu, *Single soft gluon emission at two loops*, *JHEP* **11** (2013) 080 [[1309.4391](#)].
- [92] P. Banerjee, P.K. Dhani and V. Ravindran, *Gluon jet function at three loops in QCD*, *Phys. Rev. D* **98** (2018) 094016 [[1805.02637](#)].
- [93] R. Brüser, Z.L. Liu and M. Stahlhofen, *Three-Loop Quark Jet Function*, *Phys. Rev. Lett.* **121** (2018) 072003 [[1804.09722](#)].
- [94] L.J. Dixon, E. Herrmann, K. Yan and H.X. Zhu, *Soft gluon emission at two loops in full color*, *JHEP* **05** (2020) 135 [[1912.09370](#)].
- [95] S. Catani, D. Colferai and A. Torrini, *Triple (and quadruple) soft-gluon radiation in QCD hard scattering*, *JHEP* **01** (2020) 118 [[1908.01616](#)].
- [96] V. Del Duca, C. Duhr, R. Haindl, A. Lazopoulos and M. Michel, *Tree-level splitting amplitudes for a gluon into four collinear partons*, *JHEP* **10** (2020) 093 [[2007.05345](#)].

- [97] S. Catani and L. Cieri, *Multiple soft radiation at one-loop order and the emission of a soft quark–antiquark pair*, *Eur. Phys. J. C* **82** (2022) 97 [2108.13309].
- [98] V. Del Duca, C. Duhr, R. Haindl and Z. Liu, *Tree-level soft emission of a quark pair in association with a gluon*, *JHEP* **01** (2023) 040 [2206.01584].
- [99] M. Czakon, F. Eschment and T. Schellenberger, *Revisiting the double-soft asymptotics of one-loop amplitudes in massless QCD*, *JHEP* **04** (2023) 065 [2211.06465].
- [100] M. Czakon and S. Sapeta, *Complete collection of one-loop triple-collinear splitting operators for dimensionally-regulated QCD*, *JHEP* **07** (2022) 052 [2204.11801].
- [101] S. Catani, L. Cieri, D. Colferai and F. Coradeschi, *Soft gluon–quark–antiquark emission in QCD hard scattering*, *Eur. Phys. J. C* **83** (2023) 38 [2210.09397].
- [102] L. Magnea, E. Maina, G. Pelliccioli, C. Signorile-Signorile, P. Torrielli and S. Uccirati, *Factorisation and Subtraction beyond NLO*, *JHEP* **12** (2018) 062 [1809.05444].
- [103] L. Magnea, C. Milloy, C. Signorile-Signorile, P. Torrielli and S. Uccirati, *Strongly-ordered infrared limits for subtraction counterterms from factorisation*, *PoS LL2022* (2022) 075 [2209.06102].
- [104] G. Bertolotti, P. Torrielli, S. Uccirati and M. Zaro, *Local analytic sector subtraction for initial- and final-state radiation at NLO in massless QCD*, *JHEP* **12** (2022) 042 [2209.09123].
- [105] T. Becher and G. Bell, *The gluon jet function at two-loop order*, *Phys. Lett.* **B695** (2011) 252 [1008.1936].
- [106] E. Laenen, G.F. Sterman and W. Vogelsang, *Recoil and threshold corrections in short distance cross-sections*, *Phys. Rev.* **D63** (2001) 114018 [hep-ph/0010080].
- [107] S. Catani and M. Ciafaloni, *Generalized Coherent State for Soft Gluon Emission*, *Nucl. Phys. B* **249** (1985) 301.
- [108] S. Catani, M. Ciafaloni and G. Marchesini, *NONCANCELLING INFRARED DIVERGENCES IN QCD COHERENT STATE*, *Nucl. Phys. B* **264** (1986) 588.
- [109] Y.J. Zhu, *Double soft current at one-loop in QCD*, 2009.08919.
- [110] G. Falcioni, E. Gardi and C. Milloy, *Relating amplitude and PDF factorisation through Wilson-line geometries*, *JHEP* **11** (2019) 100 [1909.00697].
- [111] Z. Bern, V. Del Duca and C.R. Schmidt, *The Infrared behavior of one loop gluon amplitudes at next-to-next-to-leading order*, *Phys. Lett. B* **445** (1998) 168 [hep-ph/9810409].
- [112] D.A. Kosower and P. Uwer, *One loop splitting amplitudes in gauge theory*, *Nucl. Phys. B* **563** (1999) 477 [hep-ph/9903515].
- [113] G. Leibbrandt, *Introduction to Noncovariant Gauges*, *Rev. Mod. Phys.* **59** (1987) 1067.
- [114] R. Mertig, M. Böhm and A. Denner, *Feyn calc - computer-algebraic calculation of feynman amplitudes*, *Computer Physics Communications* **64** (1991) 345.
- [115] V. Shtabovenko, R. Mertig and F. Orellana, *New Developments in FeynCalc 9.0*, *Comput. Phys. Commun.* **207** (2016) 432 [1601.01167].
- [116] V. Shtabovenko, R. Mertig and F. Orellana, *FeynCalc 9.3: New features and improvements*, *Comput. Phys. Commun.* **256** (2020) 107478 [2001.04407].
- [117] R.N. Lee, *Presenting LiteRed: a tool for the Loop InTEgrals REDuction*, 1212.2685.
- [118] R.N. Lee, *LiteRed 1.4: a powerful tool for reduction of multiloop integrals*, *J. Phys. Conf. Ser.* **523** (2014) 012059 [1310.1145].
- [119] S. Catani, S. Dittmaier, M.H. Seymour and Z. Trócsányi, *The Dipole formalism for next-to-leading order QCD calculations with massive partons*, *Nucl. Phys.* **B627** (2002) 189 [hep-ph/0201036].

- [120] J.M. Henn, *Multiloop integrals in dimensional regularization made simple*, *Phys. Rev. Lett.* **110** (2013) 251601 [[1304.1806](#)].
- [121] T. Hahn, *CUBA: A Library for multidimensional numerical integration*, *Comput. Phys. Commun.* **168** (2005) 78 [[hep-ph/0404043](#)].
- [122] S. Borowka, G. Heinrich, S. Jahn, S.P. Jones, M. Kerner, J. Schlenk et al., *pySecDec: a toolbox for the numerical evaluation of multi-scale integrals*, *Comput. Phys. Commun.* **222** (2018) 313 [[1703.09692](#)].